

**BIOSTRATIGRAPHIC SETUP AND DEPOSITIONAL MODEL  
OF MARGALLA HILL LIMESTONE, HAZARA BASIN  
NORTHWEST HIMALAYAS, PAKISTAN**



**By**

***Muhammad Ismail***

**Department of Earth & Environmental Sciences**

**Bahria University, Islamabad**

**2024**

**BIOSTRATIGRAPHIC SETUP AND DEPOSITIONAL MODEL  
OF MARGALLA HILL LIMESTONE, HAZARA BASIN  
NORTHWEST HIMALAYAS, PAKISTAN**



**By**

**MUHAMMAD ISMAIL**

**Department of Earth & Environmental Sciences**

**Bahria University Islamabad**

**October 2024**

**BIOSTRATIGRAPHIC SETUP AND DEPOSITIONAL MODEL  
OF MARGALLA HILL LIMESTONE, HAZARA BASIN  
NORTHWEST HIMALAYAS, PAKISTAN**



**By**

**MUHAMMAD ISMAIL**

**A thesis presented to meet the requirement for the award of the degree of  
Master of Science (Geology)**

**Department of Earth and Environmental Sciences  
Bahria University Islamabad**

**October 2024**

## APPROVAL OF EXAMINATION

Scholar Name: Mr. Muhammad Ismail, Registration No: 01-262212-008, Program of Study: MS Geology

Thesis Title: BIOSTRATIGRAPHIC SETUP AND DEPOSITIONAL MODEL OF MARGALLA HILL LIMESTONE, HAZARA BASIN NORTHWEST HIMALAYAS, PAKISTAN

It is to certify that the above scholar's thesis has been completed to my satisfaction and to my belief, its standard is appropriate for submission for examination. I have also conducted plagiarism test of this thesis using HEC prescribed software and found similarity index 17% that is within the permissible limit set by the HEC for the MS degree thesis. I have also found the thesis in format recognized by the BU for the MS thesis.

NOTE: The plagiarism report is attached at the end of thesis.

Principal Supervisor's

Signature:

Date:

Name: Dr. Mumtaz Ali Khan

## AUTHOR'S DECLARATION

I, "Mr. Muhammad Ismail" is hereby state that my MS thesis titled "BIOSTRATIGRAPHIC SETUP AND DEPOSITIONAL MODEL OF MARGALLA HILL LIMESTONE, HAZARA BASIN NORTHWEST HIMALAYAS, PAKISTAN" is my own work and has not been submitted previously by me of taking any degree from this university "Bahria University Islamabad Campus" or anywhere else in the country/world.

At any time, if my statement is found to be incorrect even after my graduation, the University has the right to withdraw /cancel my MS degree.

Name of Scholar: Mr. Muhammad Ismail

Date:

Signature:

---

## PLAGARISM UNDERTAKING

I solemnly declare that research work presented in the thesis titled “BIOSTRATIGRAPHIC SETUP AND DEPOSITIONAL MODEL OF MARGALLA HILL LIMESTONE, HAZARA BASIN NORTHWEST HIMALAYAS, PAKISTAN” is solely my research work with no significant contribution from any other person. Small contribution/help wherever taken has been duly acknowledged and that complete thesis has been written by me.

I understand the zero-tolerance policy of the HEC and Bahria University towards plagiarism. Therefore, I as an author of the above titled thesis declare that no portion of my thesis has been plagiarized and any material used as reference is properly referred/cited.

I understand that if I am found guilty of any formal plagiarism in the above titled thesis even after award of my MS degree, the university reserves the right to withdraw, revoke my MS degree and that HEC and the university has the right to publish my name on the HEC/University website on which names of the scholars are placed who submitted plagiarized thesis.

Scholar/Author's

Sign: \_\_\_\_\_

Name of Scholar: Mr. Muhammad Ismail

## DEDICATION

I dedicate this thesis to my beloved parents, whose unwavering support, endless sacrifices, and unconditional love have been the cornerstone of my academic journey. Their constant encouragement and belief in my abilities have provided me with the strength and determination to overcome every challenge, enabling me to pursue my dreams with confidence and resolve. Without their enduring presence and prayers, this achievement would not have been possible.

I also extend my heartfelt gratitude to my respected teachers, whose wisdom, guidance, and dedication have been a source of inspiration throughout my academic endeavors. Their relentless efforts in imparting knowledge and shaping my intellectual growth have significantly contributed to the person I am today. Their mentorship has not only enhanced my understanding of the subject but has also instilled in me the values of perseverance and excellence. This thesis is a reflection of their profound impact on my educational journey.

## ACKNOWLEDGEMENTS

In the journey of completing this thesis, I was in contact with many people. I have had the privilege of receiving guidance, and encouragement from researchers, academicians, and faculty members, as they have contributed towards my understanding and thoughts. First and foremost, I would like to express my profound gratitude to my thesis supervisor, Dr. Maryam Saleem, X-Assistant Professor of Earth and Environmental Sciences at Bahria University Islamabad Campus, for her unwavering support, insightful guidance, and invaluable friendship. I am equally indebted to my current supervisor, Dr. Mumtaz Ali Khan, Assistant Professor of Earth and Environmental Sciences at Bahria University Islamabad, for his critical insights and encouragement that have significantly shaped this work. Their combined mentorship has been instrumental in bringing this thesis to its present form, and I am deeply appreciative of their contributions.

I would also like to extend my heartfelt thanks to my fellow students and colleagues, whose camaraderie and support have been a source of strength throughout this academic journey. Their thoughtful perspectives and shared experiences have enriched my understanding in more ways than I can express. I am deeply grateful to my family, whose unwavering love, patience, and belief in me have been the cornerstone of my success. Though it is impossible to name everyone individually in this limited space, I want to acknowledge each person who has played a part in this journey—your support has made a lasting impact on me.



## ABSTRACT

This study investigates the biofacies identification, stratigraphic distribution, and depositional model of the Eocene Margalla Hill Limestone in the Ayubia and Nathiagali sections, located in the southeastern Hazara sub-basin of the NW Himalayas, Pakistan. Fieldwork involved collecting rock samples at regular intervals, where diagenetic features were observed, and log charts were created using CorelDraw. A total of 76 samples, 40 from Ayubia and 36 from Nathiagali, were collected, and after preparing thin sections, the samples were analyzed under a petrographic microscope for microfacies, fossils, porosity, and permeability. The limestone, which is approximately 60 meters thick at Ayubia and 54 meters at Nathiagali, consists of grey to pale grey limestone interbedded with shale and argillaceous limestone. At the Ayubia section, eight microfacies were identified, including Mudstone, Bioclastic Mudstone, Bioclastic Wackestone, Algal Wackestone, Assilinid Nummulitic Wackestone, Nummulitidae Alveolina Wackestone, Assilinid Wackestone, and Alveolina Wackestone. In contrast, the Nathiagali section revealed nine microfacies, such as Mudstone, Bioclastic Wackestone, Assilinid Wackestone, Nummulitidae-Lockhartian Wackestone, Coralline-Algal Wackestone, Assilinid-Discocyclinal Wackestone, Discocyclinal-Assilinid Wackestone, Discocyclinal Mudstone, and Assilinid Packstone. The study also highlights larger foraminifera fauna and explores the depositional environment. Diagenetic processes such as compaction, cementation, micritization, bioturbation, dissolution, and dolomitization affected the reservoir's porosity, with dissolution, dolomitization, and fracturing enhancing porosity, while compaction and cementation reduced it. The formation's development is linked to a single 3rd-order cycle with several 2nd-order system tracts (TST and HST), driven by sea-level fluctuations, with local tectonic effects playing a significant role, leading to deviations from global sea-level models.

## TABLE OF CONTENTS

<b>APPROVAL OF EXAMINATION</b> .....	i
<b>AUTHOR’S DECLARATION</b> .....	ii
<b>PLAGARISM UNDERTAKING</b> .....	iii
<b>DEDICATION</b> .....	iv
<b>ACKNOWLEDGEMENTS</b> .....	v
<b>ABSTRACT</b> .....	vi
<b>Chapter 1 INTRODUCTION</b> .....	1
1.1 General description .....	1
1.2 Location and Accessibility.....	4
1.3 Purpose of study.....	5
1.4 Aims and Objectives .....	5
1.5 Stratigraphic sections of the studied area.....	6
1.5.1 Nathiagali Section.....	6
1.5.2 Ayubia Section .....	8
1.6 Literature Review .....	8
<b>Chapter 2 REGIONAL GEOLOGY</b> .....	10
2.1 Introduction.....	10
2.2 Himalayas .....	12
2.3 Local Geology of the Study Area.....	15
2.4 Stratigraphy of the Study Area.....	15
<b>Chapter 3 FIELD OBSERVATIONS</b> .....	18
3.1 Field Work.....	18
3.2 Nathiagali section .....	20
3.3 Ayubia section.....	25
<b>Chapter 4 BIOSTRATIGRAPHY OF MARGALLA HILL LIMESTONE</b> .....	29
4.1 Introduction.....	29

4.2 Larger Benthic Foraminiferas (LBF) .....	29
4.3 Current Study .....	30
4.4 Description of the Species .....	30
4.4.1 Genus Asilina .....	31
4.4.1.1 Assilina Spinosa .....	31
4.4.1.2 Assilina Sub-Spinosa.....	32
4.4.1.3 Assilina Laminosa .....	33
4.4.1.4 Assilina granulosa .....	33
4.4.1.5 Assilina Placentula .....	34
4.4.2 Genus Nummulites.....	35
4.4.2.1 Nummulite Aticacus.....	36
4.4.2.2 Nummulite Mamilatus.....	37
4.4.2.3 Nummulite Globulus .....	37
4.4.3 Genus Lockhartia .....	39
4.4.3.1 Lockhartia Conditti .....	40
4.4.3.2 Lockhartia Tippri.....	41
4.4.4 Genus Alveolina.....	42
4.4.4.1 Alveolina Indicatrix.....	43
4.4.4.2 Alveolina sp., Drobne 1977.....	43
4.4.5 Genus Discocyclina.....	45
4.4.5.1 Discocyclina Dispensa .....	46
4.4.5.2 Discocyclina sp. 1 .....	46
4.5 Age Range of Margalla Hill Limestone .....	48
<b>Chapter 5 MICROFACIES ANALYSIS AND DEPOSITIONAL ENVIRONMENT ..</b>	<b>51</b>
5.1 Introduction.....	51
5.2 Microfacies Analysis and depositional environment of Margalla Hill Limestone .	52
5.2.1 Microfacies Analysis of Ayubia section.....	52
5.2.1.1 Mudstone Microfacie AS1 .....	53

5.2.1.2 Bioclastic Mudstone Microfacie AS2 .....	53
5.2.1.3 Bioclastic Wackstone Microfacie AS3 .....	53
5.2.1.4 Algal Wackstone Microfacie AS4 .....	54
5.2.1.5 Assilinid Nummulitic Wackstone Microfacie AS5.....	54
5.2.1.6 Nummulitidae Alveolinal Wackstone Microfacie AS6 .....	54
5.2.1.7 Assilinid Wackstone Microfacie AS7 .....	55
5.2.1.8 Alveolinal Wackstone Microfacie AS8 .....	55
5.2.2 Depositional Environment of Ayubia Section .....	56
5.2.3 Microfacies Analysis of Nathiagali Section.....	63
5.2.3.1 Mudstone Microfacie NS1 .....	63
5.2.3.2 Bioclastic Wackstone Microfacie NS 2.....	64
5.2.3.3 Assilinid Wackstone Microfacie NS 3.....	64
5.2.3.4 Nummulitidae-Lockhartian Wackstone Microfacie NS 4 .....	65
5.2.3.5 Coralline Algal Wackstone Microfacie NS 5 .....	65
5.2.3.6 Assilinid-Discocyclinal Wackstone Microfacie NS 6 .....	65
5.2.3.7 Discocyclinal-Assilinal wackstone Microfacie NS 7.....	66
5.2.3.8 Discocyclinal mudstone Microfacie NS 8.....	66
5.2.3.9 Assilinid packstone Microfacie NS 9 .....	68
5.2.4 Depositional Environment of Nathiagali Section .....	68
5.3 Depositional Model.....	75
<b>Chapter 6 DIAGENESIS AND ITS IMPACT ON RESERVOIR PROPERTIES IN</b>	
<b>THE MARGALLA HILL LIMESTONE .....</b>	<b>77</b>
6.1 DIAGENESIS .....	77
6.2 Compaction.....	77
6.3 Stylolitization.....	78
6.4 Fractures.....	78
6.5 Calcite veins.....	78
6.6 Pyritization.....	79

6.7 Micritization.....	79
6.8 Cementation .....	80
6.9 Dolomitization .....	80
6.10 Burrowing .....	81
6.11 Bioturbation .....	81
6.12 Dissolution .....	82
6.13 Paragenetic Sequence .....	86
6.14 Effect of diagenesis on reservoir properties.....	87
6.15 Characterization of Margalla Hill Limestone as a Reservoir.....	88
<b>Chapter 7 SEQUENCE STRATIGRAPHY .....</b>	<b>90</b>
7.1 Introduction.....	90
7.2 Sequence Stratigraphy of Margalla Hill Limestone.....	91
7.2.1 Ayubia section .....	92
7.2.2 Nathiagali Section .....	92
7.2.3 Correlation with Global Eustatic Curve.....	92
7.2.4 Correlation of Microfacies with Sequence stratigraphy of Ayubia section.....	95
7.2.5 Correlation of Microfacies with Sequence stratigraphy of Nathiagali section	95
<b>Chapter 8 DISCUSSION.....</b>	<b>97</b>
<b>Chapter 9 CONCLUSION .....</b>	<b>99</b>
<b>REFERENCES .....</b>	<b>101</b>

## LIST OF TABLES

<b>Table 1.1:</b> Cordinates of Ayubia and Nathia-Gali Section .....	8
--	---

## LIST OF FIGURES

<b>Figure 1.1:</b> Regional tectonic map of Pakistan depicting the exposure of Eocene strata along the Axial Belt. The study area is indicated by the white box (modified from (Shah, 1977)).	3
<b>Figure 1.2:</b> Location map of the study area, specifically Nathiagali and Ayubia, within the South Eastern Hazara Sub-Basin. (Source: Google Earth)	4
<b>Figure 1.3:</b> Geological map of South-Eastern Hazara, with the Nathiagali Section indicated as [1] and the Ayubia section indicated as [2] along the Murree-Nathiagali Road (modified from (Latif, 1970)).	7
<b>Figure 2.1:</b> Representing the Northward movement of Indian plate (i.e. Indo-eurasian plate collision) (Patriat, 1984).	12
<b>Figure 2.2:</b> Regional tectonic map of Pakistan with the location of study area showing major thrust faults in northern Pakistan along with major sub-divisions of Himalayas, (SH: Sub-Himalayas, LH: Lesser Himalayas, and HH: Higher Himalayas), Kohistan Island Arc (KIA), and Karakoram Block (KB). The principal thrust faults that occur in the Upper Indus Basin include the Salt Range Thrust (SRT), the Main Boundary Thrust (MBT), the Main Central Thrust (MCT), the Main Mantle Thrust (MMT), and the Main Karakoram Thrust (MKT). The red box represents the study area in the Hazara sub-basins (modified after (Calkins, 1975; Baig, 2006)).	14
<b>Figure 2.3:</b> Stratigraphic column of Hazara-Sub Basin (Latif, 1970).	17
<b>Figure 3.1:</b> Field outcrop view of Nathiagali section of the study area (a) Thick to thin bedded limestone unit (b) Closeup view of thick bedded limestone and nodular limestone.	22
<b>Figure 3.2:</b> Field photographs (a) Contact between dark grey limestone and light grey limestone (b) bioclastic limestone (c) nodular bioclastic limestone (d) nummulites indicated with arrows.	23
<b>Figure 3.3:</b> Field outcrop photographs Nathiagali section (a-b) Several bioclasts of ostracods and nummulites (c) Multiple calcite veins cross cutting each other (d) bioclasts of ostracods along with stylolites (os: Ostracods, st: Stylolites, cv: Calcite Veins, Nu: Nummulites).	24

<b>Figure 3.4:</b> Field outcrop view of Ayubia section (a) Thick to thin bedded limestone of Margalla Hill Limestone (b) Nodular limestone beds. ....	26
<b>Figure 3.5:</b> Field photographs of the Ayubia section: (a) Bioclasts of ostracods in a limestone bed (b) Various foraminifera species including nummulites and lockhartia (c) Assilina and nummulites in Margalla Hill limestone (d) Bioclastic limestone beds (os: ostracods, nu: nummulites, lo: lockhartia, as: assilina, bi: bioclast).....	27
<b>Figure 3.6:</b> Field photographs of the Ayubia section in the study area: (a) Brachiopod indicated with an arrow in Margalla Hill limestone (b) Facies variation showing bioclastic limestone and mudstone (c) Contact between dark and light limestone (d) Calcite veins cross-cutting bioclastic limestone.....	28
<b>Figure 4.1:</b> Age distribution of various Larger Benthic Foraminifera (LBF) in the Margalla Hill Limestone. The yellow lines indicate relatively limited age ranges of the diagnostic fossils compared to the red lines. The "Margalla Hill Limestone Biozone (MFBZ)" spans from Late Ilerdian (Shallow Benthic Zone SBZ9, 53 Ma) to Lower Cuisian (Shallow Benthic Zone SBZ10, 51.5 Ma) (modified from (Schaub, 1981; Serra-Kiel, 1998; Ahmad, 2011; Sameeni, 2013; Zhang Q. W., 2013)). ....	50
<b>Figure 5.1:</b> Facies depositional model of a carbonate ramp showing the temporal distribution of the Eocene facies of the Margalla Hill Limestone, South-Eastern Hazara sub-basin at Ayubia section.....	61
<b>Figure 5.2:</b> Microfacies distribution, depositional environments, and a mean relative sea level curve inferred from the faunal paleoecology (Racey, 1995) and facies criteria (Flügel E. , 2004) of the Margalla Hill Limestone exposed in the Ayubia section, south-eastern hazara sub-basin. (The shaded area depicts the range of variation in the deposition environment).....	62
<b>Figure 5.3:</b> Facies depositional model of a carbonate ramp illustrating the temporal distribution of the Eocene facies within the Margalla Hill Limestone, located in the southeastern Hazara sub-basin at the Nathiagali section. ....	73
<b>Figure 5.4:</b> Microfacies distribution, depositional environments, and a mean relative sea level curve inferred from the faunal paleoecology (Racey, 1995) and facies criteria (Flügel E. , 2004) of the Margalla Hill Limestone exposed in the Nathiagali section, southeastern Hazara sub-basin. (The shaded area depicts the range of variation in the deposition environment).....	74
<b>Figure 6.1:</b> Field photographs (a) Burrowing (b) bioturbation (c) dissolution (bu; burrows, bt; bioturbation and Ds; dissolution) .....	85



- Figure 6.2:** Representing paragenetic sequence of the study area ..... 87
- Figure 7.1:** Stratigraphic log displaying variable lithology, microfacies distribution, depositional environments, sequence stratigraphy, and eustatic curve. light yellow colour line shows long term global eustatic changes and dark yellow colour line shows short term global eustatic changes. HST (Highstand system tract), TST (Transgressive system tract), MFS (Maximum Flooding surface) and TS (Transgressive surface). ..... 93
- Figure 7.2:** Stratigraphic log displaying variable lithology, microfacies distribution, depositional environments, sequence stratigraphy, and eustatic curve. light yellow colour line shows long term global eustatic changes and dark yellow colour line shows short term global eustatic changes. HST (High-stand system tract), TST (Transgressive system tract), MFS (Maximum Flooding surface) and TS (Transgressive surface). ..... 94

## LIST OF PLATES

<b>Plate 4.1:</b> The above plate depicts various species of the genus Assilina: a) & b) show Assilina Spinosa, c) & d) show Assilina sub-spinosa, e) & f) show Assilina Laminosa, g), h), & i) depict Assilina Granulosa, and j) & k) show Assilina Placentula.....	35
<b>Plate 4.2:</b> The above chart depicts various Species of Nummulites. a) & b) Shows Nummulite Aticacus c) & d) Nummulite Mamilatus e) & f) Nummulite Globulus.....	39
<b>Plate 4.3:</b> The above Plate depicts Various Species of Genus Lockhartia. a) Lockhartia Conditti b) Lockhartia Tippri.....	42
<b>Plate 4.4:</b> The above Chart depicts various Species of Genus Alveolina. a) & b) Shows Cross Sectional view of Alveolina Indicatrix c) Alveolina sp cross cutted by numerous calcite veins.....	45
<b>Plate 4.5:</b> The above chart depicts various species of Discocyclina. a) Discocyclina Dispensa b) Discocyclina Sp 1 .....	47
<b>Plate 4.6:</b> The above plate showcases various fossils: A) & B) Assilina spinosa, C) & D) Assilina subspinosa, E), F), & G) Assilina granulosa, H) & I) Assilina laminosa, J) & K) Assilina placentula, L) Nummulites atacicus, M) Nummulites globulus, N) Nummulites mamilatus, O) Lockhartia conditi, P) Lockhartia tipperi, Q) Alveolina sp., R) Alveolina indicatrix, S) Discocyclina sp. 1, T) Discocyclina dispensa.....	48
<b>Plate 5.1:</b> The above Plate depicts the Photomicrographs of various microfacies of Margalla Hill Limestone, Ayubia section a) Mudstone microfacie b) Bioclastic Mudstone microfacie c) Bioclastic Wackstone microfacie d) Algal Wackstone microfacie e) Assilinitic Nummulitic Wackstone microfacie f) Nummulitidae Alveolinal Wackstone microfacie g) Assilinitic Wackstone microfacie h) Alveolinitic wackstone microfacie. ....	56
<b>Plate 5.2:</b> The photomicrographs of various microfacies of Margalla Hill Limestone, Nathiagali section: a) Mudstone microfacies b) Bioclastic wackstone microfacies c) Assilinitic wackstone microfacies d) Nummulitidae-Lockhartian wackstone microfacies e) Algal-Assilina wackstone microfacies f) Assilinitic-discocyclinal wackstone microfacies g) Discocyclinal-Assilina wackstone microfacies h) Discocyclinal mudstone microfacies i) Assilina grainstone microfacies.....	67

**Plate 6.1:** Thin section view illustrating mechanical and chemical compaction (a-b), pyritization (c), and micritization (d). ie St - stylolite, Fr - fracture, Py - pyrite, CV - calcite veins. .... 83

**Plate 6.2:** Photomicrographs (a-b) cementation (c) Dolomitization (i.e, bl; blocky and bo; botryoidal cementation) (c) dolomitization. .... 84

# Chapter 1

## INTRODUCTION

### 1.1 General description

Eocene sedimentary rocks, primarily carbonates, hold immense commercial significance. Limestone and dolomites, prevalent within this period, serve agricultural and industrial purposes, being utilized as building stones. Most notably, they function as reservoir rocks for over one third of the world's petroleum reserves. These rocks have been subject to intensive research due to their environmental and economic importance (Sam boggs, 2006)

In Pakistan, carbonate lithologies prevail over other lithologies such as shales and evaporites in the Eocene succession. The Eocene strata extend across a vast region from the southern side of the Himalayan Mountains in the north to the Arabian Sea in the south (see Figure 1.1). Outcrops of the Eocene strata are present in both the Indus (upper and lower) and Baluchistan basins of Pakistan, where it is exposed along the Axial Belt and NW Himalayan Fold-Thrust Belt (Shah, 1977; Kadri, 1995). Tectonic shifts induced by the Himalayas have led to the subdivision of the Upper Indus Basin into the Kohat, Peshawar, Potwar, Hazara, and Kashmir sub-basins (Shah, 1977; Kazmi, 2008; Afzal, Revised stratigraphy of the lower Cenozoic succession of the Greater Indus Basin in Pakistan, 2009; Umar, 2015).

The Eocene strata hold significant economic value for Pakistan due to the presence of numerous oil and gas fields, including the country's largest gas field, the "Sui Gas Field," located in the southern region (Shah, 1977; Siddiqui, 1998). The Potwar sub-basin, in particular, is rich in oil fields, with active extraction occurring in the Dakhni, Meyal, Dhulian, FimKassar, and Balkassar fields. The area south of the Main Boundary Thrust (MBT) is a critical region, known for housing a vast number of oil and gas

reserves. Notable hydrocarbon reserves are found in the Upper and Lower Indus basins, especially within the Eocene strata, with formations such as the Sakesar and Chorgali formations playing a key role, particularly in the Adhi and Pindori oil fields (Kadri, 1995).

In 2002, oil production from the Eocene rocks was substantial, with a total of 2,071,298 barrels extracted. However, in 2003, the output slightly decreased to 116,311 barrels. The Eocene successions in the Kohat, Hazara, and Potwar sub-basins of the Upper Indus Basin are of particular interest, as these sub-basins are home to formations like the Kuldana, Margalla, Chorgali, and upper Patala formations.

The Kuldana Formation is unique, primarily comprising a mix of siliciclastic and carbonate sediments formed in a shallow marine environment, with fossils of freshwater vertebrates (Shah, 1977; Kazmi, 2008; Gingerich, 1977; Gingerich, 1981). In contrast, the other units predominantly consist of various carbonate lithologies with distinct facies. This study focuses on the Margalla Hill Limestone, a distinct type of limestone primarily found in the Upper Indus Basin. The limestone is exposed in various locations along the Murree to Abbottabad road in the southeastern Hazara Sub-Basin, Pakistan. The primary aim of this study is to characterize the reservoir through an integrated approach, involving diagenesis, microfacies, and bio-sequence stratigraphic analysis.

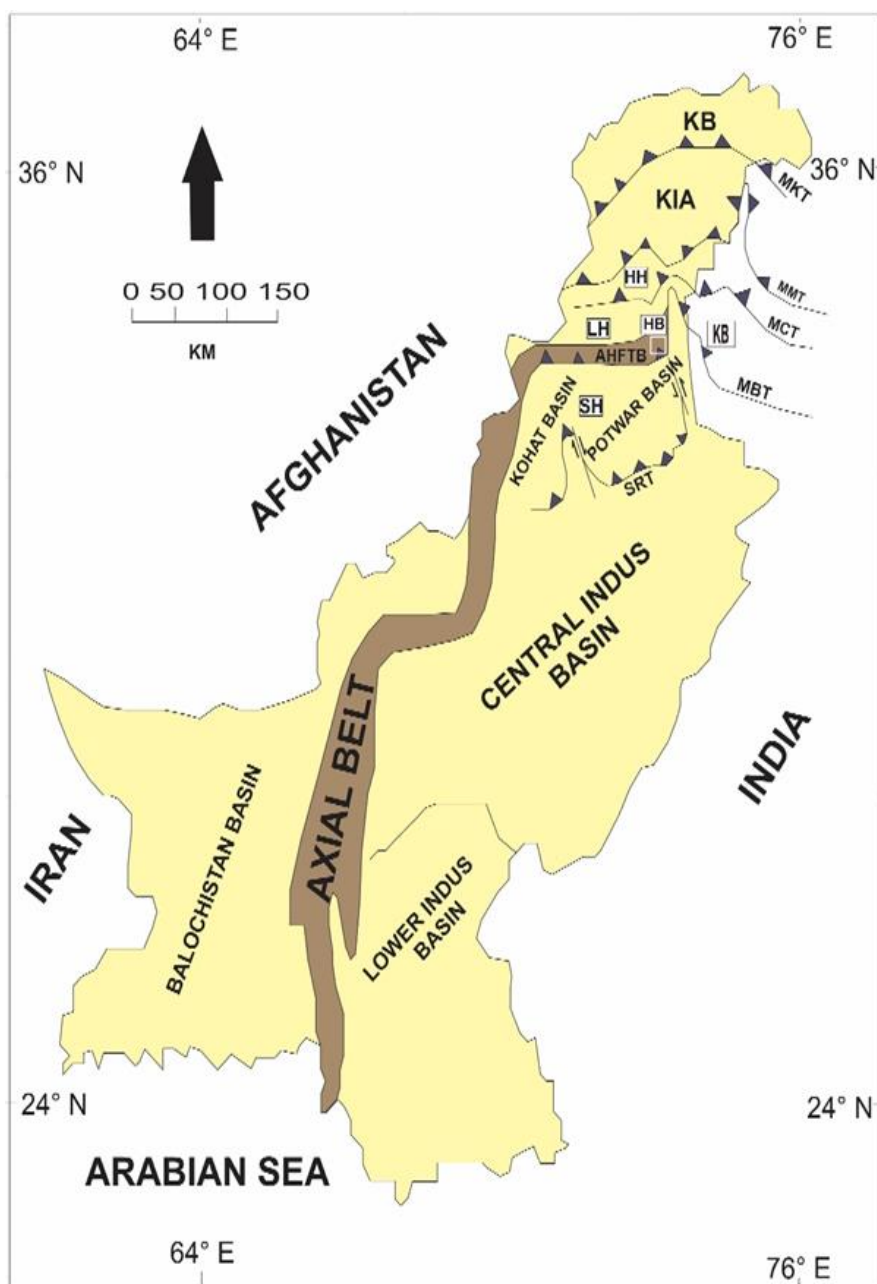


**Figure 1.1:** Regional tectonic map of Pakistan depicting the exposure of Eocene strata along the Axial Belt. The study area is indicated by the white box (modified from (Shah, 1977)).

## 1.2 Location and Accessibility

The southeastern portions of the Hazara district in West Pakistan constitute the primary focus area of the research (see Figure 1.2). This region is situated between latitudes  $34^{\circ}04'$  and  $34^{\circ}01'$  north and longitudes  $73^{\circ}23'$  east. Near Islamabad, the elevation in the study area ranges from just under 2,000 feet to 9,780 feet at Miranjani, near Nathiagali. The majority of the region lies above 4,000 feet. The Galis group, positioned between Murree and Abbottabad, encompasses the highest points in the area and serves as a natural boundary between the Indus and Jhelum river systems.

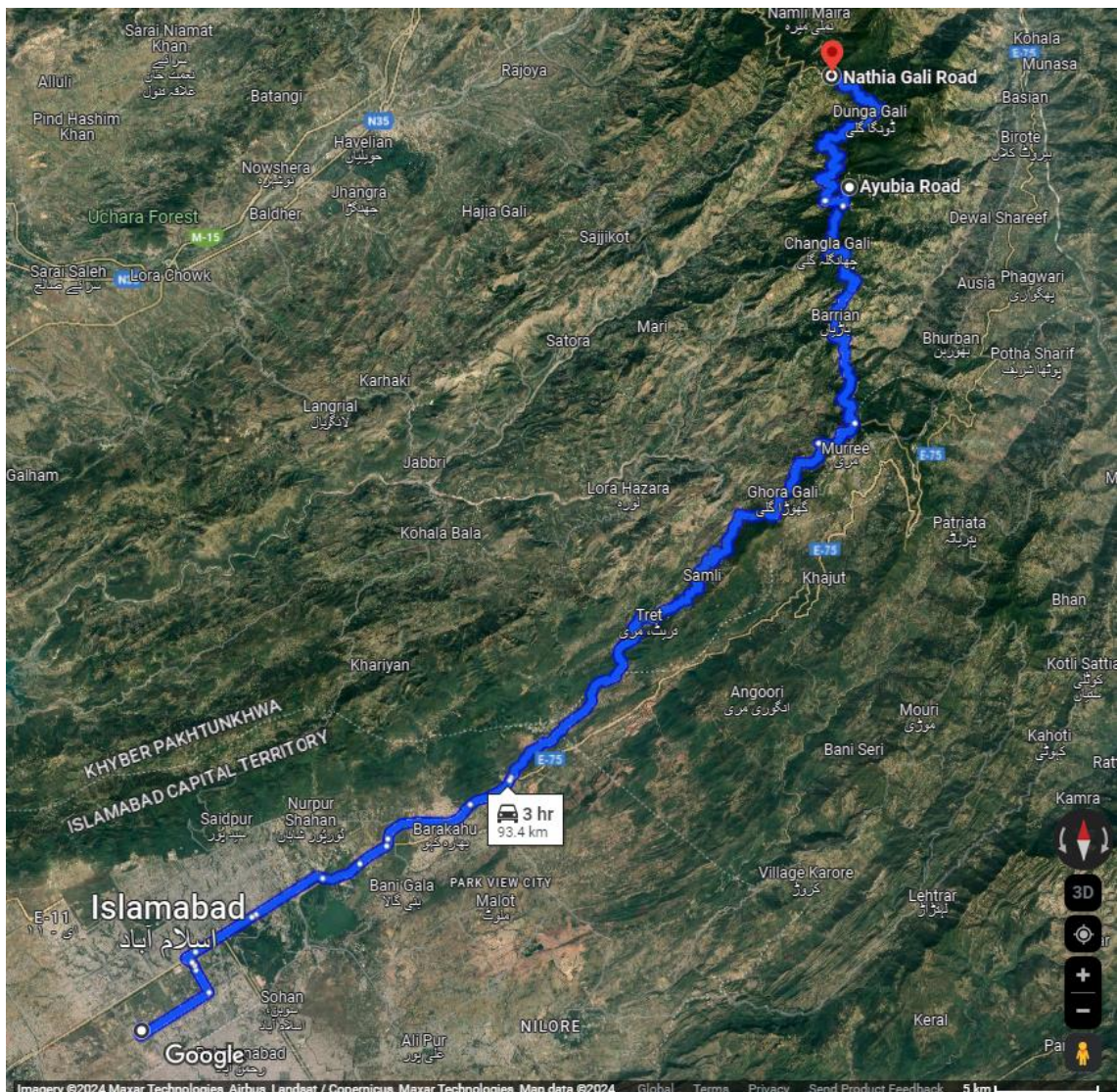


**Figure 1.2:** Location map of the study area, specifically Nathiagali and Ayubia, within the South Eastern Hazara Sub-Basin. (Source: Google Maps)

### **1.3 Purpose of study**

Despite their economic significance, the tectonically complex structural geology, dense vegetation, and limited accessibility of the Hazara sub-basin have hindered thorough exploration of its Eocene strata. Understanding the complete geological evolution of the Eocene strata in this region has been difficult due to these limitations. While there are numerous locations where the Margalla Hill Limestone outcrops are exposed, none of them reveal the entire formation. Prior studies have mostly concentrated on paleontological research, generic descriptions of different lithofacies qualities, and regional mapping utilizing small outcrop sections (Latif, 1970; Shah, 1977; Swati, 2013). The primary purpose of this study is to enhance the understanding of the geological evolution and reservoir potential of the Eocene strata in the tectonically complex Hazara sub-basin. This study will utilize diagenesis, microfacies, and biostratigraphic analysis to characterize the reservoir and provide new insights into the stratigraphy, depositional environments, and geological history of the Eocene strata in the Hazara sub-basin.

### **1.4 Aims and Objectives**

The objectives of this research are as follows:

1. Defining biostratigraphic zones and assessing their correlations with the physical stratigraphy of the study area.
2. Conducting a detailed investigation of stratigraphic, chronostratigraphic, and geological data derived from high-resolution biostratigraphic analysis, logging, and sequence stratigraphic analyses in the study area.
3. Determining and reconstructing the depositional environment.



These objectives aim to enhance understanding of the stratigraphic framework, depositional history, and environmental conditions of the study area, contributing to broader geological and paleontological knowledge.

## **1.5 Stratigraphic sections of the studied area**

### **1.5.1 Nathiagali Section**

This outcrop section is situated along the Nathiagali to Abbottabad Road, designated as [1] in (Figure 1.3), approximately 50 to 80 kilometers northeast of Islamabad, and around 2 kilometers from the major Nathiagali bazaar. The coordinates for the Nathia-Gali section are provided in (Table 1.1). This section comprises several Eocene formations, notably including the Chorgali and Kuldana formations. The Margala Hill Limestone rests above the Patala Formation and is overlain by the Chorgali Formation in this region. Lower and upper connections are both conformable. Samples were collected from the formation for petrographic and palaeontologic examination.

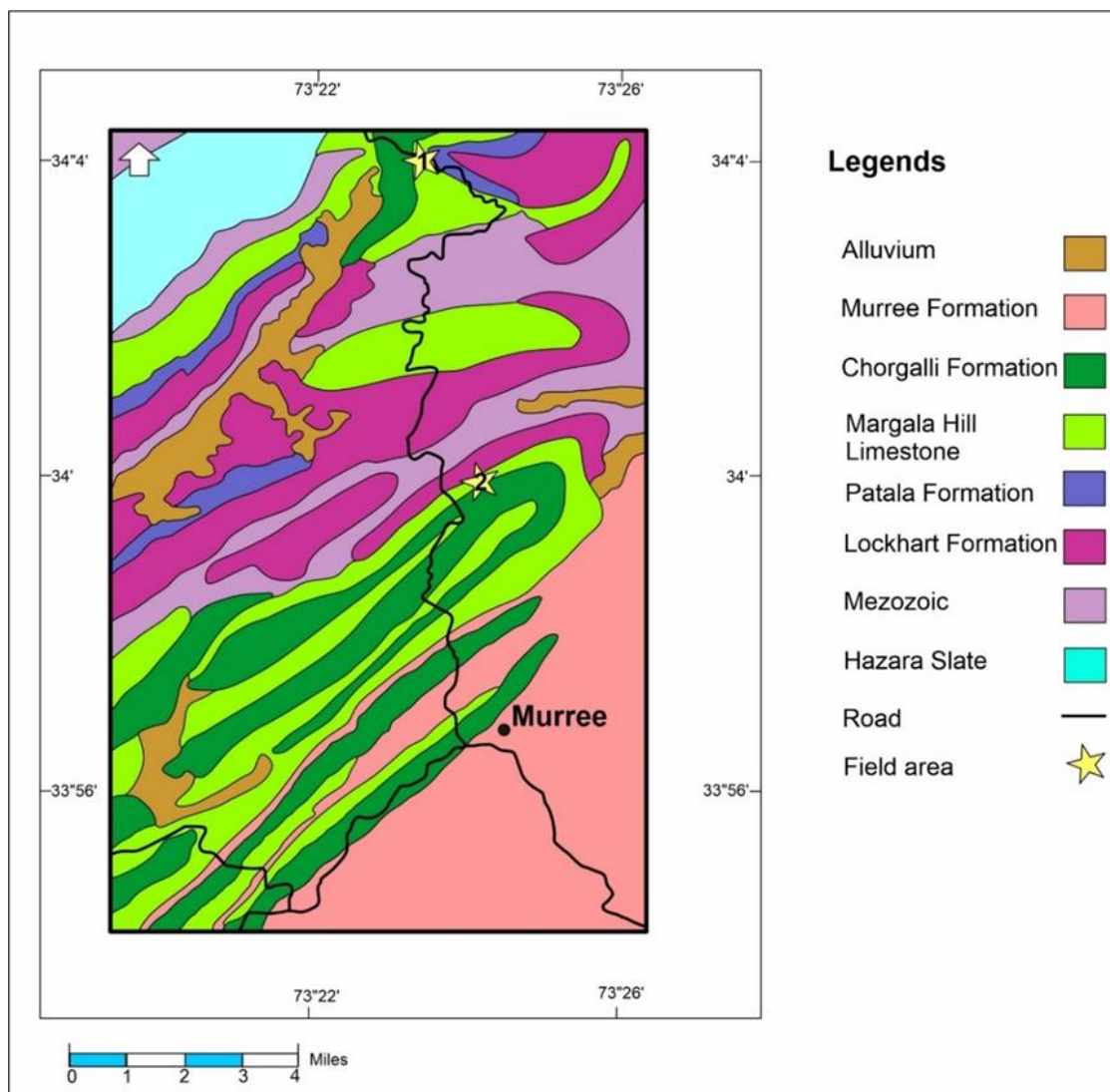


**Figure 1.3:** Geological map of South-Eastern Hazara, with the Nathiagali Section indicated as [1] and the Ayubia section indicated as [2] along the Murree-Nathiagali Road (modified from *Latif, 1970*).

**Table 1.1:** Coordinates of Ayubia and Nathia-Gali Section

Locality Number	Locality Name	Geographical Coordinates of the Study Area	
		Latitude N	Longitude E
1	Nathia-Gali Section	34°04'17" N	73°23'24" E
		34°04'19"N	73°23'21"E
2	Ayubia Section	34°01'34"N	73°23'49"E
		34°01'31"N	73°23'48"E

### 1.5.2 Ayubia Section

Exposed along the Murree-Nathiagali Road, the outcrop section illustrated in Figure 1.3 showcases preserved Eocene formations, including the Kuldana, Murree, and Chorgali formations. The coordinates for the Ayubia section are detailed in Table 1.1. The Margala Hill Limestone rests above the Patala Formation and is overlain by the Chorgali Formation in this region. Lower and upper connections are both conformable. Samples were collected from the formation for petrographic and palaeontologic examination.

### 1.6 Literature Review

A comprehensive understanding of the Margalla Hill Limestone and its geological context is achieved through the collective efforts of several authors. The Margalla Hill Limestone is characterized by interbedded shale and bioclastic limestone. It is conformably overlain by the Eocene Chorgali Formation and is underlain by the Paleocene Patala Formation in the Hazara sub-basin. In the second decade of the twentieth century, (Pinfold, 1918; Pascoe, 1920) conducted the earliest investigations into Paleogene strata in the Upper Indus Basin. Based on the examination of Eocene strata underlying the Margalla Hill Limestone (Latif, 1970) and Margalla-equivalent strata in

the Attock region of the northern Kohat sub-basin (Pascoe, 1920), a new nomenclature for Margalla-equivalent strata in the Hazara sub-basin was suggested. The formalization of the name "Margalla Hill Limestone" was later authorized by Pakistan's Stratigraphic Committee (Shah, 1977), a term utilized in this work.

The formation is divided into two sections and is primarily made up of shale and limestone that are interbedded (Shah, 1977). The lower part is made up of interbedded shale and thin to medium bedded, extremely fine crystalline dolomite, whereas the upper section of the lower part is composed of greenish-grey, calcareous shale. The upper part of the formation primarily consists of shale, featuring a nodular argillaceous limestone bed near the top and a thick, grey limestone deposit nearby (Shah, 1977). (Gill, W. D., 1953) suggested that the deposition of the Margalla Hill Limestone occurred in an open-shelf/ramp setting. The limestone has been reported to contain foraminifera, ostracods, and mollusks (Davies, 1937; Gill, 1953) with few miliolids, ostracods, and echinoid clasts observed at the type locality of the formation's dolomitic portion (Kazmi, 2008).

(Sameeni, 2013) conducted biostratigraphic studies in the northern Potwar subbasin (Kala Chitta Range), recognizing numerous bigger Benthic Foraminifera species, such as *Nummulites* sp. and *Alveolina* sp., and various microfacies through petrographic analyses. Consequently, the current study aims to investigate the diagenetic, depositional, and bio-sequence stratigraphic constraints on reservoir characterization of the early Eocene Margalla Hill Limestone in the Hazara sub-basin, NW Himalaya, Pakistan.

## Chapter 2

# REGIONAL GEOLOGY

### 2.1 Introduction

The Indo-Pakistan Plate colliding with the Eurasian Plate, which closed the eastern Neo-Tethys Ocean, was the most significant event of the Cenozoic Era (Bender, 1995). Approximately fifty million years ago, the Indian Plate initiated its collision with the Eurasian Plate (Beck, 1995). Subsequently, the Indian Plate underwent counterclockwise rotation until its eastern half collided with Eurasia. This collision event occurred diachronously from east to west, spanning from 55 Ma to 41 Ma (Scotese, 1988; Yoshida, 2018). The deformation front's southward migration within the Indian Plate resulted in the formation of significant geological structures such as the Main Central Thrust (MCT), Main Frontal Thrust, and Main Boundary Thrust (MBT). The Khairabad-Panjtal thrust, an extension of the MCT in western Pakistan, displaced Precambrian rocks over unmetamorphosed rocks within the Indian Plate approximately 20 million years ago (Treloar, 1992). Furthermore, according to (Treloar, 1992; Meigs, 1995), the MBT juxtaposes unmetamorphosed Jurassic rocks of the lesser Himalayan over Post Eocene molasse sediments of the Himalayan Foredeep, dating to approximately 13 to 10 million years ago.

The movement of the Indian plate northward commenced approximately 130 million years ago, leading to the narrowing of the Neo-Tethys due to intra-oceanic subduction in the north (Johnson, 1976). This process resulted in the formation of an island arc system in present-day Pakistan, including the Kohistan Island Arc. The Tethys Ocean in southern Eurasia transitioned into back-arc basins during the formation of this island arc system (Searle, 1991). Subsequently, a back-arc basin in North Pakistan collapsed following the collision of the Kohistan Island Arc with the Karakorum block (Eurasia) via a suture zone known as the Main Karakorum Thrust (MKT) (TahirKheli,

1979). (Coward, 1986) estimated this impact to have occurred between 102 and 75 million years ago.

The convergence of the Indian and Eurasian plates ensued after the consumption of the Tethyan oceanic crust beneath the Eurasian plate around 50 million years ago (Powell, 1979). This collision led to the Himalayan orogeny, with its intensity peaking in the early stages (Figure 2.1). The spectacular Himalayan Mountain belt, which is estimated to be 3500 km long and stretches from the northeastern boundary of India to the Afghan Block, was created as a result of the collision between the Indian and Eurasian plates (Shah, 1977; Yoshida, 2018). The NW-Himalayas Fold-Thrust belt is the name given to Pakistan's Himalayan Mountain range (Shah, 1977; Bender, 1995).

The collision between the Indo-Pakistan Plate and the Eurasian Plate resulted in the formation of towering mountain peaks composed of various materials, including sedimentary, metamorphic, and volcanic rocks. At the early stages, the Indian subcontinent collided at a speed of 18 cm/year (Chatterjee, 2013) (Figure 2.1).

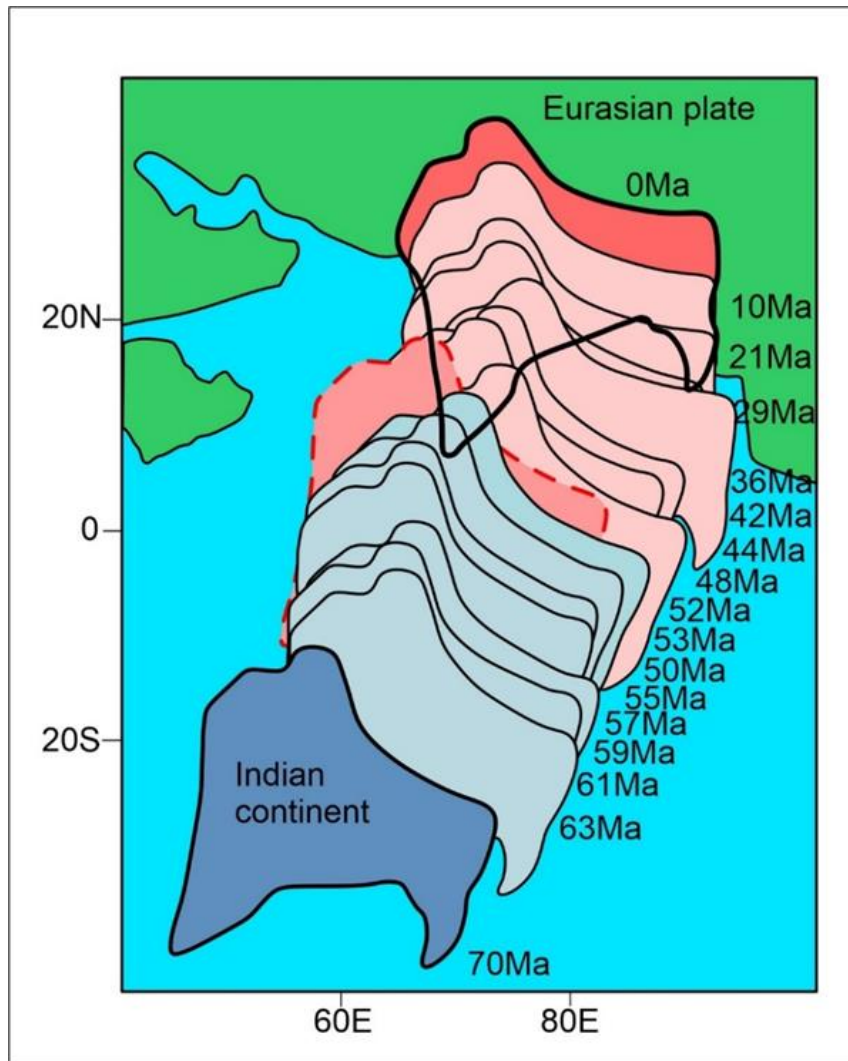


**Figure 2.1:** Representing the Northward movement of Indian plate (i.e. Indo- Eurasian plate collision) (*Patriat, 1984*).

## 2.2 Himalayas

The NW-Himalayas Fold-Thrust belt stretches from the border of Pakistan and Afghanistan to the northwest of India, measuring roughly 560 km in length and 250 km in length from south to north. The Lesser Himalayas (LH), Sub Himalayas (SH), and Higher Himalayas (HH) are its three tectono-morphologic sectors. Thrust faults - Salt Range Thrust (SRT), Main Boundary Thrust (MBT), Main Central Thrust (MCT), Main Mantle Thrust (MMT), and Main Karakoram Thrust (MKT) - impose constraints on these

sectors, arranged from south to north (Figure 2.2). The sedimentary rocks in the southernmost Sub Himalayas (SH) sector range in age from Precambrian to Recent. It is bordered to the north and south by the Main Boundary Thrust (MBT) and Salt Range Thrust (SRT), respectively. The Lesser Himalayas (LH) sector, situated between the Higher Himalayas (HH) to the south and the Sub Himalayas (SH) to the north, is bounded by the MBT to the south and the Main Central Thrust (MCT) to the north. It consists of metamorphic and sedimentary rocks dating from the Cambrian to the Miocene. The Main Mantle Thrust (MMT) forms its northern boundary, while the MCT forms its southern boundary. Its composition primarily comprises Precambrian to Cambrian igneous and metasedimentary rocks (Shah, 1977; Bender, 1995; Kazmi, 2008).

The Higher Himalayas (HH) lie to the north of the Kohistan Island Arc (KIA), with the Main Mantle Thrust (MMT) and Main Karakoram Thrust (MKT) defining its southern and northern boundaries, respectively. It constitutes an intra-oceanic island arc with a wedge-shaped configuration, positioned between the Indo-Pakistan Plate in south and the Karakoram Block (KB) in the north (Figure 2.2). Late Cretaceous-Paleocene igneous rocks make up the Main Karakoram Thrust (MKT), and the north and west portions of the Kohistan Island Arc (KIA). (Tahirkheli, 1982) states that the middle part of the arc is covered by the Kohistan Batholith sequence, which consists of diorite and gabbro from an earlier suite (110-85 Ma). Mafic and ultramafic rocks are densely packed in the southern arc. North of the MKT lies the Karakoram Block (KB), while Pakistan's western and northwestern regions encompass the Afghan and Turban Blocks. The Tibet Block's direction is north and northeast (Shah, 1977).



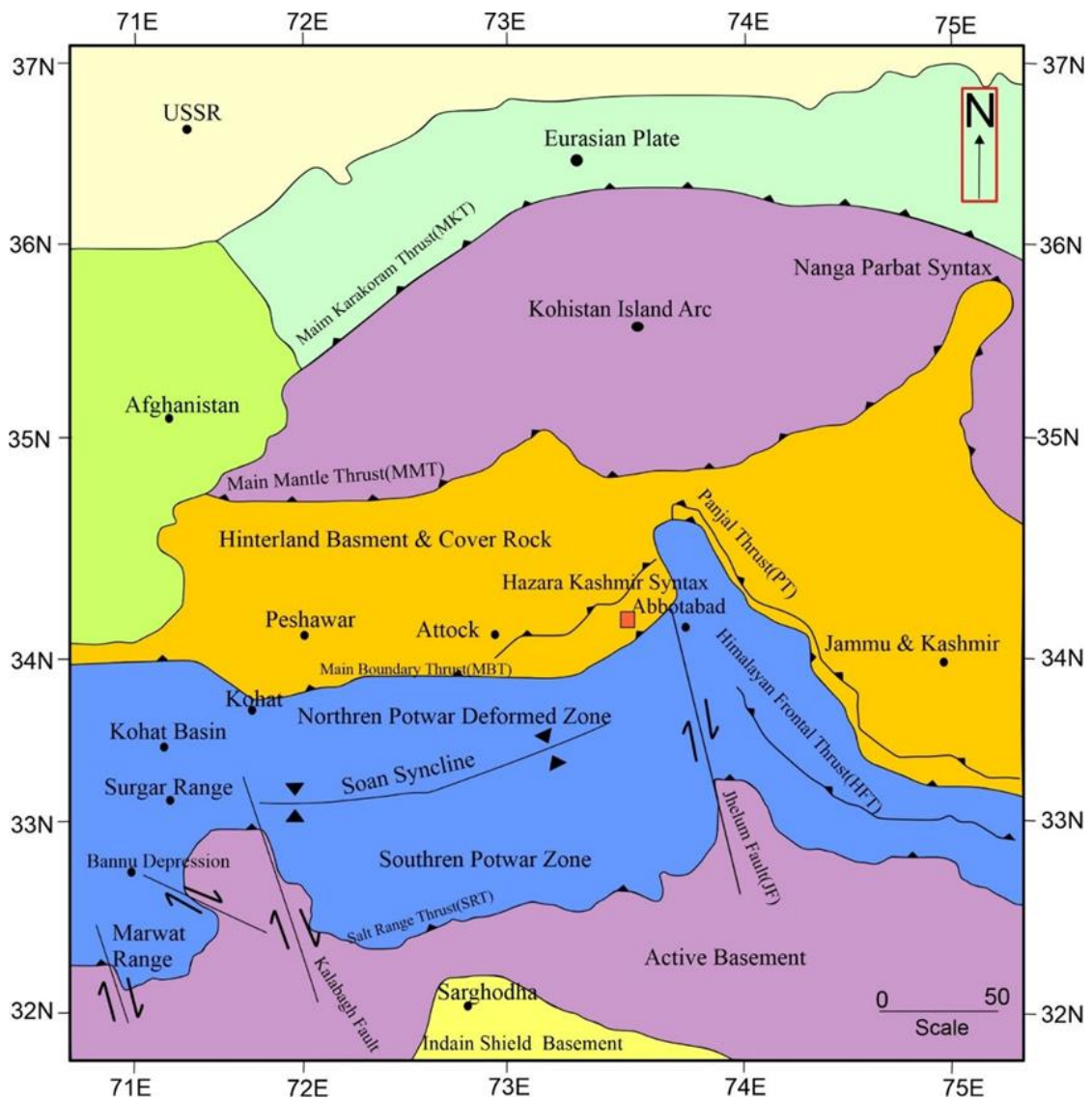


**Figure 2.2:** Regional tectonic map of Pakistan with the location of study area showing major thrust faults in northern Pakistan along with major sub-divisions of Himalayas, (SH: Sub-Himalayas, LH: Lesser Himalayas, and HH: Higher Himalayas), Kohistan Island Arc (KIA), and Karakoram Block (KB). The principal thrust faults that occur in the Upper Indus Basin include the Salt Range Thrust (SRT), the Main Boundary Thrust (MBT), the Main Central Thrust (MCT), the Main Mantle Thrust (MMT), and the Main Karakoram Thrust (MKT). The red box represents the study area in the Hazara sub-basins (modified after (Calkins, 1975; Baig, 2006)).

### **2.3 Local Geology of the Study Area**

The studied region in the Upper Indus Basin is severely deformed, and the structure and geology in the northern region of the basin are more complex than in the southern regions due to several tectonic activity stages. There are numerous thrust faults that arise as older rocks are layered on top of younger strata. The sedimentary strata in the area have moved as a result of numerous microscopic and mesoscopic folds and faults (Baker, 1988; Bender, 1995). The research site is located in the Hazara sub-basin of the Lesser Himalayas based on structural geology. Figure 2.3 depicts the Panjal and Murree faults (Calkins, 1975) along with their corresponding lateral counterparts that border the Attock-Hazara fold and thrust belt to the north and south, respectively. The two faults gradually merge close to Hassa, north of Garhi Habibullah, as they approach each other from the east and then the north. The megasynclinorium of the Attock-Hazara fold and thrust belt along the Murree-Abbottabad road is divided into at least two synclinoria, the larger Kuzagali synclinorial complex towards Murree and the smaller Nawashahr synclinorial complex towards Abbottabad, according to the geologic map of southeast Hazara (Latif, 1970). The MBT (Murree fault) limits the Kuzagali Synclinorial Complex in the south, while the Nathiagali fault, also known as the Hazardara fault, limits it in the northwest against the Hazara slates.

### **2.4 Stratigraphy of the Study Area**

On the Murree-Abbottabad road, the study area was confined to the Kuzagali synclinorial complex so, the Kuzagali synclinorial complex gets restricted in the north-west by the Nathiagali Fault against the hazara slate. However, rocks older than the Mesozoic are not exposed in the South-East. (Latif, 1970) suggested that the depositional axis of the basin was systematically migrating towards the south-east and south, as a result of Himalayan uplift. (Latif, 1970) provided a concise description of the stratigraphy of South-Eastern Hazara, accompanied by a geological map. He divided the lithostratigraphic units into seven groups separated by unconformities, and then further

subdivided them into 21 formations, correlating them with neighboring areas. He renamed the majority of the units to match the stratigraphic code.

The sedimentary sequence in the study area comprises of Samana Suk, Chichali, Lumshiwal, Kawagarh, Hangu, Lockhart, Patala, Margala Hill limestone, Chorgali, Kuldana and Murree Formations. The Margala Hill Limestone rests above the Patala Formation and is overlain by the Chorgali Formation in this region. Lower and upper connections are both conformable. The exposed stratigraphic successions in the study area are mentioned in (Figure 2.3).

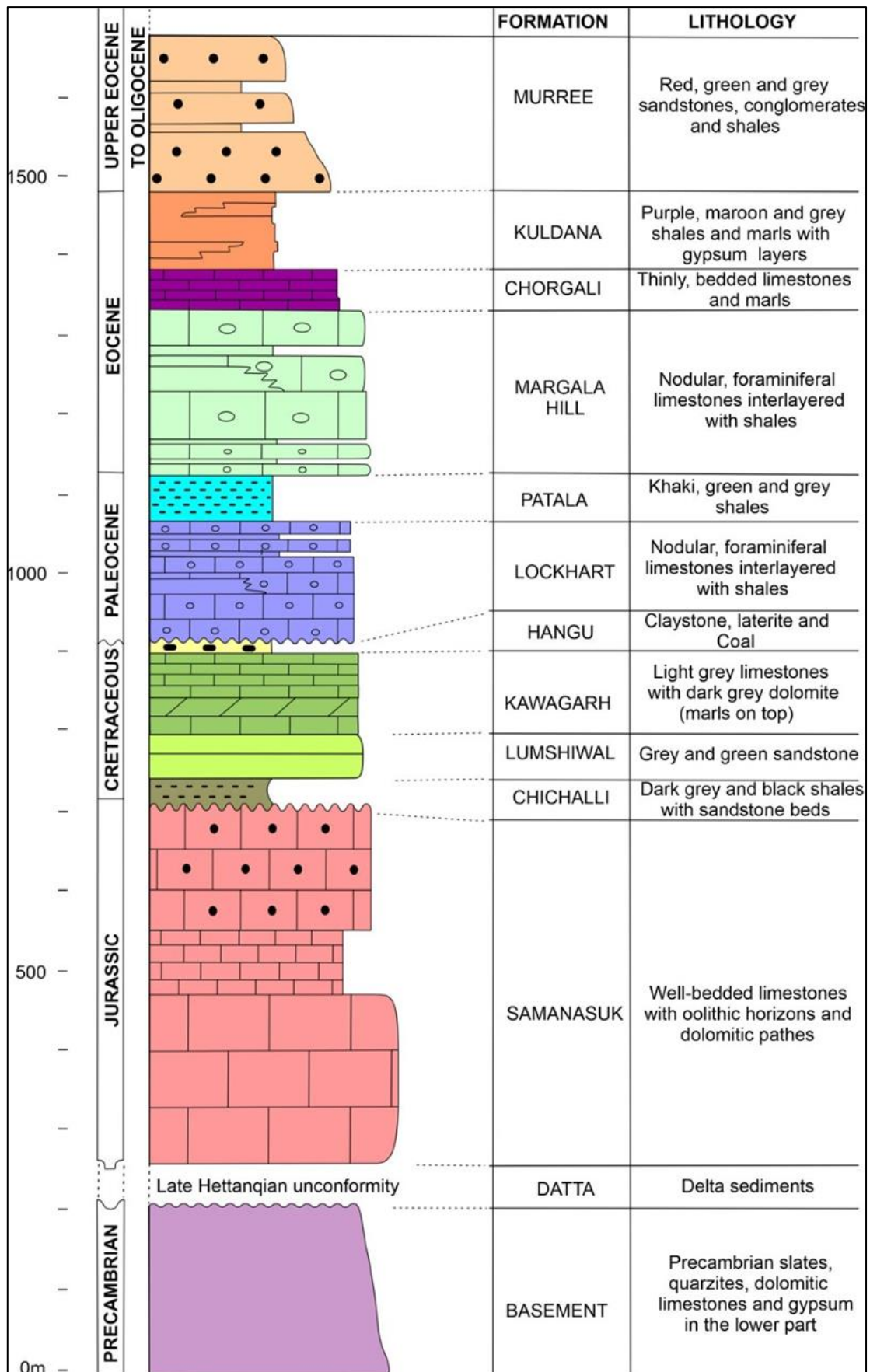


Figure 2.3: Stratigraphic column of Hazara-Sub Basin (Latif, 1970).

## Chapter 3

### FIELD OBSERVATIONS

#### 3.1 Field Work

A comprehensive geological fieldwork was undertaken to explore and analyze the Margalla Hill Limestone located in the southeastern Hazara sub-basins, particularly focusing on two sections: Nathiagali and Ayubia. These sections were strategically chosen based on their accessibility and the relatively minimal structural deformation they exhibit, making them ideal for detailed geological analysis. The primary objective of this fieldwork was to gather rock samples systematically and study the depositional environment, microfacies, and diagenetic processes of the Margalla Hill Limestone, with a special focus on the early Eocene period.

The fieldwork spanned two days, carried out under the supervision of an experienced geological supervisor. The process was meticulous, with significant emphasis on precise data collection and sampling. Two sections, the Nathiagali and Ayubia sections, were selected for the investigation based on accessibility and structural integrity. The geographic coordinates of these two sections, their location details, and the number of samples collected from each section are presented in (Table 1.1)

The field team, equipped with geological tools, including hammers, measuring tapes, and GPS devices, initiated the sampling process. A total of 76 rock samples were collected across both sections, with the sampling interval determined based on stratigraphic variation. Regular sampling intervals were maintained to ensure uniform data, but deviations were made in cases where distinct diagenetic features or notable variations in lithology were observed.

The thickness of the beds was measured using a measuring tape, which allowed for accurate stratigraphic correlation and documentation. The sections were logged from the bottom to the top, capturing changes in lithology, bed thickness, and diagenetic features. These observations provided valuable insights into the depositional sequence of the limestone and any structural deformations that may have occurred over time.

In both sections, specific attention was given to the collection of samples from areas exhibiting unusual diagenetic textures such as cementation and fossil preservation. This attention to detail ensured that the subsequent laboratory analysis would yield accurate data regarding the depositional environment and post-depositional alterations.

The rock samples were then transported to the Central Laboratory of Peshawar for further analysis. Thin sections were prepared from each sample to allow for petrographic examination. This process involved vacuum impregnation with blue epoxy to enhance the visibility of porosity and permeability features under the microscope. The prepared thin sections were then examined for detailed microfacies analysis, fossil content, and diagenetic features.

The microfacies analysis was based on the Dunham classification of limestones (Dunham, 1962) a widely accepted method for categorizing carbonate rocks. The samples were carefully examined to identify skeletal grains, non-skeletal grains, and cementation types. This allowed for a thorough interpretation of the depositional environment of the Margalla Hill Limestone. The study of fossils within the limestone provided additional evidence for dating the strata and contributed to the overall understanding of the sequence stratigraphy of the area.

The analysis of porosity and permeability, key factors in evaluating the reservoir potential of limestone formations, was also conducted using petrographic microscopy. Porosity types, including interparticle, intraparticle, and moldic porosity, were identified and measured, providing insights into the diagenetic history and potential fluid flow within the rock.

Several digital tools and software applications were employed to assist with the analysis and presentation of the field data. CorelDRAW was used to create detailed stratigraphic log charts, which helped visualize the geological sections from bottom to top. These log charts were essential for understanding the vertical distribution of the limestone beds, their thicknesses, and any variations in lithology or diagenesis observed in the field.

In addition to CorelDRAW, Google Earth Pro was utilized to access satellite imagery and geographic data for the field locations. This allowed the team to map the exact coordinates of the sampling sites and visualize the broader geological context of the study area. By overlaying field observations with satellite images, a more comprehensive understanding of the local tectonics and structural features could be achieved.

### **3.2 Nathiagali section**

Sampling was conducted in two sections, with the Nathiagali section being precisely sampled, yielding a total of 40 samples. These samples were collected at specific intervals, covering a total thickness of 54 meters. The section summarizes diverse lithostratigraphic sequences, each distinguished by unique characteristics. Figure 3.1a features alternating thick to thin bedding carbonate units, followed by Figure 3.1b, which illustrates the contact of these beds with nodular limestone. This plate provides a comprehensive overview of the stratigraphic variations within the examined geological section. In the Margalla Hill limestone, there is significant facies variation, as shown in Figure 3.2a. Additionally, various massive and nodular beds of bioclastic limestone have been observed (Figures 3.2 b-c).

Moreover, nummulitic beds in Margalla Hill limestone have been observed. Figure 3.3a showcases the co-occurrence of ostracods and calcite veins, while Figure 3.3b

presents a notable presence of abundant ostracods, accompanied by a few nummulites and indications of stylolite development. In Figure 3.3c, the dominance of calcite veins signifies a particular geological process. Finally, Figure 3.3d highlights the significance of ostracods, coexisting with prominently developed stylolite features, adding to the complexity of the sedimentary history.





**Figure 3.1:** Field Outcrop View of Nathiagali Section of the Study Area: (a) The outcrop shows a well-exposed sequence of thick to thin bedded limestone units, representing the main lithology of the section. (b) A closer view highlights the thick-bedded limestone with well-developed nodular limestone layers. The nodularity indicates localized diagenetic features within the thicker beds, reflecting subtle variations in sedimentary processes.



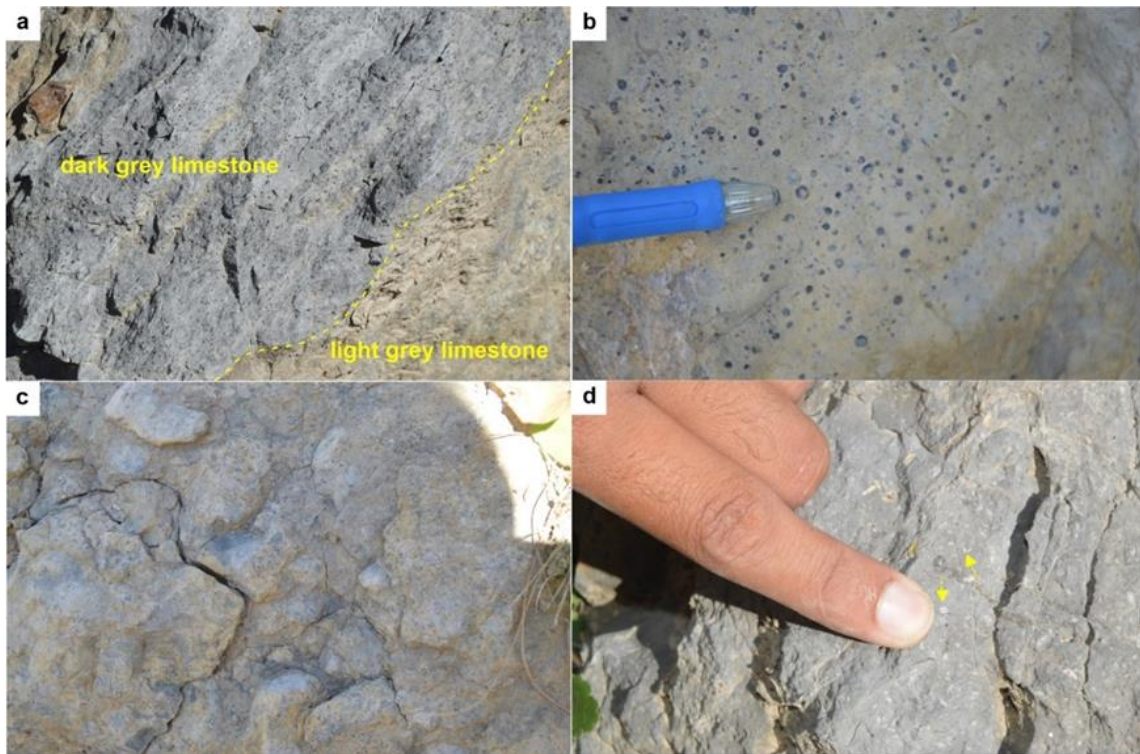


**Figure 3.2:** Field Photographs: (a) Contact between dark grey limestone and light grey limestone, representing a noticeable lithological boundary, (b) Bioclastic limestone, showing an accumulation of biogenic debris, (c) Nodular bioclastic limestone, displaying nodular texture within the bioclastic framework, (d) Nummulites indicated with arrows, highlighting the presence of large benthic foraminifera within the limestone matrix.

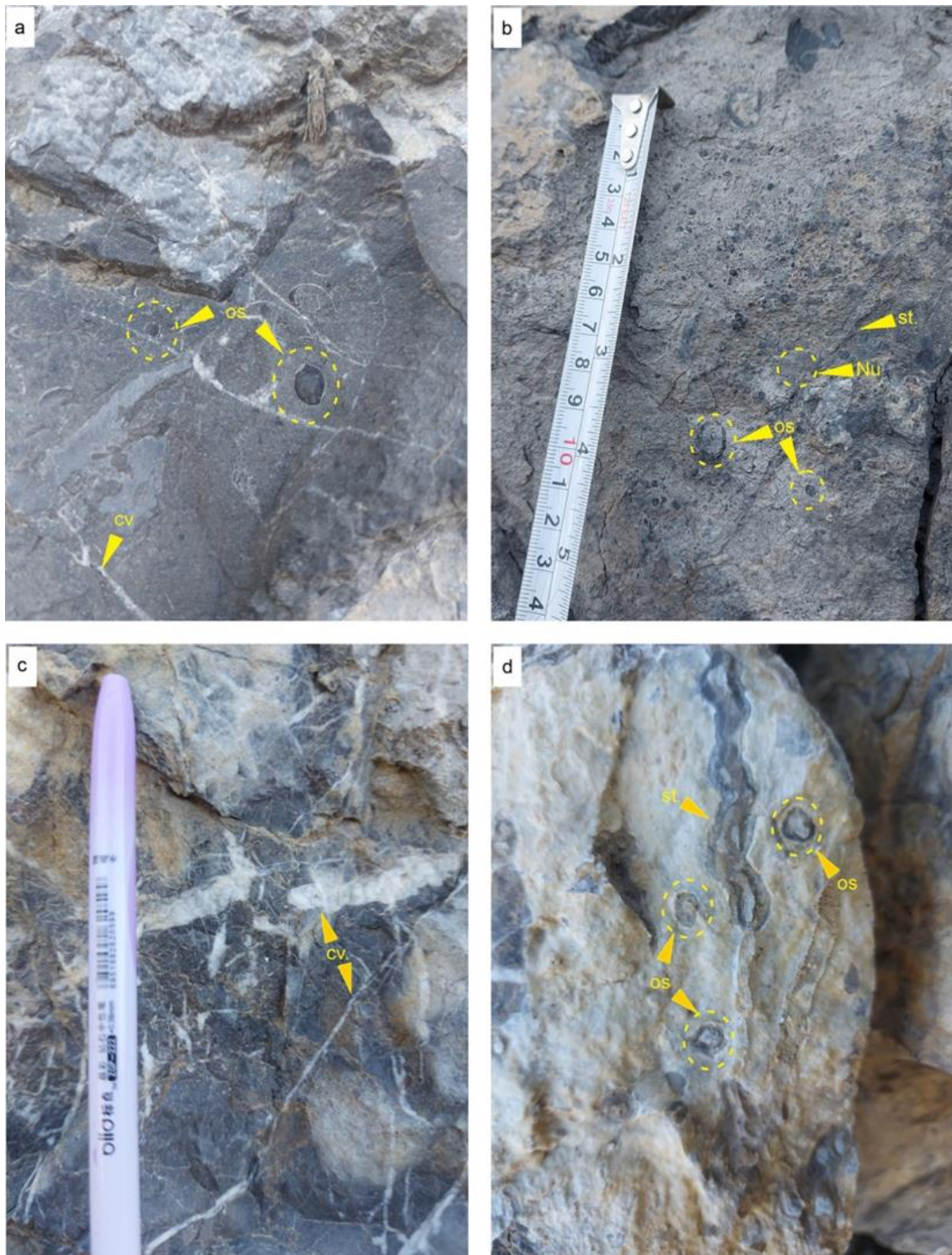


**Figure 3.3:** Field Outcrop Photographs of Nathiagali Section: (a-b) Outcrop showing several bioclasts of ostracods and nummulites, indicating fossil-rich limestone, (c) Multiple calcite veins cross-cutting each other, highlighting diagenetic processes, (d) Bioclasts of ostracods accompanied by stylolites, marking areas of pressure solution (os: Ostracods, st: Stylolites, cv: Calcite Veins, Nu: Nummulites).

### 3.3 Ayubia section

In the Ayubia section, a total of 36 samples were collected at specific intervals, covering total thickness of 60 meters. The lithological sequences within this section are distinguished by their characteristic features, such as thick-bedded nodular to massive limestone and brecciated to finely bedded nature. Figure 3.4a evidently exhibits an alternating sequence of bedding, characterized by a pronounced thick-thin massive stratification. This stratigraphic variation indicates fluctuating depositional regimes, possibly driven by dynamic environmental conditions. Figure 3.4b highlights nodular limestone beds, providing insight into sedimentary dynamics that could suggest changes in sediment supply, energy levels, or depositional settings, requiring careful consideration.

Figure 3.5a shows the occurrence of fossils, suggesting localized ecological conditions during deposition. Figure 3.5b presents a significant faunal group dominated by abundant Nummulites and Lockhartia, indicating a successful marine habitat and offering paleontological insights for further interpretation. Figure 3.5c deepens the subject matter by showing the dominance of Assilina, accompanied by benthic foraminifera bioclasts, revealing complex interactions within the microfaunal dominion. Figure 3.5d displays the cast of foram bioclasts, introducing a layer of complexity to the sedimentary sequences. Figure 3.6a shows brachiopod shells protruding in the bioclastic limestone beds, while Figure 3.6b reveals facies variations in beds. Figure 3.6c displays the contact between dark grey limestone and light grey limestone, and Figure 3.6d shows calcite veins in bioclastic limestone.





**Figure 3.4:** Field outcrop view of Ayubia section: (a) Thick to thin bedded limestone characteristic of the Margalla Hill Limestone formation, (b) Nodular limestone beds, displaying distinct nodularity within the stratigraphic sequence.



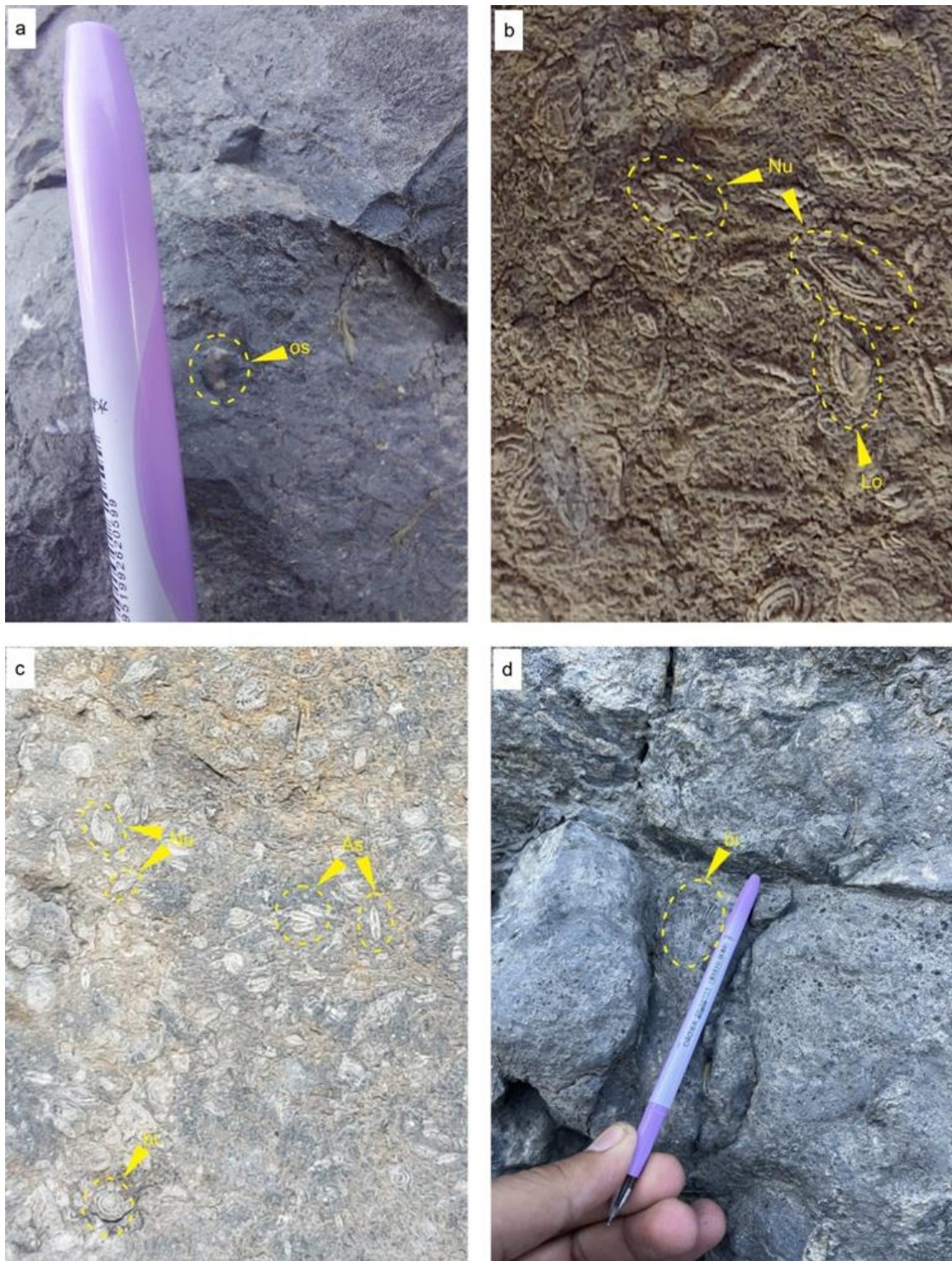


**Figure 3.5:** Field photographs of the Ayubia section: (a) Bioclasts of ostracods within a limestone bed, (b) Various foraminifera species, including nummulites and lockhartia, (c) Assilina and nummulites present in the Margalla Hill Limestone, (d) Bioclastic limestone beds, containing abundant bioclasts (os: ostracods, nu: nummulites, lo: lockhartia, as: assilina, bi: bioclast).

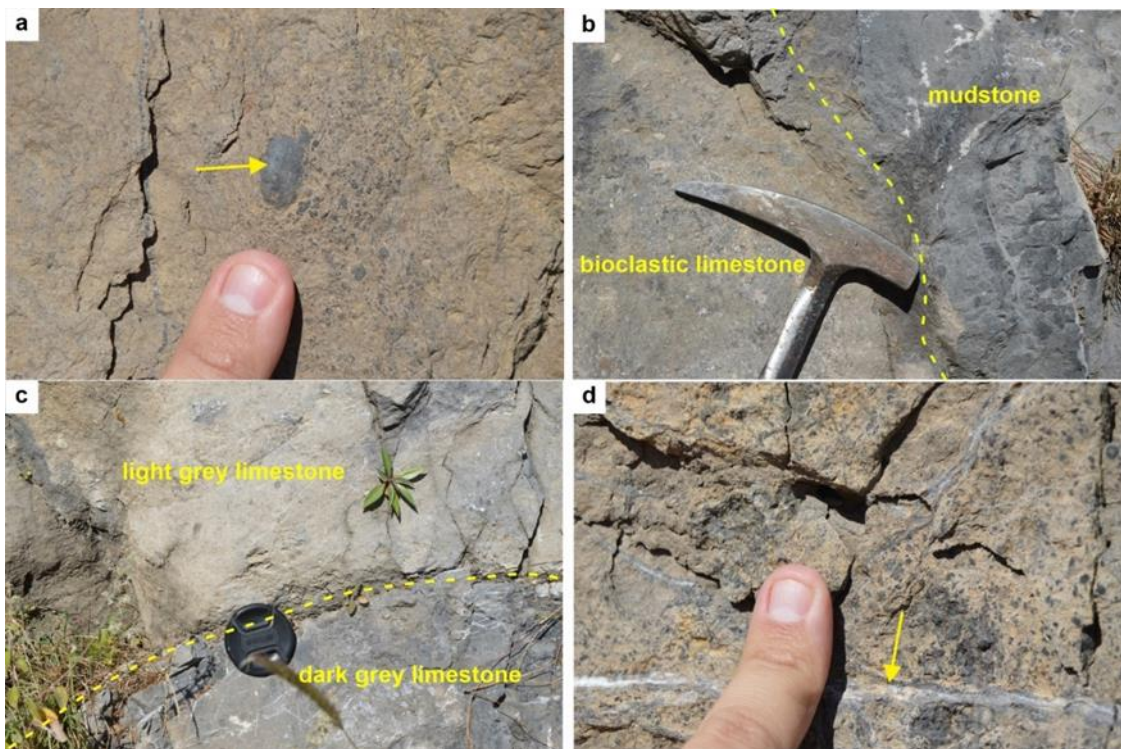


**Figure 3.6:** Field photographs of the Ayubia section in the study area: (a) Brachiopod indicated by an arrow within the Margalla Hill Limestone, (b) Facies variation, showing alternating bioclastic limestone and mudstone, (c) Contact between dark and light limestone, highlighting lithological contrast, (d) Calcite veins cross-cutting bioclastic limestone, illustrating post-depositional diagenetic features.

## **Chapter 4**

# **BIOSTRATIGRAPHY OF MARGALLA HILL LIMESTONE**

### **4.1 Introduction**

Larger Benthic Foraminiferas (LBF) and planktonic organisms are found in moderate to well-preserved abundance in the Eocene rocks of the research area. These fossils are essential for paleoenvironmental studies and biostratigraphic dating. Reported fossils include Alveolina, Assilina, Nummulites, Lockhartia, Discocyclina, corals, ostracods, and algae, as noted by various researchers (Hottinger, 1960; Cheema, 1968; Latif, 1970; Serra-Kiel, 1998; Ahmad, 2011; Afzal, 2011; Swati, 2013). This research project identified several significant LBF species. Planktons are exceedingly fine (silt-sized) and because of diagenetic changes, they are difficult to identify at the genus or species level. The Margalla Hill Limestone is known for its abundance of LBF fossils; more detailed information on these fossils is provided below.

### **4.2 Larger Benthic Foraminiferas (LBF)**

Foraminiferas exhibit a diverse range of sizes, shapes, and habitats, from deep-sea floors to shallow marine environments (BouDagher-Fadel, 2008). These marine protozoans possess small holes and shells that can be either linear or coiled. Foraminifera are categorized into two main groups: planktonic and benthic (BouDagher-Fadel, 2008). Benthic species live on the ocean floor, while planktonic species float in open marine environments near or at the water's surface. Planktonic foraminifera serve as significant index fossils due to their rapid evolutionary changes and widespread global distribution. Several biostratigraphic zonal approaches have been used to classify rocks from the Cenozoic Era that are located on the eastern shelf of the Neo-Tethys Ocean by (Hottinger,



1960; Schaub, 1981; Serra-Kiel, 1998). Index fossils, including Assilinids, Nummulitids, and Alveolinids, have been employed to distinguish between several Cenozoic Era epochs and phases. These biozones were further separated into shallow benthic zones (SBZ) by (Serra-Kiel, 1998). Several researchers have validated the validity of these biozones (Racey, 1994; Racey, 1995; Sameeni, 2013; Swati, 2013).

### **4.3 Current Study**

Two sections of the Margalla Hill Limestone in the Hazara sub-basin were selected for microfacies and biostratigraphic dating studies. Samples were collected and meticulously examined for this purpose. Fourteen species of limestone-forming foraminifera (LBFs) were identified and assigned to the Margalla Hill Limestone Biozone (MFBZ). The study indicates that, biostratigraphically, the Margalla Hill Limestone spans from SBZ9 to SBZ10. Researchers have compared the typical biozones identified by (Schaub, 1981) and (Serra-Kiel, 1998) with the Margalla Hill Limestone Biozone (MFBZ). The MFBZ corresponds to the SBZ 9 and SBZ 10 biozones as defined by (Serra-Kiel, 1998; Afzal, 2011; Ahmad, 2011; Sameeni, 2013). Additionally, it aligns with the *Assilina subspinosa*, *Assilina placentula*, *Assilina laminosa*, *Nummulites globulus*, *Nummulites atacicus*, and *Alveolina indicatrix* biozones described by (Schaub, 1981). This investigation indicates that the formation occurred between the Late Ilerdian (Shallow Benthic Zone - SBZ9, 53 Ma) and the Lower Cuisian (Shallow Benthic Zone - SBZ10, 51.5 Ma) during the early Eocene.

### **4.4 Description of the Species**

The following section provides information on the various species of Larger Benthic Foraminifera identified in the Margalla Hill Limestone.

#### 4.4.1 Genus *Assilina*

The genus *Assilina* is distinguished by its unique lenticular-planispiral morphology, which is a prominent characteristic that differentiates it from other genera. Some species within this genus display a central depression, resulting from the overlapping of chambers, and in certain instances, a proloculus can also be observed. The coiling within these species is particularly tight, contributing to their distinctive shape and structural integrity. These morphological features are not only crucial for species identification but also provide valuable insights into the evolutionary adaptations and ecological strategies of *Assilina*.

Species within the genus *Assilina* are of significant importance in biostratigraphy, serving as key indicators for dating geological formations. Their presence is often utilized to establish the relative ages of sedimentary layers, particularly in the context of the middle Eocene to the late Paleocene epochs, as noted by various studies (Hottinger, 1960; Schaub, 1981; Serra-Kiel, 1998; Ahmad, 2011; Sameeni, 2013). The detailed descriptions of the recognized species, along with photomicrographs, are provided to facilitate accurate identification and further research. These comprehensive records underscore the genus's relevance in paleoenvironmental reconstructions and stratigraphic correlations, emphasizing its role in advancing our understanding of historical geological and climatic conditions.

##### 4.4.1.1 *Assilina spinosa*

*Assilina spinosa* is distinguished by its distinct lenticular morphology, which features a centrally positioned depression. This unique depression causes the granules on the test surface to decrease in size as they approach the center, resulting in a gradual transition of granule size from the periphery towards the middle. The species exhibits

variability in test size, ranging from 0.2 to 2 mm. Furthermore, the proloculus of *Assilina spinosa* is notably developed, as highlighted in Plate 4.1 (a & b).

In terms of its geological distribution, *Assilina spinosa* is known to have a stratigraphic range from the lower Ilerdian (Shallow Benthic Zone - SBZ5) to the upper Ilerdian (Shallow Benthic Zone - SBZ9). This temporal range has been supported by various studies, including those by (Ahmad, 2011) and (Zhang Q. W., 2013), which have documented its occurrence within these specific stratigraphic intervals. The species' well-defined stratigraphic presence provides valuable insights into the paleoenvironmental conditions of the Ilerdian stage.

#### **4.4.1.2 Assilina Sub-Spinosa**

The subspecies *Assilina sub-spinosa* is distinguished by its shell morphology, which varies from flat to lenticular. The external surface of the test is notably marked by prominent, thick ridges that are closely spaced, providing a textured appearance. A majority of specimens exhibit sharply defined test edges, with a poorly developed proloculus. The walls of the shell are notably thick, contributing to its robust structure. The size of the test in this subspecies can range significantly, measuring between 0.3 and 3 mm in diameter (as illustrated in Plate 4.1: c & d).

The stratigraphic distribution of *Assilina Sub-Spinosa* spans from the middle Ilerdian (Shallow Benthic Zone - SBZ8) to the lower Cusian (Shallow Benthic Zone - SBZ10), indicating its presence in sedimentary deposits from this geological timeframe. This temporal range has been substantiated by several studies, including those conducted by (Ahmad, 2011; Sameeni, 2013; Zhang Q. W., 2013). These findings highlight the significance of *Assilina Sub-Spinosa* in understanding the paleoenvironmental conditions and biostratigraphic frameworks of the regions where it is found.

#### 4.4.1.3 *Assilina Laminosa*

The species *Assilina laminosa* is characterized by a distinct lenticular shape with sharp, well-defined edges and notably thick walls. The proloculus, which is the initial chamber in the foraminiferal shell, is often either underdeveloped or entirely absent in some specimens. Additionally, many examples of this species lack internal pillars, contributing to its unique structural formation. The external surface of *Assilina laminosa* is predominantly smooth, featuring only minimal granulation, which differentiates it from other closely related species. The overall size of this species varies significantly, ranging from as small as 0.2 mm to as large as 2 mm (Plate 4.1: e, f).

Stratigraphically, *Assilina laminosa* has been identified across a range extending from the middle Ilerdian (Shallow Benthic Zone - SBZ8) to the lower Cusian (Shallow Benthic Zone - SBZ10). This age span indicates that the species existed during a specific interval within the Paleogene period, corresponding to well-defined epochs of the early Eocene. The presence of this species in various stratigraphic layers has been well-documented in the literature, with significant references provided by (Ahmad, 2011; Sameeni, 2013; Zhang Q. W., 2013). These studies contribute valuable insights into the paleoenvironmental conditions and biostratigraphic frameworks of the time, highlighting the significance of *Assilina laminosa* in the broader context of geological and paleontological research.

#### 4.4.1.4 *Assilina granulosa*

*Assilina granulosa* is a subspecies distinguished by its unique flat, elongated morphology, which features sharp, well-defined edges. The external surface of its test is characterized by a pattern of distributed ridges and granules, providing a textured appearance that is distinctive to this subspecies. Notably, the proloculus, or the initial chamber of the test, is not visible in this subspecies. The size of the test varies

considerably, ranging from 0.2 mm to 4 mm, as illustrated in Plate 4.1 (g, h, & i). These morphological characteristics play a significant role in the identification and classification of *Assilina granulosa* within its genus.

The temporal range of *Assilina granulosa* spans from the lower Ilerdian (Shallow Benthic Zone - SBZ5) to the upper Cusian (Shallow Benthic Zone - SBZ11), indicating its presence in the geological record during these specific stratigraphic zones. This time frame suggests that the subspecies existed from the early to the middle Eocene, providing valuable insight into the paleoenvironmental conditions of that era. The work of (Ahmad, 2011) has been instrumental in documenting the stratigraphic occurrence and morphological features of *Assilina granulosa*, contributing significantly to the understanding of its evolutionary history and paleogeographic distribution.

#### **4.4.1.5 *Assilina Placentula***

*Assilina placentula* is a subspecies distinguished by its thick, lenticular-shaped walls, which exhibit smooth and well-defined edges. A notable characteristic of this subspecies is the variability in the visibility and development of the proloculus; in some specimens, the proloculus is either poorly developed or not visible at all. The external surface of *Assilina placentula* is predominantly smooth, with minimal granulation. The size of this subspecies can vary significantly, typically ranging from 1 to 5 mm, as observed in specimens illustrated in Plate 4.1 (j & k).

The stratigraphic distribution of *Assilina placentula* is quite specific, extending from the lower Ilerdian (Shallow Benthic Zone - SBZ5) to the late middle Ilerdian (Shallow Benthic Zone - SBZ9). This indicates a presence during a distinct interval in the Paleogene period, reflecting both the subspecies' evolutionary adaptations and environmental conditions of that era. Studies by (Ahmad, 2011) and (Zhang Q. W., 2013) have provided valuable insights into its age and stratigraphic significance, contributing to a more comprehensive understanding of its paleobiological and geological context.

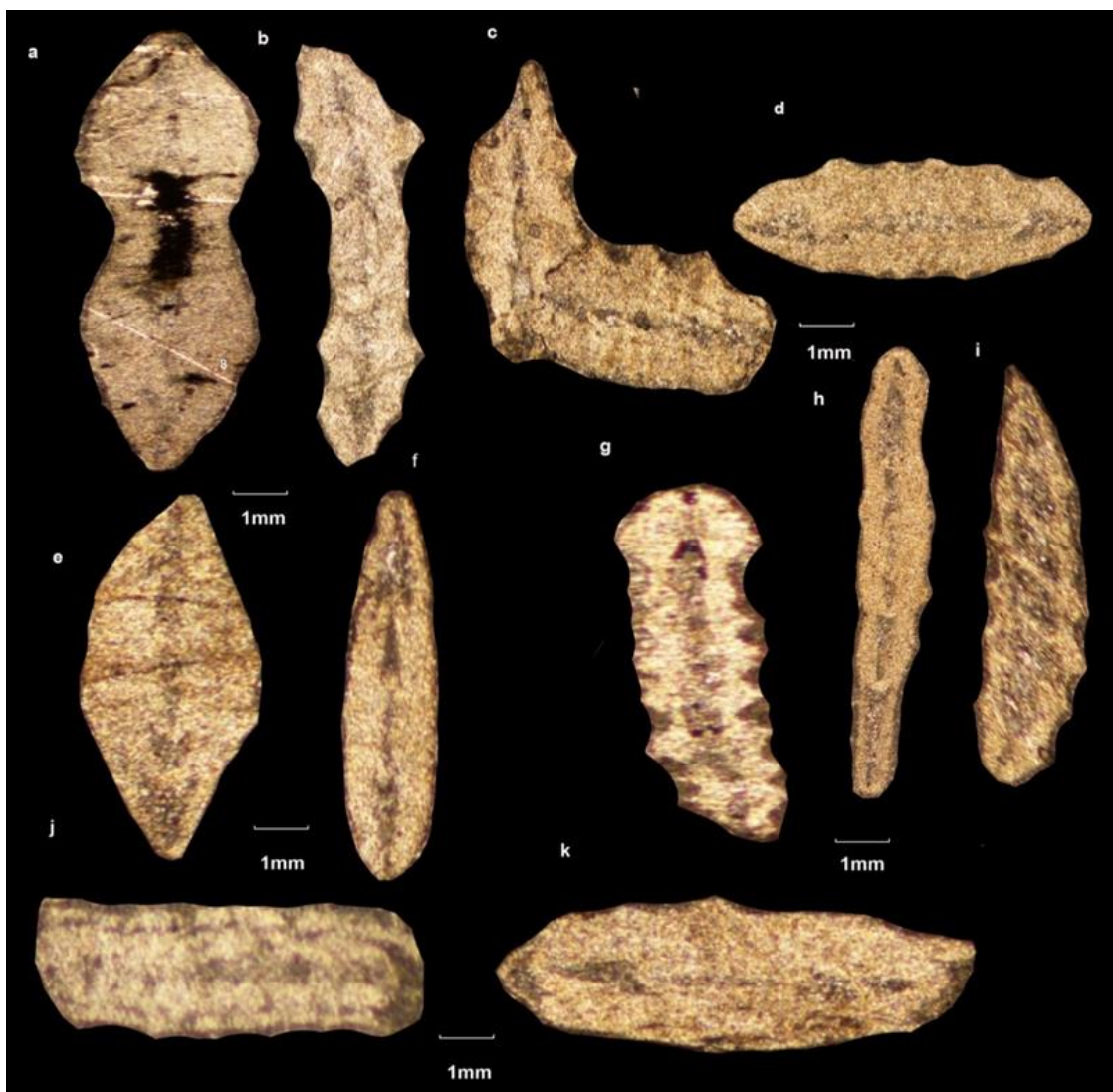


**Plate 4.1:** The above plate depicts various species of the genus *Assilina*: a) & b) show *Assilina Spinosa*, c) & d) show *Assilina sub-spinosa*, e) & f) show *Assilina Laminosa*, g), h), & i) depict *Assilina Granulosa*, and j) & k) show *Assilina Placentula*.

#### 4.4.2 Genus *Nummulites*

The genus *Nummulites* is characterized by its distinctive shell morphology, which ranges from lenticular to globular in shape. The coiling of these shells is initially tightly wound in the early whorls, transitioning to a looser configuration as the whorls move

outward from the center. This coiling is segmented into multiple compartments by septa, contributing to the complex structure of the shell. The size of the test, or shell, varies significantly within this genus, ranging from as small as 1 mm to as large as 7 mm, reflecting a broad morphological diversity.

Extensive research has been conducted on the genus *Nummulites*, with findings suggesting that these organisms existed from the early Eocene to the early Oligocene. Earlier studies by (Hottinger, 1960; Schaub, 1981; Serra-Kiel, 1998; Ahmad, 2011; Sameeni, 2013; Ghazi, 2014) have documented the temporal range of these foraminifera, highlighting their evolutionary significance and biostratigraphic importance. The widespread presence of *Nummulites* during this period provides crucial insights into the paleoenvironmental conditions and geological history of the early Tertiary period.

#### 4.4.2.1 Nummulite *Aticacus*

*Nummulite Aticacus* is distinguished by its lenticular shape and notably thin test walls, setting it apart from other species within the *Nummulites* genus. The test's central region features well-established umbilical pillars, while the proloculus is relatively small in size. This species typically reaches a shell diameter of up to 7 mm. The coiling pattern of *Nummulite Aticacus* is characterized by tightly wound coils near the proloculus, which gradually become more loosely coiled further from the center. These morphological traits are illustrated in Plate 4.2 (a & b), which provide a visual representation of the coiling pattern.

Ecologically, *Nummulite Aticacus* is found within the middle Ilerdian (Shallow Benthic Zone - SBZ8) biozone, as noted by (Ahmad, 2011; Sameeni, 2013; Zhang Q. W., 2013). Its presence in this specific biozone highlights its relevance to the biostratigraphy and paleoenvironmental conditions of the time. The detailed structural features and the ecological context of *Nummulite Aticacus* contribute to its significance in the study of foraminiferal taxa and their evolutionary history.

#### 4.4.2.2 Nummulite Mamilatus

The *Nummulite mamilatus* subspecies is characterized by its robust, thick walls and a distinct globular to lenticular shell morphology. Central to its structure is a notable radial proloculus, which is prominently positioned at the core of the shell. Notably, the development of the pillars is still in its nascent stage, with their formation incomplete. The coiling of the shell exhibits a marked contrast: it is tightly wound around the proloculus and progressively becomes more loosely coiled as it extends away from this central region. The maximum size of this test can reach up to 3 mm, as illustrated in Plate 4.2 (c & d).

This subspecies is found in sedimentary strata ranging from the middle Ilerdian (Shallow Benthic Zone - SBZ8) through to the upper Cusian (Shallow Benthic Zone - SBZ10). Its presence in these geological periods provides valuable insights into the evolutionary and environmental conditions of the time. The observed morphological characteristics, including the unique coiling pattern and initial pillar formation, contribute to the understanding of the subspecies' adaptation and development within its historical context.

#### 4.4.2.3 Nummulite Globulus

This subspecies *Nummulite Globulus* is characterized by its distinct morphological features, including chambers that are thick and exhibit a biconvex to spherical shape. One of the notable characteristics of this subspecies is the presence of relatively weak pillars situated at the center of the test, providing structural support but with less prominence compared to other subspecies. The initial chamber, known as the proloculus, is relatively small in size when compared to the overall dimensions of the



shell. This feature contributes to the compactness of the subspecies, which can reach a maximum size of up to 4 mm in diameter, as evidenced by fossil samples in Plate 4.2 (e & f).

*Nummulite globulus* species have been identified predominantly within the intermediate Ilerdian (Shallow Benthic Zone - SBZ8) age zone, suggesting a specific geological and chronological distribution. This stratigraphic range highlights their prevalence during this particular time period, contributing valuable information to paleontological and stratigraphic studies. The presence of these species in this age zone has been well-documented in various studies, including those by (Ahmad, 2011; Sameeni, 2013), which underscore the importance of *Nummulite globulus* in understanding the paleoenvironmental conditions of the time.

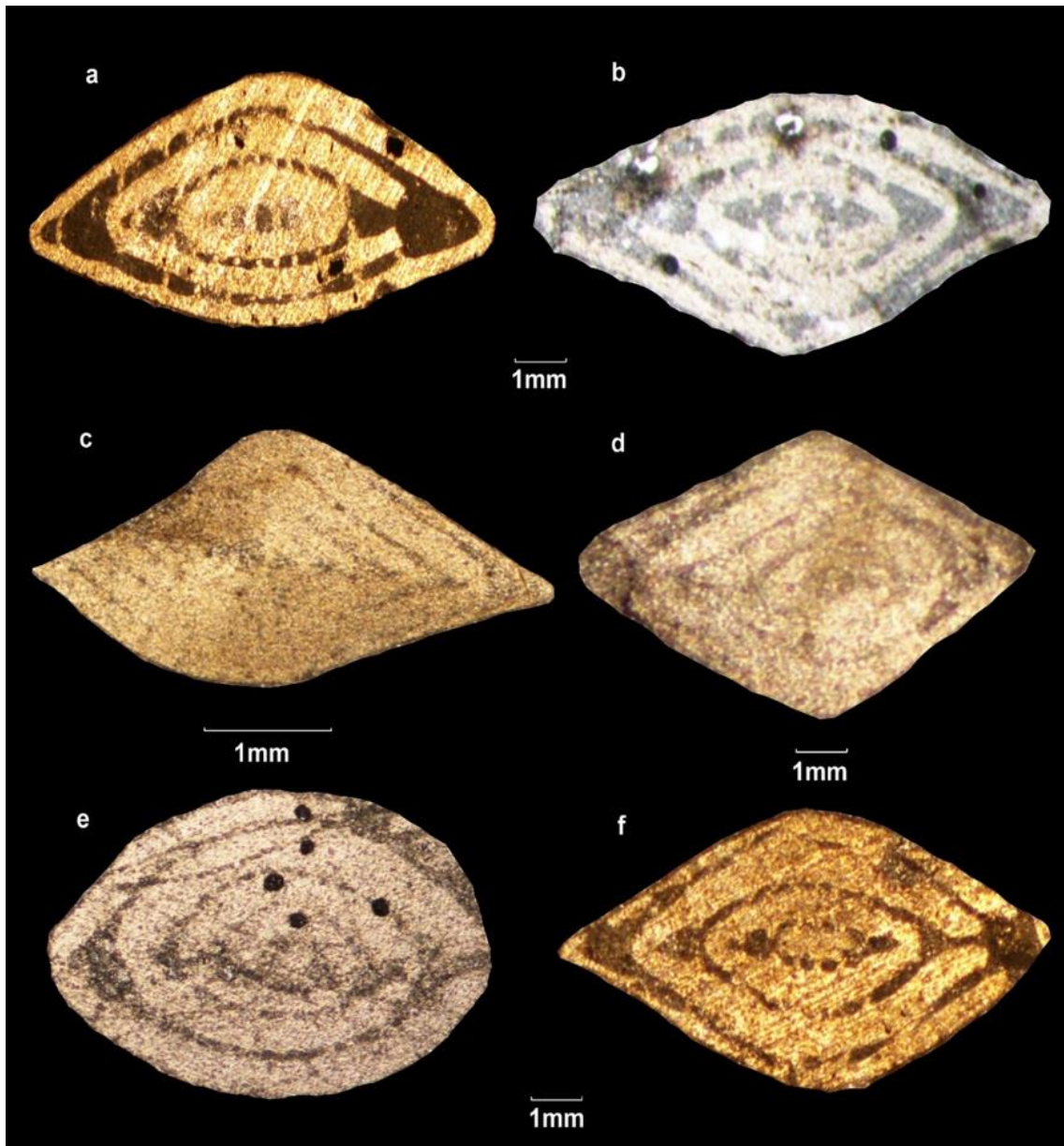


**Plate 4.2:** The above chart depicts various Species of *Nummulites*. a) & b) Shows *Nummulite Aticacus* c) & d) *Nummulite Mamilatus* e) & f) *Nummulite Globulus*

#### 4.4.3 Genus *Lockhartia*

The genus *Lockhartia* is distinguished by its distinctive morphology, characterized by its planispiral to trochospiral coiling and the presence of well-developed, thick pillars within the central region of the test. The shells of *Lockhartia* species exhibit

variations in size, generally ranging from 2 mm to 4 mm, with some species displaying a convex profile and rounded edges. The umbilical region of certain species is filled with pillars, adding to the structural complexity of the test. These morphological features are essential for species identification and provide valuable insights into the genus's evolutionary adaptations and ecological niches. *Lockhartia* species are significant in biostratigraphy, particularly within the Thanetian to Ilerdian stratigraphic ranges, where they serve as key indicators for dating sedimentary formations and understanding the paleoenvironmental conditions of the Paleocene to early Eocene epochs (Ahmad, 2011; Zhang Q. W., 2013).

#### 4.4.3.1 *Lockhartia Conditti*

*Lockhartia conditti* is a notable subspecies within the genus *Lockhartia*, distinguished by its well-developed and robust central pillars within the test. These structural characteristics are prominent features that aid in the identification and differentiation of the species. *L. conditti* is predominantly found in the lower and middle strata of the Margalla Hill Limestone, a geological formation known for its rich fossil content. The shell of this species can attain a size of up to 3 mm, as evidenced in specimens documented in Plate 4.3 (a).

The stratigraphic distribution of *Lockhartia conditti* is broad, encompassing a significant temporal range. It is observed from the lower Thanetian stage, corresponding to the Shallow Benthic Zone 2 (SBZ2), to the late middle Ilerdian stage, associated with Shallow Benthic Zone 9 (SBZ9). This range indicates its persistence through a considerable portion of the Paleocene and early Eocene epochs, highlighting its adaptability to changing environmental conditions during this period (Ahmad, 2011; Zhang Q. W., 2013).

#### 4.4.3.2 *Lockhartia Tippri*

The subspecies *Lockhartia tippri* is characterized by its distinctively low trochospiral shell structure, which exhibits a fairly convex profile with rounded edges. Notably, the umbilicus of this subspecies is uniquely filled with pillars, adding to its identifiable morphology. This subspecies achieves a maximum size of approximately 3.5 mm, as illustrated in Plate 4.3b. The geological distribution of *Lockhartia tippri* extends from the late Paleocene to the early Eocene epoch, reflecting its significant presence during this time period.

The stratigraphic range of *Lockhartia tippri* is well-documented, spanning from the upper Thanetian (Shallow Benthic Zone - SBZ4) to the late middle Ilerdian (Shallow Benthic Zone - SBZ9). This extensive range provides valuable insights into the evolutionary timeline and environmental conditions of the species. Key references detailing this subspecies include (Ahmad, 2011; Zhang Q. W., 2013), which contribute to our understanding of its paleontological and geological context.

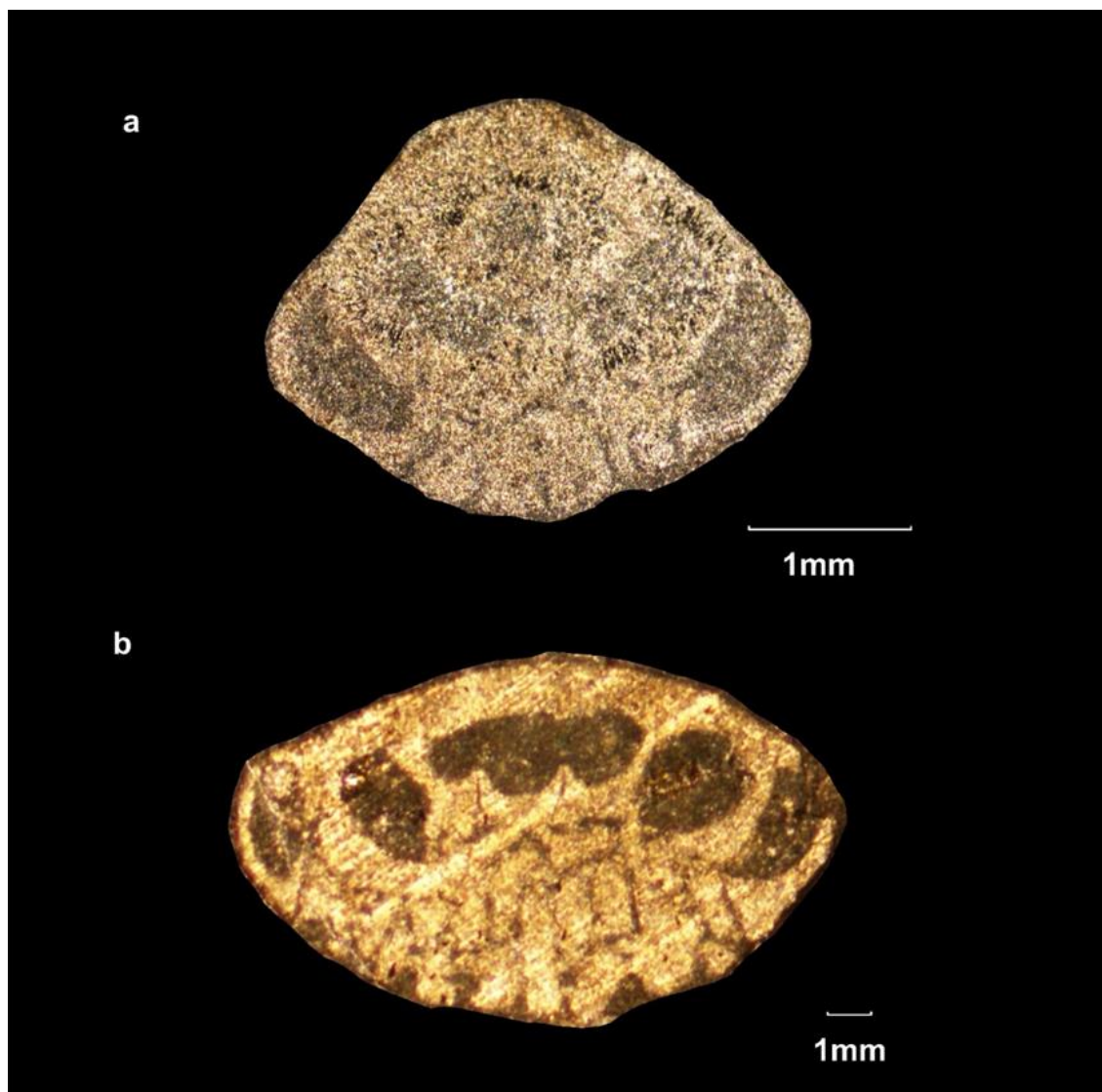


**Plate 4.3:** The above Plate depicts Various Species of Genus *Lockhartia*. a) *Lockhartia Conditti* b) *Lockhartia Tippri*.

#### 4.4.4 Genus *Alveolina*

The genus *Alveolina* is characterized by its distinctive spiral coiling and highly ornamented test structure. The shells of *Alveolina* species typically exhibit a coiling pattern that ranges from tight in early whorls to more loosely arranged in later stages, with a pronounced, spherical to globular shape. The test is often divided into multiple chambers by numerous septa, with varying degrees of thickening and ornamentation. These features, including the presence of internal pillars and the intricate arrangement of chamberlets, are crucial for identifying species within this genus. *Alveolina* species are

important for biostratigraphic studies, particularly in the Late Paleocene to early Eocene epochs, as they provide valuable information on the relative ages of sedimentary layers and insights into paleoenvironmental conditions (Hottinger, 1960; Ahmad, 2011; Sameeni, 2013).

#### **4.4.4.1 *Alveolina Indicatrix***

The subspecies *Alveolina indicatrix*, prevalent in the Margalla Hill Limestone, is characterized by its spherical to globular shell morphology, which notably lacks distinct pillars. The proloculus, or the initial chamber, is considerably reduced in size and may be obscured under certain observational conditions. In the early stages of development, the shell exhibits tightly coiled whorls, but as the organism matures, these coils become more spaced apart and begin to diverge from one another. The size of the chambers within the shell varies according to the specific species, with the overall dimensions of the test reaching up to 2 mm, as illustrated in Plate 4.4 (a & b).

Geological studies have dated this subspecies to the Late Ilerdian (Shallow Benthic Zone - SBZ9) through to the Lower Cuisian (Shallow Benthic Zone - SBZ10) periods, as documented in the works of (Hottinger, 1960; Ahmad, 2011; Sameeni, 2013). The stratigraphic context of *Alveolina indicatrix* provides valuable insight into the temporal distribution of this species, offering a means to better understand the evolutionary and environmental conditions of its time.

#### **4.4.4.2 *Alveolina* sp., Drobne 1977**

The test *Alveolina* sp., Drobne 1977, is distinguished by its medium-sized, sub-spherical morphology. Initially, the test features a spherical proloculus with a diameter ranging between 150 and 180  $\mu\text{m}$ , which is followed by two to three tightly coiled spherical nepionic whorls. In its adult stage, the test evolves to include three to four

additional whorls that exhibit significant flosculinization, leading to a considerable thickening of the test both axially and equatorially. However, during the senile stage, the test undergoes a reduction in axial and equatorial thickening, with the basal layer becoming less pronounced over the course of five to seven tightly coiled whorls at the periphery. The inner chamberlets of the whorls are small and spherical, whereas those in the outer whorls are comparatively larger and elongated (Rahman et al., 2021).

Stratigraphically, *Alveolina* sp. is documented within the time range from SBZ7 to SBZ9, as noted by (Zhang Q. W., 2013). This stratigraphic distribution provides valuable insights into the temporal presence and evolutionary progression of the species, reflecting its adaptability and morphological changes throughout its life cycle. The detailed description of the test structure and its variations at different developmental stages contribute to a comprehensive understanding of the species' taxonomy and its paleobiological significance.



**Plate 4.4:** The above Chart depicts various Species of Genus Alveolina. a) & b) Shows Cross Sectional view of Alveolina Indicatix c) Alveolina sp cross cutted by numerous calcite veins.

#### 4.4.5 Genus Discocyclina

Three *Discocyclina* species have been identified in the Margalla Hill Limestone. Here is a description of these species: *Discocyclina* has a flat and discoidal test characterized by numerous tiny chambers. Some species exhibit a bulge in the middle, where the core bulge is surrounded by slender flanks. According to sources (Hottinger,



1960; Schaub, 1981; Serra-Kiel, 1998), *Discocyclusina* species have a geologic range extending from the Middle Paleocene to the Late Eocene.

#### 4.4.5.1 *Discocyclusina* *Dispensa*

*Discocyclusina dispensa* is a species distinguished by its distinctive test morphology, which is spherical and biconvex, with a pronounced globular central region (see Plate 4.5 a). Extending outward from this central core are flat, thin, discoidal flanks that define the overall shape of the test. Many observed specimens display fractured flanks, indicating potential alterations or stresses experienced by the test post-formation. This species' test structure is marked by a complex arrangement of numerous chambers that vary in size, contributing to the overall architectural complexity of the test.

The preservation of the internal structure and coiling of *Discocyclusina dispensa* specimens is notably compromised due to the high micrite content present in the matrix. As a result, finer details of the test's coiling and internal features are not well-preserved in the fossil record. Despite this, specimens from this formation can attain sizes up to 3 mm, demonstrating the significant growth potential of this species. The combination of micritic infill and chamber variability provides key insights into the environmental conditions and depositional settings during the time of formation.

#### 4.4.5.2 *Discocyclusina* sp. 1

The test of *Discocyclusina* sp. 1 is characterized by its distinct spherical shape, exhibiting a biconvex profile with a prominent, globular central region. This central structure is surrounded by radiating, flat, and thin discoidal flanks that extend outward, creating a well-defined, symmetrical outline. The design and structure of this test are detailed in (Zhang Q. W., 2013), who provide a comprehensive examination of its

morphological features, which include the unique arrangement of the flanks that contribute to its overall spherical and biconvex appearance (Plate 4 b).

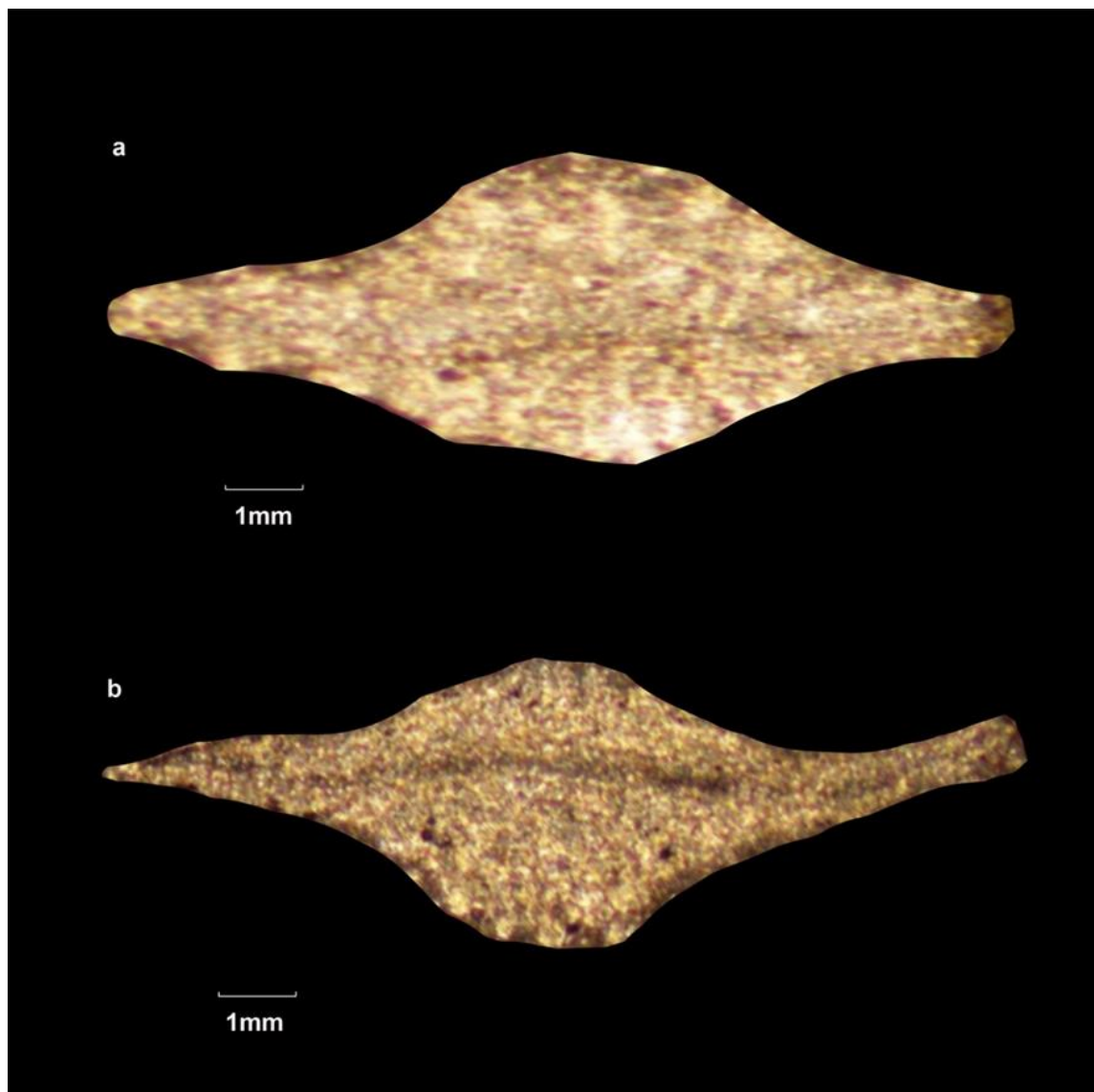


**Plate 4.5:** The above chart depicts various species of *Discocyclina*. a) *Discocyclina Dispensa* b) *Discocyclina Sp 1*

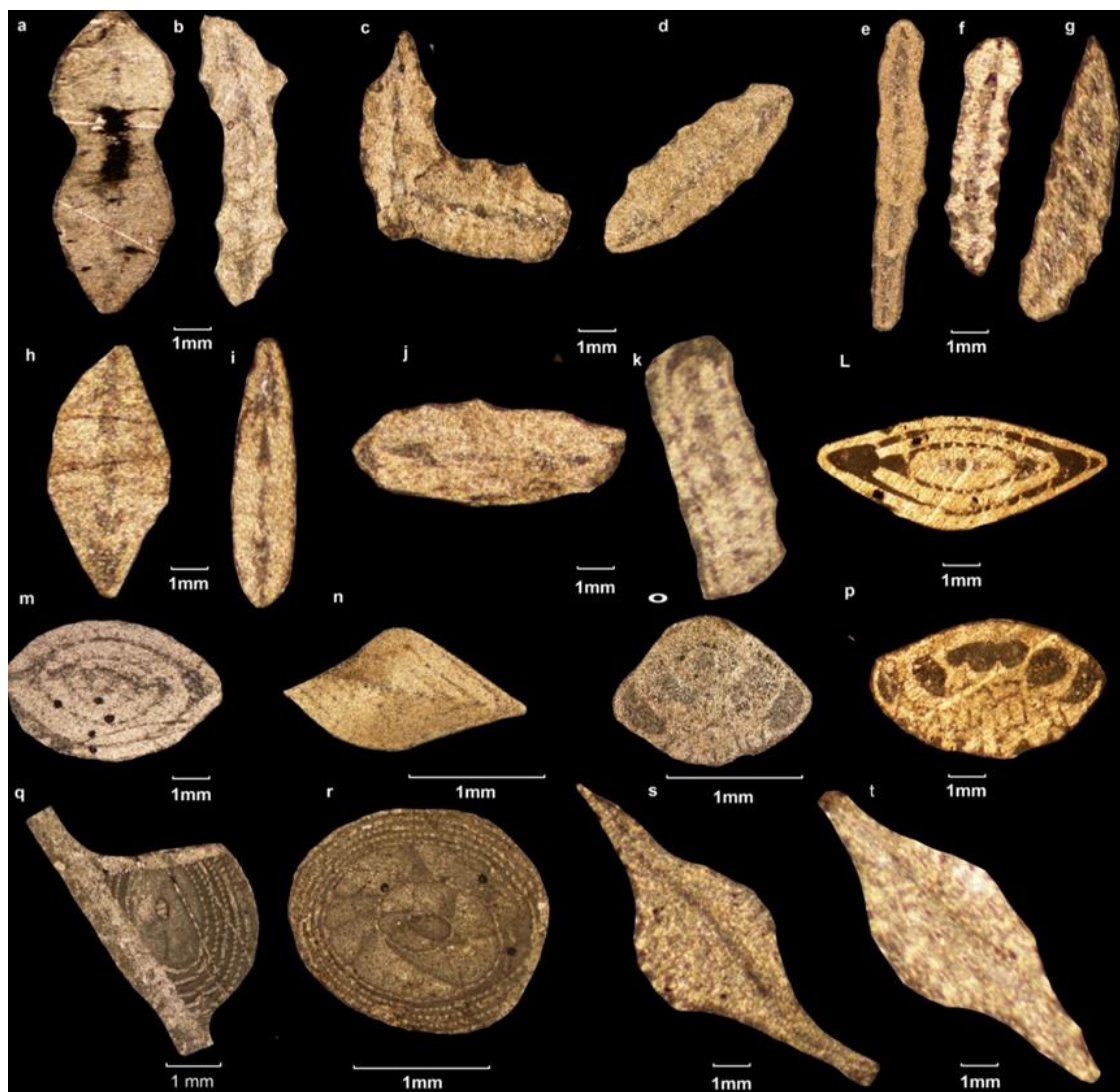


**Plate 4.6:** The above plate showcases various fossils: A) & B) *Assilina spinosa*, C) & D) *Assilina subspinosa*, E), F), & G) *Assilina granulosa*, H) & I) *Assilina laminosa*, J) & K) *Assilina placentula*, L) *Nummulites atacicus*, M) *Nummulites globulus*, N) *Nummulites mamilatus*, O) *Lockhartia conditi*, P) *Lockhartia tipperi*, Q) *Alveolina sp.*, R) *Alveolina indicatrix*, S) *Discocyclina sp. 1*, T) *Discocyclina dispensa*.

#### 4.5 Age Range of Margalla Hill Limestone

The Margalla Hill limestone primarily consists of carbonate material and it has a significant amount of larger benthic foraminiferas (LBF), which are valuable for age

determination. The index fossils identified are *Lockhartia tipperi*, *Lockhartia conditi*, *Assilina placentula*, *Assilina granulosa*, *Assilina laminosa*, *Assilina subspinosa*, *Assilina spinosa*, *Nummulites mammillatus*, *Nummulites globulus*, *Nummulites atacicus*, *Lockhartia tipperi*, *Lockhartia conditi*, and *Alveolina indicatrix* according to studies by (Latif, 1970; Shah, 1977; Swati, 2013). From the early Eocene to the late Paleocene, these species were present (Schaub, 1981; Serra-Kiel, 1998; Sameeni, 2013). The species with the shortest age ranges are *Assilina subspinosa*, *Assilina laminosa*, *Nummulites atacicus*, *Nummulites globulus*, *Alveolina indicatrix*, *Alveolina sp.*, and *Discocyclina sp. 1*, which date from the Upper Cuisian (Shallow Benthic Zone - SBZ11) to the Lower Ilerdian (Shallow Benthic Zone - SBZ5). The age range for *Alveolina indicatrix* spans from Late Ilerdian (Shallow Benthic Zone - SBZ9) to Lower Cuisian (Shallow Benthic Zone - SBZ10) (Schaub, 1981; Serra-Kiel, 1998; Ahmad, 2011; Sameeni, 2013). These fossils are thus considered key index fossils.

The Margalla Hill Limestone is dated from the Late Ilerdian (Shallow Benthic Zone - SBZ9, approximately 53 Ma) to the Lower Cuisian (Shallow Benthic Zone - SBZ10, approximately 51.5 Ma). This chronological framework is established through the formation's stratigraphic placement between the Upper Cuisian Kuldana Formation and the Middle Ilerdian Sakesar Formation, as well as the age ranges of associated index fossils (Ahmad, 2011; Sameeni, 2013). The upper boundary of the formation is marked by the presence of *Nummulites* fossils from the Upper Cuisian stage (Shallow Benthic Zone - SBZ10) as reported by (Sameeni, 2013) and (Zhang Q. W., 2013). The identified species of Larger Benthic Foraminiferas (LBF) within this context are considered reliable indicators for dating the formation in the examined sections (see Figure 4.1).

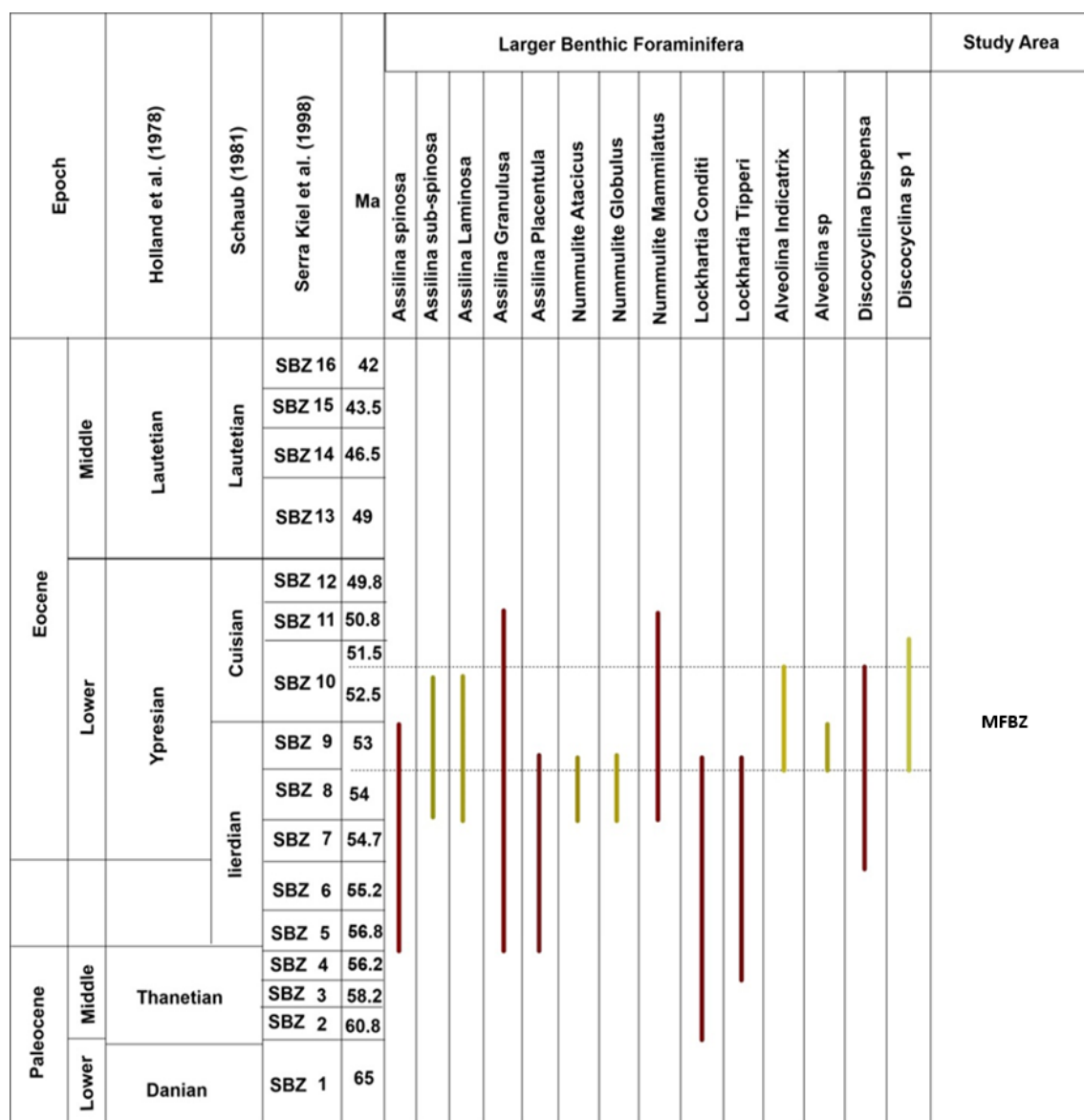


**Figure 4.1:** Age distribution of various Larger Benthic Foraminifera (LBF) in the Margalla Hill Limestone. The yellow lines indicate relatively limited age ranges of the diagnostic fossils compared to the red lines. The "Margalla Hill Limestone Biozone (MFBZ)" spans from Late Ilerdian (Shallow Benthic Zone SBZ9, 53 Ma) to Lower Cuisian (Shallow Benthic Zone SBZ10, 51.5 Ma) (modified from (Schaub, 1981; Serra-Kiel, 1998; Ahmad, 2011; Sameeni, 2013; Zhang Q. W., 2013)).

## Chapter 5

# MICROFACIES ANALYSIS AND DEPOSITIONAL ENVIRONMENT

### 5.1 Introduction

In 1838, Swiss geologist Gressly introduced the term "facies" as part of his foundational work in modern stratigraphy. The same methodology applied to siliciclastic rocks is used to interpret the environment of carbonate rocks. Facies represent the properties of a rock or sediment unit that reflect its depositional environment and distinguish it from those in adjacent environments (Nichols, 2007). Facies can be defined as "the sum of the characteristics of sedimentary units resulting from a specific set of physical, chemical, and biological parameters that produce a unit with distinct textural, structural, and compositional properties." According to (Middleton, 1973), facies encompass "any lithological, structural, and organic aspects of rock observable in the field."

Historically, "microfacies" as a term was specifically associated with paleontological and petrographic criteria examined in thin sections, as initially described by (Brown, 1943). Presently, this term has broadened to encompass a comprehensive range of paleontological and sedimentological data derived from various rock samples, including thin sections, polished slabs, and peels. In the current study, data were systematically gathered from thin sections, peels, and polished slabs to identify and analyze microfacies, with a primary focus on elucidating the composition and texture of limestone, as outlined by (Boggs Jr, 2009).

## **5.2 Microfacies Analysis and depositional environment of Margalla Hill Limestone**

For the microfacies analysis of the Margalla Hill Limestone, a total of 76 samples were collected from the Ayubia and Nathiagali sections and subjected to detailed petrographic examination via thin section study. This analysis aimed to identify and describe essential microfacies components such as allochems, cementing materials, matrix, and textural features. Notably, the examination of the relative percentages of foraminifera, skeletal grains, and non-skeletal grains offered critical insights into the depositional environment and paleoecological conditions of the limestone formation. The study employed the Dunham classification of limestones (Dunham, 1962), a widely recognized method for categorizing carbonate rocks, to systematically analyze skeletal grains, non-skeletal grains, and cementation types, facilitating a comprehensive interpretation of the Margalla Hill Limestone's depositional environment. Additionally, the analysis of fossils within the limestone provided further evidence for dating the strata and enhanced the understanding of the area's sequence stratigraphy.

### **5.2.1 Microfacies Analysis of Ayubia section**

Based on field data and petrographic research, eight distinct microfacies have been identified within the Margalla Hill Limestone at the Ayubia Section, situated in the southeastern Hazara sub-basin of the NW Himalayas, Pakistan. These microfacies have been systematically compared with findings from other studies, with each facies reflecting a unique depositional environment as outlined by (Benchilla, 2002). The identified microfacies for the Margalla Hill Limestone in this Ayubia section are designated as AS1 to AS8, where "AS" refers to the Ayubia Section and the numerals 1 to 8 correspond to the different types of microfacies documented in this study:

1. Mudstone microfacies AS1
2. Bioclastic Mudstone microfacies AS2
3. Bioclastic Wackestone microfacies AS3

4. Algal Wackestone microfacies AS4
5. Assilinid Nummulitic wackestone microfacies AS5
6. Nummulitidae Alveolinal wackestone microfacies AS6
7. Assilinid Wackestone microfacies AS7
8. Alveolinal Wackestone microfacies AS8

#### **5.2.1.1 Mudstone Microfacie AS1**

This microfacies is characterized by micritic limestone comprising approximately 2% allochems within a micritic ground mass of about 96%. The preservation of biogenic content is notably poor. Examination of the thin section indicates the presence of calcite-filled veins, constituting approximately 5% of the observed features (see Plate 5.1a)

#### **5.2.1.2 Bioclastic Mudstone Microfacie AS2**

The Bioclastic Mudstone Microfacies AS2 is characterized by a predominant micritic limestone matrix, with less than 10% of grains and 85-90% matrix content. The primary allochems in this facies include green algae and larger benthic foraminifera, such as *Nummulite* and *Lockhartia*. Notable features include visible calcite veins constituting approximately 4% of the composition, alongside minor traces of miliolid foraminifera (Plate 5.1b).

#### **5.2.1.3 Bioclastic Wackstone Microfacie AS3**

The Bioclastic Wackstone Microfacies AS3 is characterized by a composition of 15-25% bioclasts, with an average proportion of 18%. The matrix constitutes 60-80% of the facies, averaging 70%. The bioclasts present in this facies include miliolids, green



algae, mollusks, echinoids, and fragmented remains of *Nummulites*, *Alveolina*, and *Lockhartia*. Additionally, the facies features approximately 9% calcite-filled veins.

#### **5.2.1.4 Algal Wackstone Microfacie AS4**

The Algal Wackstone Microfacies AS4 is characterized by a composition of approximately 25-30% allochems, with an average of 28%, and 60-70% matrix. This microfacies is notably rich in Zygnematales, which are filamentous and unbranched, forming extended chains of cells joined end-to-end (Margulis, L., 1990). In addition to the abundant Zygnematales, a moderate presence of green algae is observed. Stylolites are also present, comprising about 9% of the facies (Plate 5.1d).

#### **5.2.1.5 Assilinid Nummulitic Wackstone Microfacie AS5**

The Assilinid Nummulitic Wackstone Microfacies AS5 is characterized by a composition comprising 29% allochems and 62% micrite. The dominant allochems, which include Assilina and Nummulite, constitute the primary framework grains of this microfacies. Furthermore, calcite veins account for 13% of the observed composition (Plate 5.1e).

#### **5.2.1.6 Nummulitidae Alveolinal Wackstone Microfacie AS6**

The Nummulitidae Alveolina Wackstone Microfacies AS6 comprises 38% allochems and 45-55% micrite. This microfacies is characterized by the predominance of nummulites and Alveolina as the main allochems, with Lockhartia present in a lesser

proportion. The wackstone texture suggests deposition in a low to moderately energetic environment, as detailed by (Tucker M. E., 1990; James & Dalrymple, 2010). Additionally, the presence of 4% calcite veins was noted (Plate 5.1f).

#### **5.2.1.7 Assilinid Wackstone Microfacie AS7**

This microfacies is characterized by 36% allochems and 60% micrite. It features a predominance of *Assilina*, accompanied by a minor presence of *Nummulites*, *Lockhartia*, and occasional occurrences of *Discocyclina* and green algae. Additionally, stylolites are present, constituting 4% of the composition (see Plate 5.1g).

#### **5.2.1.8 Alveolinal Wackstone Microfacie AS8**

The Alveolinal wackstone microfacies, designated as AS8, consists of approximately 35% allochems and 50-65% micrite, with an average micrite content of 60%. This microfacies is characterized by a high abundance of *Alveolina*, supplemented by a relatively minor presence of nummulite, *Lockhartia*, and 3-5% green algae, as depicted in (Plate 5.1h).

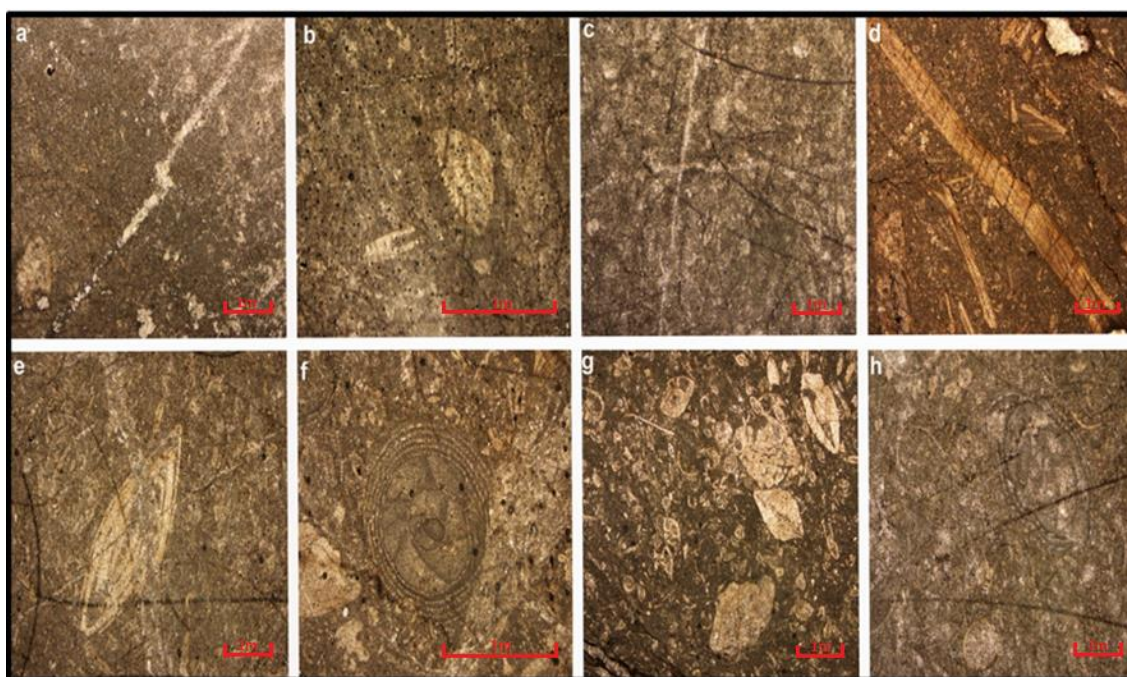


**Plate 5.1:** The above Plate depicts the Photomicrographs of various microfacies of Margalla Hill Limestone, Ayubia section a) Mudstone microfacie b) Bioclastic Mudstone microfacie c) Bioclastic Wackstone microfacie d) Algal Wackstone microfacie e) Assilinid Nummulitic Wackstone microfacie f) Nummulitidae Alveolinal Wackstone microfacie g) Assilinid Wackstone microfacie h) Alveolinid wackstone microfacie.

### 5.2.2 Depositional Environment of Ayubia Section

According to (Tucker M. E., 1990; James & Dalrymple, 2010), the depositional model shown in Figure 5.1 suggests that AS1 microfacie with mudstone texture represents a low-energy, nutrient-rich, semi-restricted environment. The micritic limestone with a high proportion of matrix (96% micrite) and only 2% allochems suggests a low-energy depositional environment where sediment accumulation occurs slowly, often seen in settings with limited wave action or current. The poor preservation of biogenic content, along with the presence of calcite-filled veins, indicates a nutrient-rich setting. This is characteristic of environments like tidal flats, where sediments can be fine-grained, and organic material is often buried rapidly, leading to poor preservation. (Tucker M. E., 1990;

James & Dalrymple, 2010) depositional model characterize mudstones in similar contexts as being deposited in **tidal flats**. These areas are generally influenced by tidal cycles, leading to periodic flooding and exposure, which can create the semi-restricted conditions.

AS2 microfacie with high matrix content (85-90%), predominance of micritic limestone and the presence of allochems like green algae and larger benthic foraminifera (*Nummulite* and *Lockhartia*) support a lagoonal environment. These organisms are typically found in shallow, warm, and nutrient-rich waters, which are characteristic of inner lagoonal settings. The significant matrix content and the presence of calcite veins (4%) suggest that deposition occurred in a low-energy environment, which is typical for lagoonal settings where wave action is minimal, allowing fine sediments to accumulate without disturbance. The presence of larger benthic foraminifera indicates a favorable environment for these organisms, often associated with healthy lagoon ecosystems. The inclusion of green algae further supports the idea of a nutrient-rich setting.

Based on textural characteristics and faunal composition, the AS3 microfacies is identified as an **inner proximal ramp habitat or lagoonal environment** (Tucker M. E., 1990; Geel, 2000; James & Dalrymple, 2010). The presence of bioclasts, such as larger benthic foraminifera, green algae, and miliolids, supports this classification, indicating deposition in shallow (10–15 meters), warm, and nutrient-rich waters (Heckel, 1972; Flügel E. , Introduction to Facies Analysis, 1982). These conditions are conducive to the growth of diverse biota, including the bioclasts we've identified. The Wackestone texture further suggests deposition in a low- to mildly energetic environment (Tucker M. E., 1990; James & Dalrymple, 2010). (Racey, 1994) observes that the coexistence of open marine fauna (Dasycladean algae) and hypersaline species (miliolids) points to deposition within an inner proximal ramp setting or a transition zone between a lagoon and a sand shoal. The observed calcite-filled veins (approximately 9%) can also indicate diagenetic processes occurring in a relatively stable environment, further supporting the conclusion of a low-energy setting.

The AS4 microfacies is characterized with composition of approximately 25-30% allochems, along with the notable abundance of Zygnematales, indicates a depositional setting influenced by both lagoonal and marine conditions. The presence of dasycladean algae suggests a productive environment, typical of shallow, warm waters. The Wackestone texture implies a relatively low-energy setting, which is conducive to the deposition of fine sediments while still allowing for some energy from water movement. This aligns well with environments found along the **inner proximal ramp**. The suggested depth range of 10-15 meters is consistent with conditions that would support abundant algal growth, particularly Zygnematales and other green algae. These conditions are typically found in areas with ample sunlight and nutrients, promoting diverse marine life. (Heckel, 1972; Flügel E. , Introduction to Facies Analysis, 1982). The occurrence of stylolites (9%) suggests that the sediment underwent some degree of compaction and diagenesis, which can be indicative of a stable environment, further supporting the idea of low-energy conditions. This texture, along with the presence of open marine fauna (Dasycladean algae), suggests deposition in an inner proximal ramp setting or a transitional area between a sand shoal and a lagoonal environment (Racey, 1994).

The AS5 microfacies is characterized by a Wackestone texture with *Assilina* and *Nummulites* as the dominant framework grains combined with a significant micritic component (62%), strongly indicates that this microfacies was deposited in a relatively deeper environment, below the influence of typical wave action. Their close association suggests deposition below the **Fairweather Wave Base (FWWB)** (Racey, 1994) where sedimentation is primarily influenced by bottom currents rather than wave activity. While the microfacies is characterized by a Wackestone texture, which typically indicates low- to moderate-energy conditions, the specific composition of dominant foraminifera suggests a setting where energy is sufficient to allow for the accumulation of these larger benthic foraminifera, yet still stable enough to allow micrite deposition. The association of *Assilina* and *Nummulites* may indicate a transitional environment between deeper marine and more shallow settings, potentially influenced by local bathymetric variations or changes in sediment supply. The presence of calcite veins (13%) further supports the idea of post-depositional alteration, which is often observed in more stable, low-energy environments where bioturbation and other diagenetic processes can occur.

The AS6 microfacies with the presence of 38% allochems and 45-55% micrite, combined with the predominance of *Nummulites* and *Alveolina*, indicates a relatively stable and low-energy environment conducive to the accumulation of these organisms. The composition and texture of the Wackestone suggest deposition in shallow waters, where light can penetrate to support photosynthetic organisms and contribute to the growth of benthic foraminifera like *Nummulites* and *Alveolina*. The presence of these specific foraminifera suggests that deposition occurred in a range of shallow water settings spanning from the **proximal middle ramp to the distal inner ramp**, possibly influenced by local topography and sediment dynamics. The presence of calcite veins (4%) indicates post-depositional diagenetic processes, which can be common in low-energy environments where sediments are stable over longer periods, allowing for calcite precipitation.

The AS7 microfacies, characterized by the predominance of *Assilina* along with smaller quantities of *Nummulites* and *Discocyclina* indicates a depositional environment likely transitioning between the **distal inner ramp and proximal middle ramp settings**. (Racey, 1994). The 36% allochems and 60% micrite content indicate a stable sedimentary environment where fine-grained micrite can accumulate alongside larger foraminiferal fragments. This is characteristic of environments where energetic conditions are moderate, allowing for the deposition of both fine and coarse materials. The presence of green algae suggests a shallow marine environment that is conducive to photosynthesis, typically found in warm, nutrient-rich waters. The stylolites (4% presence) imply post-depositional processes that are consistent with low-energy environments where sediments can undergo diagenetic alteration. The Wackestone texture suggests deposition under low to moderate energy conditions, suitable for the accumulation of these allochems without significant disturbance.

The AS8 microfacies, is characterized by the high abundance of *Alveolina*, combined with low concentrations of *Nummulites* and *Lockhartia*, indicates a tranquil setting conducive to the accumulation of these larger foraminifer, reflects deposition in low-energy, shallow water environments near the **inner ramp**. The average micrite

content of 60% suggests a stable environment with minimal disturbance, allowing for the fine sediment to settle and accumulate alongside the allochems. This aligns with environments where sedimentation is primarily influenced by biological activity, such as algal blooms. The 3-5% presence of green algae supports the notion of warm, shallow waters where photosynthetic activity is prevalent. This environment is typically rich in nutrients, further enhancing the growth of marine organisms. The overall characteristics of the microfacies suggest deposition near the inner ramp, where conditions are often calm, allowing for the preservation of delicate structures and organisms.

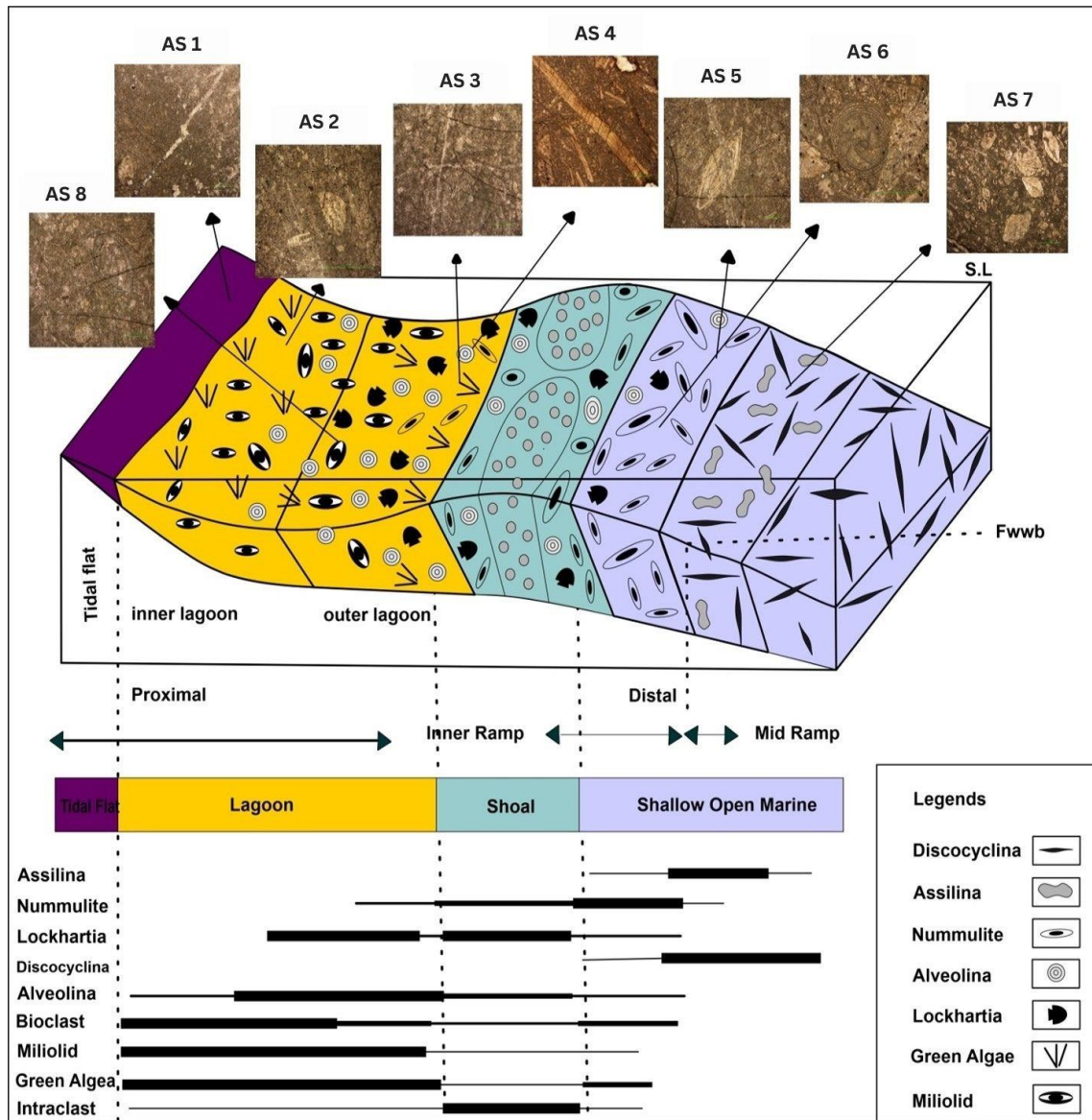


**Figure 5.1:** Facies depositional model of a carbonate ramp showing the temporal distribution of the Eocene facies of the Margalla Hill Limestone, South-Eastern Hazara sub-basin at Ayubia section.



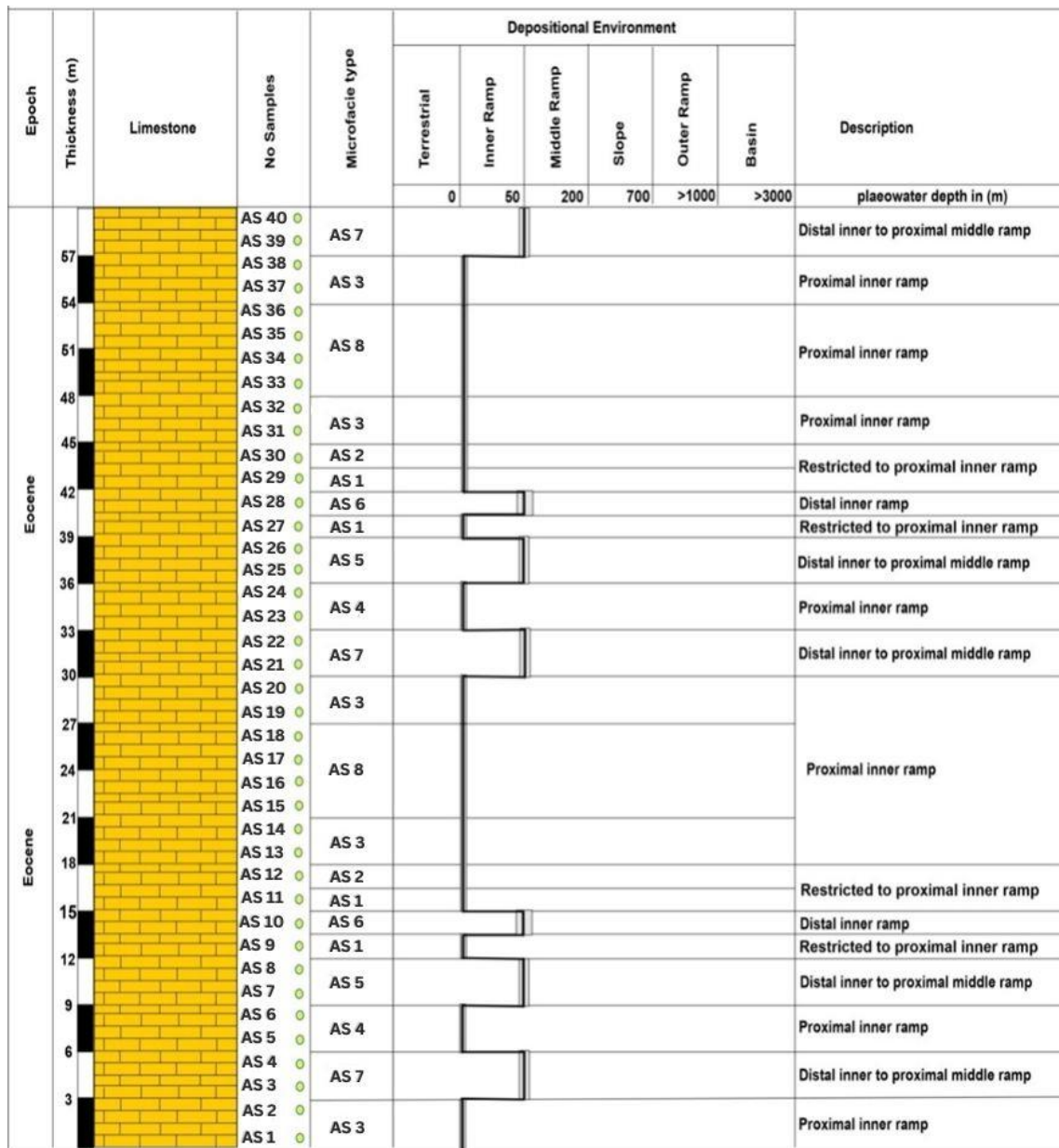


**Figure 5.2:** Microfacies distribution, depositional environments, and a mean relative sea level curve inferred from the faunal paleoecology (*Racey, 1995*) and facies criteria (*Flügel E. , 2004*) of the Margalla Hill Limestone exposed in the Ayubia section, south-eastern hazara sub-basin. (The shaded area depicts the range of variation in the deposition environment).

### 5.2.3 Microfacies Analysis of Nathiagali Section

Based on comprehensive field data and petrographic analysis, nine distinct microfacies have been identified within the Margalla Hill Limestone at the Nathiagali Section, located in the southeastern Hazara sub-basin of the NW Himalayas, Pakistan. These microfacies have been analyzed and compared with findings from other studies, each representing a unique depositional environment. The identified microfacies for the Margalla Hill Limestone in this section are designated as NS1 to NS9, where "NS" refers to the Nathiagali Section and the numerals 1 to 9 correspond to the different types of microfacies documented in this study.

1. Mudstone Microfacies NS 1
2. Bioclastic Wackstone microfacies NS 2
3. Assilinid Wackstone microfacies NS 3
4. Nummulitidae-Lockhartian Wackstone microfacies NS 4
5. Coralline-algal Wackstone microfacies NS 5
6. Assilinid-Discocyclinal Wackstone microfacies NS 6
7. Discocyclinal-Assilinal Wackstone microfacies NS 7
8. Discocyclinal Mudstone microfacies NS 8
9. Assilinid Packstone microfacies NS 9

#### 5.2.3.1 Mudstone Microfacie NS1

Mudstone Microfacies NS1 is characterized primarily by micritic limestone, which constitutes the majority of its composition, with approximately 90% of the ground mass being micrite. The remaining 6% comprises allochems, including biogenic fragments, although these are generally poorly preserved. Within this facies, sporadic occurrences of Lockhartia, algae, and miliolid foraminifera, infilled with sparry calcite,

are observed. The facies also feature stylolites, accounting for about 7% of its composition, indicating pressure solution processes (refer to Plate 5.2a).

### **5.2.3.2 Bioclastic Wackstone Microfacie NS 2**

The Bioclastic Wackstone Microfacies NS 2 is characterized by a significant bioclast content ranging from 35% to 45%, with an average of 42%. The matrix component constitutes 50% to 60% of the facies, averaging around 58%. The bioclasts present within this microfacies predominantly include fragments of algae, miliolids, and the foraminiferal genera *Lockhartia* and *Nummulite*, the latter being present in minor quantities. Additionally, filled stylolites make up approximately 3% of the facies composition, which is illustrated in Plate 5.2b.

### **5.2.3.3 Assilinid Wackstone Microfacie NS 3**

The Assilinid wackstone microfacies, designated as NS 3, is characterized by a composition of approximately 26% allochems and a significant micrite content ranging from 65% to 75%, with an average of 72%. This microfacies predominantly includes a variety of larger benthic foraminifera species, particularly *Assilina*, which constitutes the majority. It also features a relatively lower abundance of other benthic foraminifera, such as nummulites and *Lockhartia*, along with sporadic occurrences of algae. Additionally, the microfacies contains approximately 10% unidentified bioclasts, adding to its heterogeneity (as illustrated in Plate 5.2c).

#### **5.2.3.4 Nummulitidae-Lockhartian Wackstone Microfacie NS 4**

The Nummulitidae-Lockhartian wackestone microfacies, designated as NS 4, is characterized by its composition, which includes 30-40% allochems, averaging 36%, and a matrix that comprises 50-65%, averaging 64%. The allochems within this microfacies are predominantly large benthic foraminifera, specifically the genera *Nummulites* and *Lockhartia*, with a minor presence of *Assilina*. Additionally, this microfacies contains 13% bioclasts, which are fragments derived from broken pieces of *Nummulites*, *Lockhartia*, and algae. Notably, 1% of stylolites are also present in this microfacies, as illustrated in Plate 5.2d.

#### **5.2.3.5 Coralline Algal Wackstone Microfacie NS 5**

The Coralline Algal Wackstone Microfacies NS 5 is characterized by the presence of 35-40% allochems, with an average composition of 36%, and a matrix content ranging from 55-65%, averaging 64%. The primary allochems in this microfacies are coralline algae and *Assilina*, accompanied by lesser quantities of *Nummulites*, *Discocyclusina*, and green algae. Notably, bioclasts constitute approximately 4% of the composition, consisting of fragmented remains of algae, *Assilina*, and various shell debris. This microfacies provides valuable insights into the sedimentological environment and paleoecological conditions (Plate 5.2e).

#### **5.2.3.6 Assiliniid-Discocyclusinal Wackstone Microfacie NS 6**

This microfacies consists of 35% allochems and 60-70% micrite, averaging 65%. It contains various species of larger benthic foraminifera, predominantly *Assilina* and *Discocyclusina*, with a relatively low proportion of *Nummulite*. Additionally, 11% bioclasts

were observed, including fragments of *Assilina* and planktonic foraminifera. Moreover, 12% stylolites were also observed (Plate 5.2f).

#### **5.2.3.7 Discocyclinal-Assilinal wackstone Microfacie NS 7**

The Discocyclinal-Assilinal Wackstone microfacies, designated as NS 7, is characterized by a composition of approximately 45% allochems and 50-60% micrite, with an average micrite content of 55%. This microfacies prominently features a diverse assemblage of larger benthic foraminifera, predominantly comprising *Discocyclina* and *Assilina* species, while *Nummulite* is present in relatively lower proportions. In addition, bioclasts constitute about 12% of the microfacies, including fragments of *Assilina* and other unidentified bioclasts. Stylolites are also a notable component, accounting for around 6% of the observed features (see Plate 5.2f).

#### **5.2.3.8 Discocyclinal mudstone Microfacie NS 8**

The Discocyclinal mudstone microfacies (NS 8) is characterized by a composition predominantly of micrite, accounting for 80-90% of the total matrix, and approximately 9% allochems. This microfacies is distinguished by the presence of various species of larger benthic foraminifera, with *Discocyclina* being the most prevalent, followed by lesser proportions of *Assilina* and *Nummulite*. Additionally, the microfacies includes about 3% unidentified bioclasts and features calcite-filled veins, which constitute around 12% of the observed content (as depicted in Plate 5.2g).

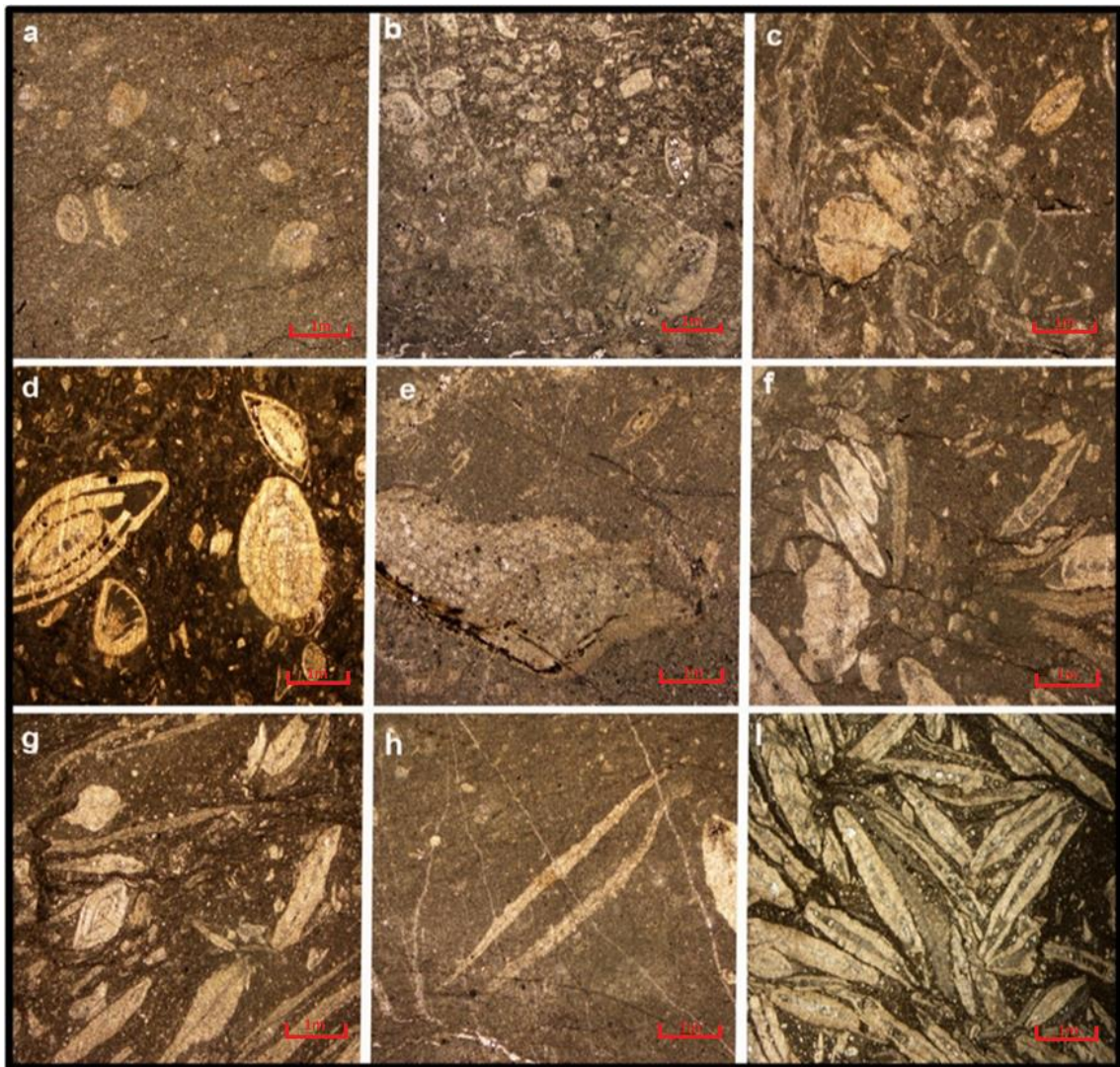


**Plate 5.2:** The photomicrographs of various microfacies of Margalla Hill Limestone, Nathiagali section: a) Mudstone microfacies b) Bioclastic wackstone microfacies c) Assilinid wackstone microfacies d) Nummulitidae-Lockhartian wackstone microfacies e) Algal-Assilina wackstone microfacies f) Assilinid-discocyclinal wackstone microfacies g) Discocyclinal-Assilina wackstone microfacies h) Discocyclinal mudstone microfacies i) Assilina grainstone microfacies.

### 5.2.3.9 Assilinid packstone Microfacie NS 9

The Assilinid Packstone microfacies, designated as NS 9, is characterized by a high concentration of allochems, comprising approximately 85% of the total composition, with the remaining 10-15% consisting of micrite. This microfacies is notable for its diverse assemblage of larger benthic foraminifera, particularly the genus *Assilina*, which dominates the assemblage, alongside a comparatively lower presence of *Discocyclina*. In addition to these foraminiferal constituents, a minor fraction (3%) of unidentified bioclasts is also present, as observed in Plate 5.2c.

### 5.2.4 Depositional Environment of Nathiagali Section

The depositional model of the Margalla Hill Limestone, as depicted in Figure 5.4, reveals a range of environments based on microfacies analysis. NS1 microfacies composition, with approximately 90% micrite, indicates a stable environment where fine sediments could accumulate with limited disturbance. The predominance of micrite suggests conditions that favor the preservation of fine particles, typically found in low-energy settings. The mudstone texture of NS1 indicates deposition in low-energy, nutrient-rich settings (Tucker M. E., 1990; James & Dalrymple, 2010). This microfacies is characterized by miliolids and a low proportion of green algae, suggests a warm, nutrient-rich, moderately turbulent, and semi-restricted environment (Geel, 2000). The presence of stylolites, accounting for about 7% of the composition, points to pressure solution processes, which are often indicative of burial and compaction. This can suggest a degree of tectonic activity or sediment loading over time. The presence of miliolids and low amounts of green algae aligns with typical conditions of an **inner ramp setting**, where water circulation allows for nutrient exchange while maintaining relatively calm conditions conducive to sediment deposition.

NS2 microfacies, with its significant bioclast content, averaging 42%, indicates an active biological environment where various organisms contributed to the sediment. This level of bioclast richness suggests a dynamic ecosystem capable of supporting a diverse array of life. With the matrix component constituting averaging around 58%, the microfacies demonstrates a balance between bioclasts and matrix material. This ratio suggests deposition in an environment where both biogenic and fine-grained sediments are present, indicative of moderate energy conditions that allow for sediment sorting. The presence of algae fragments, miliolids, and foraminifera such as *Lockhartia* and *Nummulite* (in minor quantities) indicates a rich, biologically productive environment. The limited diversity of bioclasts suggests specific ecological conditions, possibly pointing to a stable environment conducive to the preservation of certain species while limiting others. Limited bioclast diversity, including larger benthic foraminifera, green algae, and signs of miliolids, points to a shallow, nutrient-rich environment (Heckel, 1972; Flügel E. , 1982). The presence of dasycladean algae and miliolids in this microfacies supports a depositional environment within an **inner proximal ramp** or a transitional zone between a **lagoon and a sand shoal** (Racey, 1994). The 3% composition of filled stylolites reflects the history of pressure solution processes, indicating sediment compaction and potential burial over time.

NS3 microfacies, with allochems constituting approximately 26% of the composition, this facies contains a moderate bioclast presence. The dominance of *Assilina* and other larger benthic foraminifera indicates a specific ecological niche that supports these organisms, likely within a low-energy environment where fine sediment can accumulate without significant disturbance, suggests deposition in a distal inner to proximal middle ramp setting (Racey, 1994). The significant micrite content, averaging 72%, suggests a low-energy depositional environment. Micritic sediments typically accumulate in calmer waters where the finer particles can settle, pointing to environments below the **fair-weather wave base (FWWB)**. *Assilina* dominates, reflecting its adaptability to a distal inner ramp or proximal middle ramp setting. The minor presence of *Nummulites* and *Lockhartia* suggests that these species were less dominant in this setting but still present. The sporadic presence of algae further supports the idea of shallow waters, where sunlight penetrates and enables photosynthesis, though algae are less abundant compared to benthic foraminifera. The presence of approximately 10%



unidentified bioclasts adds complexity and indicates some variability in the local biota. This heterogeneity could result from fluctuating environmental conditions, such as changes in nutrient availability or water energy, which periodically introduce other organisms into the depositional system. The predominance of *Assilina*, combined with minor occurrences of *Nummulites* and *Lockhartia*, is characteristic of deposition in a **distal inner ramp to proximal middle ramp setting**. This environment is consistent with moderate water depth, below the FWWB, where both micrite and bioclasts can accumulate without significant reworking by waves or currents.

In contrast, NS 4, which contains abundant *Nummulites* and *Lockhartia* with less *Assilina*, indicates a low- to slightly energetic environment based on its Wackestone texture (Tucker M. E., 1990; James & Dalrymple, 2010). The predominance of larger benthic foraminifera (*Nummulites* and *Lockhartia*) with minor *Assilina* suggests shallow marine conditions, but the wackestone matrix and moderate levels of allochems (36%) point to lower energy settings where sediment was not highly reworked. The presence of 13% bioclasts (fragmented foraminifera and algae) implies mild energy levels that allowed for some breakage of shells and other organic material but not enough to fully destroy or transport the remains far from their source. The presence of 1% stylolites may indicate some compaction and pressure dissolution, which can occur in low-energy settings where sediments accumulate slowly over time. The wackestone texture reflects low- to slightly energetic environment, consistent with the interpretation of a lower-energy, **inner ramp setting** where water depth remains shallow, but energy levels are low enough to allow micritic material to dominate.

The NS5 microfacies, dominated by coralline algae and *Assilina* with subordinate *nummulites*, *discocyclina*, and green algae, suggests a mid-ramp environment with moderate to high energy settings (Heckel, 1972; Adams, 1998). The abundance of coralline algae and *Assilina*, along with smaller amounts of *Nummulites*, *Discocyclina*, and green algae, suggests deposition in a more open marine environment. Coralline algae thrive in well-lit, shallow water settings with moderate to high energy, often associated with mid-ramp zones where wave and current action is more pronounced. The 4% bioclast content, consisting of fragmented algae, foraminifera (*Assilina*), and shell debris,

indicates that moderate energy conditions were sufficient to break down and transport biological material, which is characteristic of mid-ramp environments. The matrix content (55-65%) suggests that while micritic sediment dominated, the energy levels were not so high as to completely wash away fine particles. This balance between matrix and allochems is typical of mid-ramp environments, where conditions are neither too turbulent nor too calm. The depositional setting likely reflects an area within the **mid-ramp zone** where energy levels fluctuate enough to allow both algal growth and moderate sediment reworking.

The NS6 microfacie is characterized by the presence of *Assilina* and *Discocyclusina* as dominant larger benthic foraminifera, with minor amounts of Nummulites, suggests a depositional environment that was relatively shallow but further offshore compared to inner ramp settings. This is typical of a proximal middle ramp environment where energy levels start to decrease but still allow for the presence of larger foraminifera. The high percentage of micrite indicates deposition in lower-energy conditions, which aligns with middle ramp settings where fine-grained sediment can accumulate. The presence of 11% bioclasts and 12% stylolites further suggests moderate energy levels, enough to fragment foraminifera but not enough to transport them far from the depositional site. Stylolites also indicate some degree of pressure dissolution, possibly related to compaction in a relatively calm environment.

The NS7 microfacies is characterized by slightly higher allochems content compared to NS6, dominated by *Discocyclusina* and *Assilina*, indicates a similar environment. The increase in allochem content reflect a slightly more energetic setting, but still within the proximal middle ramp zone. The slightly lower micrite content suggests that the depositional environment was within the middle ramp but with slightly higher energy, allowing for a bit more grain accumulation than NS6. The bioclasts (12%) and stylolites (6%) reflect similar conditions to NS6, with moderate energy leading to some bioclast fragmentation and pressure-induced stylolites.

Both NS6 and NS7 microfacies, characterized by abundant *Assilina* and *Discocyclina* with minor *Nummulites*, point to a **proximal middle ramp** setting where energy levels were moderate but not as high as in more inner ramp settings.

The NS8 microfacies, which is abundant in *discocyclina* and contains relatively few *Assilina* and *nummulites*, indicates a quiet, low-energy environment likely located in a **proximal middle ramp setting**, as suggested by its mudstone texture (Tucker M. E., 1990; James & Dalrymple, 2010). The high micrite content suggests very low-energy conditions where fine, micritic material could settle without significant disturbance. This is typical of mudstone textures, which indicate a calm environment, such as a proximal middle ramp, where energy levels are low enough to allow mud to dominate the sediment. The relatively low percentage of allochems, dominated by *Discocyclina* and minor *Assilina* and *Nummulites*, reflects a depositional setting that was not high-energy enough to accumulate larger foraminifera in abundance. *Discocyclina's* presence supports a quiet, more stable marine setting. The low bioclast content and the occurrence of calcite-filled veins suggest a quiet depositional environment with some diagenetic alteration (pressure and chemical changes post-deposition)

NS9 microfacie, dominated by *Assilina* with subordinate *Discocyclina* and a packstone texture, points to a moderate to high-energy environment in the distal inner ramp (Tucker M. E., 1990; James & Dalrymple, 2010). The high concentration of allochems, dominated by *Assilina* with some *Discocyclina*, indicates a higher-energy depositional environment. Packstone textures, with their abundance of grains and reduced micrite content, typically form in settings with moderate to high water movement, allowing for the accumulation of foraminifera and the winnowing of finer sediments. The low micrite content further supports the idea of a higher-energy environment, where finer particles are reworked or washed away, leaving behind a grain-supported structure typical of packstone. This is consistent with **distal inner ramp** settings, where water energy is sufficient to remove micrite but not as strong as in shoal or outer ramp zones. The minor fraction of bioclasts, likely fragmented due to the more turbulent conditions, reflects higher-energy environment where biological material can be broken down and redistributed.

Figure 5.5 provides a comprehensive overview of these depositional environments, summarizing various aspects of the Margalla Hill Limestone at the Nathiagali section.

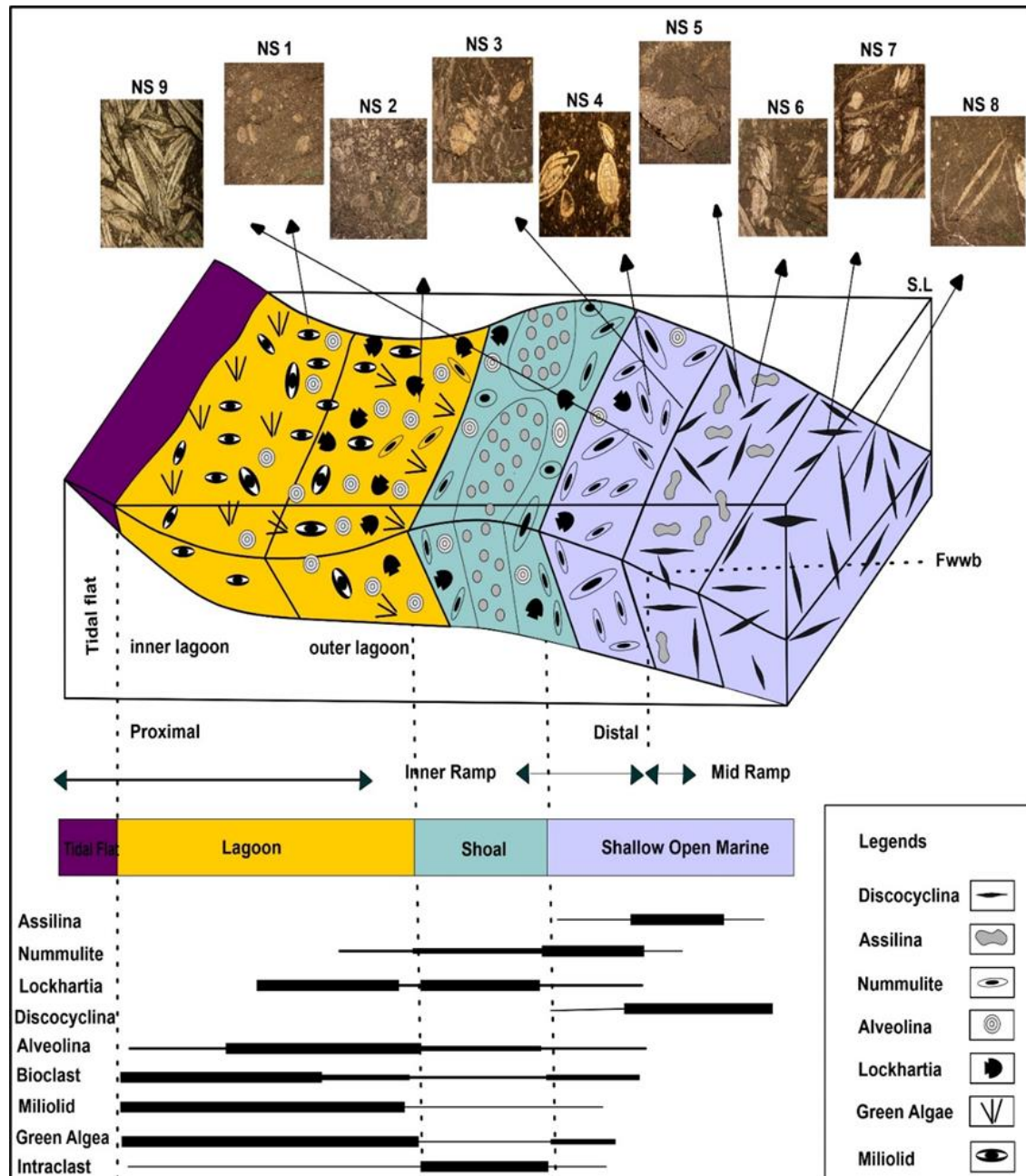


**Figure 5.3:** Facies depositional model of a carbonate ramp illustrating the temporal distribution of the Eocene facies within the Margalla Hill Limestone, located in the southeastern Hazara sub-basin at the Nathiagali section.

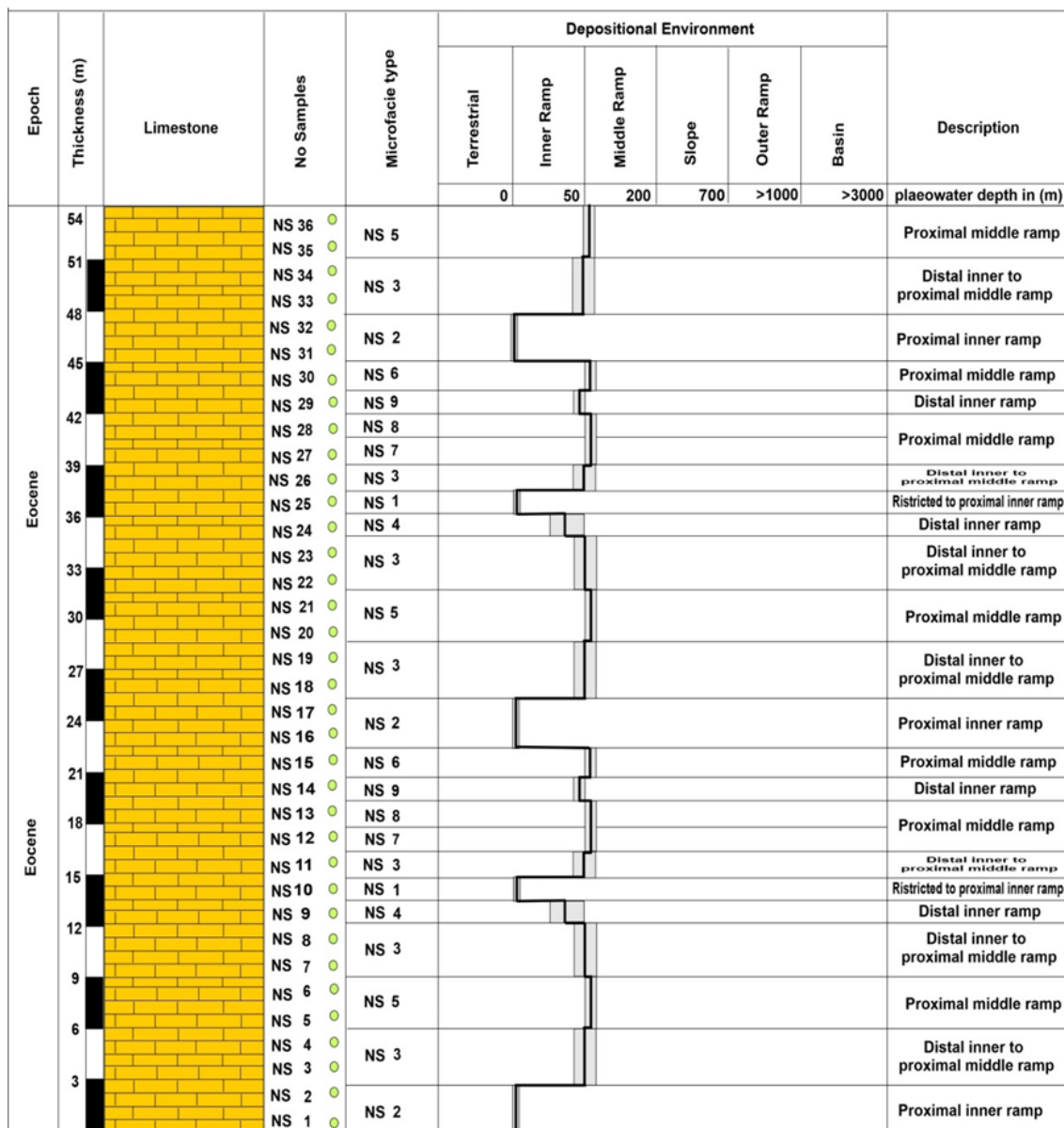


**Figure 5.4:** Microfacies distribution, depositional environments, and a mean relative sea level curve inferred from the faunal paleoecology (*Racey, 1995*) and facies criteria (*Flügel E. , 2004*) of the Margalla Hill Limestone exposed in the Nathiagali section, southeastern Hazara sub-basin. (The shaded area depicts the range of variation in the deposition environment).

### 5.3 Depositional Model

The comprehensive analysis of microfacies within the Margalla Hill Limestone, alongside the identification of age-specific fossils such as *Nummilite mamillatus* (Fichtel and Moll), *Nummilite atacicus Leymerie*, *Assilina spinosa Davies and Pinfold*, *Assilina subspinosa Davies and Pinfold*, *Assilina laminose Gill*, *Assilina granulosa (d'Archiac)*, *Locartia tippri Davies* (refer to Figure. 4.1 ,4.2 & 4.3), offers valuable insights into the Eocene carbonate ramp environment. (Buxton, 1989; Ćosović, 2004; Barattolo, 2007) highlights that the fauna distribution on the Eocene carbonate ramp, as described by (Racey, 1994) reflects a shallow marine setting, likely associated with Tethyan carbonate platform deposition. The carbonate platform facies model proposed by (Read, 1985) provides a foundational framework for understanding carbonate deposition processes within this formation. This study's depositional model has been further refined based on (Mirza, 2022) addressing the varying profiles, facies compositions, and evolutionary sequences of different carbonate platforms as outlined by (Read, 1985).

Shoal-water complexes within these environments, which include ooid-pellet sands or skeletal banks, indicates a dynamic environment that oscillated between high-energy and low-energy conditions, and can be categorized as either homoclinal or distally steepened. Homoclinal ramps transition seaward into deeper water without significant deep-water breccias, while distally steepened ramps exhibit either high-energy conditions with extensive skeletal sand blankets or low-energy conditions with widespread shallow, sub-wave-base mud blankets. Microfacies analysis reveals that packstones and wackestones were deposited in moderate-energy settings, whereas micrite-dominated mudstones indicate a low-energy, quiet-water environment (Tucker M. E., 1990; Flügel E. , 2004). The absence of significant slope breaks or deep-water breccias suggests that deposition was primarily within the inner ramp, with some facies extending into the proximal middle ramp. The combination of larger benthic foraminifera, the types of microfacies (such as packstones and wackestones), and the overall depositional settings indicate a dynamic interplay between restricted lagoonal conditions and open marine influences, typical of carbonate ramp systems. (see Figure 6.1 to 6.5). Ultimately, the evidence points to an **open marine lagoon environment** for the early Eocene Margalla

Hill Limestone, characterized by restricted lagoonal conditions and influenced by the broader Tethyan carbonate platform dynamics.

## **Chapter 6**

# **DIAGENESIS AND ITS IMPACT ON RESERVOIR PROPERTIES IN THE MARGALLA HILL LIMESTONE**

### **6.1 DIAGENESIS**

Diagenesis is a complex sequence of physical, chemical, and biological transformations that gradually convert sediment into sedimentary rock. It occurs after sediment deposition but before deep burial and metamorphism, profoundly influencing the physical properties of sedimentary rocks such as mineral composition, texture, porosity, and permeability. Diagenesis also plays a crucial role in preserving fossils through processes like mineral replacement (Tucker M. E., 1993).

The Margalla Hill Limestone in study area, exhibits various diagenetic features including physical and chemical compaction, bioturbation, burrowing, pyritization, fracturing, calcite veining, cementation, micritization, dissolution, and dolomitization. While these diagenetic processes generally enhance reservoir quality, some alterations can diminish it. Of particular importance is dolomitization, which significantly affects the reservoir characteristics.

### **6.2 Compaction**

The Margalla Hill Limestone exhibits compaction processes, both mechanical and chemical. Mechanical compaction is characterized by fractures, distorted grains, and grain-to-grain sutured contacts, while chemical compaction is evident through dissolution features and stylolites, as observed in thin sections. These features align with previous findings by (Bathurst, 1976; Read, 1985). Plate 6.1a and 6.1b illustrate the presence of stylolites and fractures in the thin sections from the study area.



### **6.3 Stylolitization**

Stylolitization refers to the process where stylolites—irregular, suture-like structures—are formed in carbonate or other sedimentary rocks due to pressure dissolution. This process occurs when increased overburden stress leads to the dissolution of minerals at grain boundaries, causing a reduction in bed thickness and the development of these distinct features. Stylolites are often indicative of significant geological stress and can impact the mechanical properties of the rock formations in which they occur (Norman, 2015). Plate 6.1a visually represents the formation and characteristics of stylolites during this process.

### **6.4 Fractures**

Fractures in rocks occur as a consequence of mechanical breakdown, which arises from the concentration of stresses around inherent defects, heterogeneities, and physical discontinuities. These stresses, which include lithostatic, tectonic, and thermal stresses, as well as high fluid pressures, lead to the development of fractures (Bathurst, 1976; Read, 1985). The thin sections analyzed in the study reveal clear instances of fracturing. This phenomenon is visually represented in Plate 6.1b, which illustrates the nature and extent of these fractures.

### **6.5 Calcite veins**

Calcite veins, also referred to as calcite-filled fractures, are geological formations that occur when mineral-rich fluids, typically containing calcium carbonate (calcite), flow

through fissures or gaps within rocks and subsequently deposit calcite minerals within these openings. The size of these veins can range from tiny, almost imperceptible cracks to more prominent and easily identifiable features. Calcite veins are prevalent across a variety of geological settings and rock types, making them a common occurrence in the study of geology (Bathurst, 1976; Read, 1985). Plate 6.1d provides a clear visual representation of several calcite veins.

## **6.6 Pyritization**

Pyritization is a hydrothermal process whereby a rock undergoes transformation through the deposition of iron and sulfur, similar to silicification. This process is frequently observed in sedimentary rocks and hydrothermal mineral deposits. Pyritization typically occurs under specific conditions, often requiring the presence of organic material, bacteria, and chemical reactions in an environment characterized by low oxygen levels, as described by (Raiswell, 1997). An example of this phenomenon can be seen in the Margalla Hill Limestone formation, where pyrite is clearly present, as evidenced in the thin sections analyzed. Plate 6.1c distinctly illustrates the occurrence of pyritization.

## **6.7 Micritization**

Micritization refers to the diagenetic process where original skeletal grain structures undergo transformation into a cryptocrystalline texture. This occurs due to the repeated growth of algal pore spaces, which are subsequently filled by micritic precipitates (Bathurst, 1976; Read, 1985). As a widespread diagenetic phenomenon, micritization is observable across nearly all facies, albeit to varying degrees. It is particularly prevalent in shallow marine environments, where such transformations are common (Flügel E. &, 2010). Plate 6.1d offers a detailed illustration of the micritization process.

## 6.8 Cementation

Cementation is a geological process where minerals dissolved in pore fluids precipitate and bind sediment particles, creating a solid rock matrix. This process involves the deposition of minerals such as calcite, silica, iron oxides, and clay minerals, which act as cementing agents. These minerals form in response to variations in pressure, temperature, and the chemical composition of pore fluids, leading to the development of a durable and stable rock structure over geological time (Choquette, 1987). In the Margalla Hill Limestone, calcite cementation is evident in several outcrops, where it appears as distinct calcite patches and veins. This cementation is observed in fractures and pore spaces within the limestone, which are either partially or fully filled with precipitated calcite.

The Margalla Hill Limestone showcases two prominent types of calcite cements: blocky and botryoidal. Blocky calcite cement (Plate 6.2a) is predominantly formed under shallow marine conditions and significantly modifies the sedimentary fabric, suggesting a diagenetic process involving interactions between mineral-rich fluids and sediment in a marine phreatic environment (Tucker M. E., 1990; Moore, 2013). Conversely, botryoidal calcite cementation (Plate 6.2b) indicates a similar environmental context, further reflecting interactions between sediment and mineral-rich fluids during diagenesis.

## 6.9 Dolomitization

Dolomitization is a geological process in which the mineral dolomite (calcium magnesium carbonate:  $\text{CaMg}(\text{CO}_3)_2$ ) replaces calcium carbonate minerals, such as limestone, either partially or fully. This transformation, which occurs over extensive geological time scales, converts limestone into dolostone, or dolomite rock. Typically found in sedimentary environments like ancient reefs, shallow marine settings, and

evaporative basins, dolomite rocks exhibit changes in porosity and permeability that can significantly affect reservoir characteristics and fluid dynamics within subsurface formations. Due to these modifications, dolostone can potentially act as a productive reservoir for hydrocarbons or groundwater (Khan E. U., 2020).

## **6.10 Burrowing**

Burrowing refers to the process by which organisms excavate cavities or tunnels within sediment or soil as they navigate through it, as depicted in Figure 6.1a. This behavior is characteristic of infauna, a category of species that reside underground, including organisms such as worms, clams, and various types of crabs. The burrows created by these infaunal species exhibit a range of sizes, shapes, and depths, which are influenced by both the specific species and the surrounding environmental conditions (Dorgan, 2015).

The process of dolomitization can be visually identified in geological samples, such as the Margalla Hill Limestone. Distinct dolomite crystals are observable in thin sections of these samples, as shown in Plate 6.2c, highlighting the occurrence and impact of dolomitization on rock formation and composition.

## **6.11 Bioturbation**

Bioturbation is a process that involves the physical mixing and disturbance of soil or sediment due to the activities of living organisms, as illustrated in Figure 6.1b. These organisms, commonly referred to as bioturbators, include a diverse range of species such as worms, crabs, and insects, which inhabit or interact with the sediment. Through their movement and behavior, these organisms rework the sediments both vertically and horizontally, which results in the blending of distinct sediment layers and the creation of

intricate patterns. This process plays a significant role in shaping the structure and composition of sedimentary environments, as highlighted by (Meysman, 2006).

## **6.12 Dissolution**

Carbonate dissolution, also referred to as the process of dissolution, involves the breakdown and removal of carbonate minerals, such as calcite ( $\text{CaCO}_3$ ) and dolomite ( $\text{CaMg}(\text{CO}_3)_2$ ), from rocks or sediments due to the action of acidic fluids. This geological process is of considerable importance across various geological contexts, as it can lead to the formation of unique landforms and features. An example of this process can be observed in the Margalla Hill Limestone, as illustrated in Figure 6.1c, where the effects of carbonate dissolution are clearly depicted (Kurganskaya, 2018).

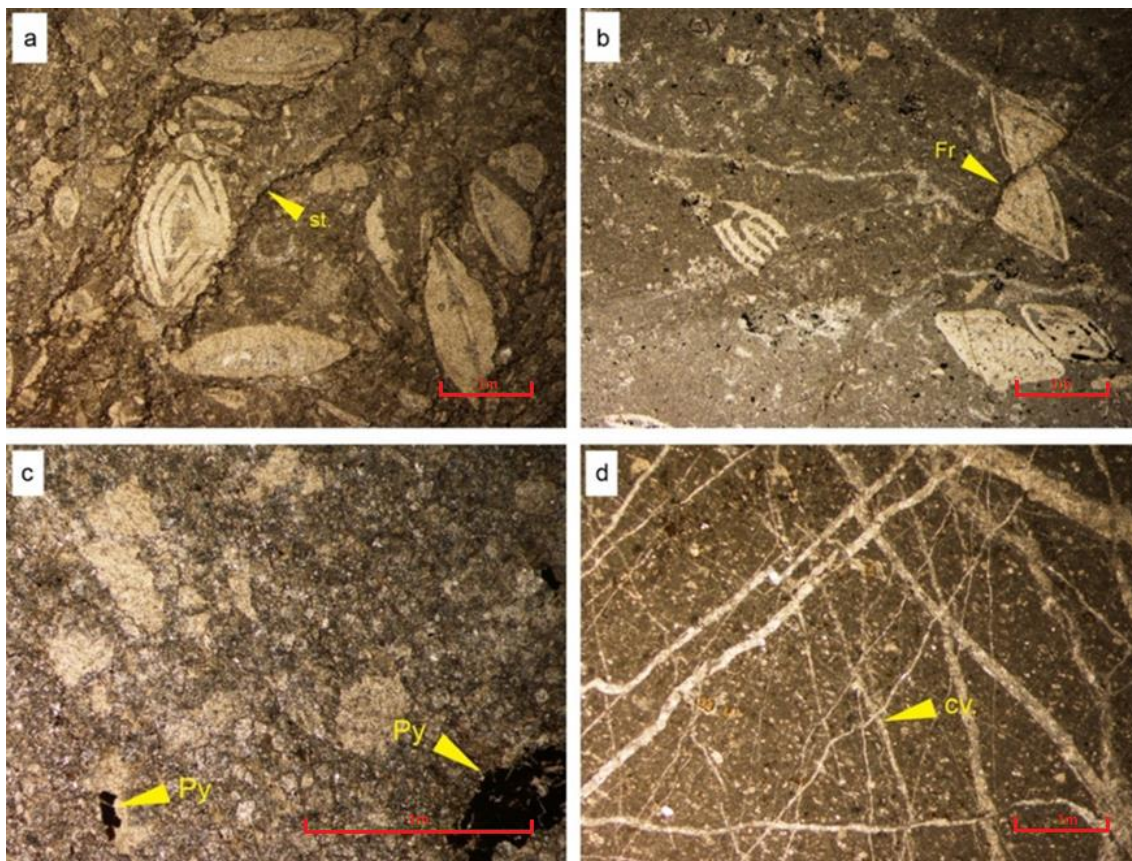


**Plate 6.1:** Thin section view illustrating mechanical and chemical compaction (a-b), pyritization (c), and micritization (d). i.e. St - stylolite, Fr - fracture, Py - pyrite, CV - calcite veins.

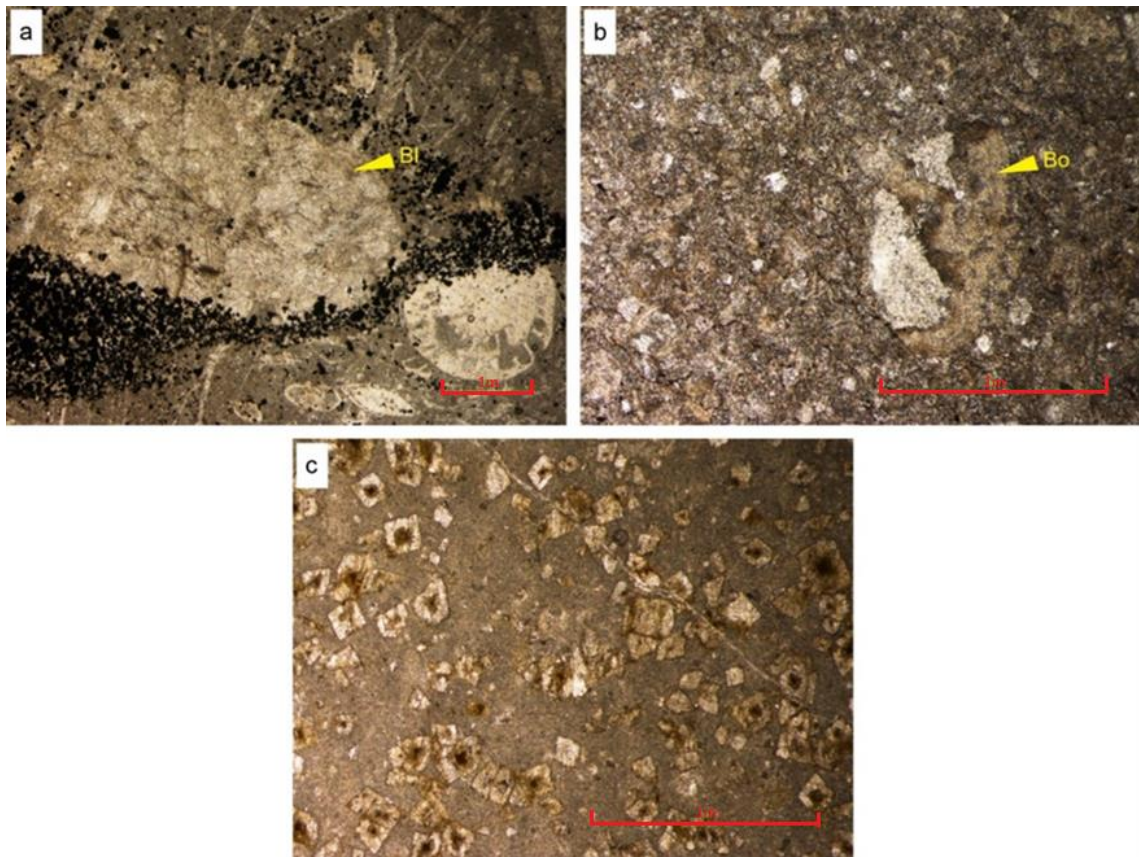


**Plate 6.2:** Photomicrographs (a-b) cementation (c) Dolomitization (i.e, bl; blocky and bo; botryoidal cementation) (c) dolomitization.



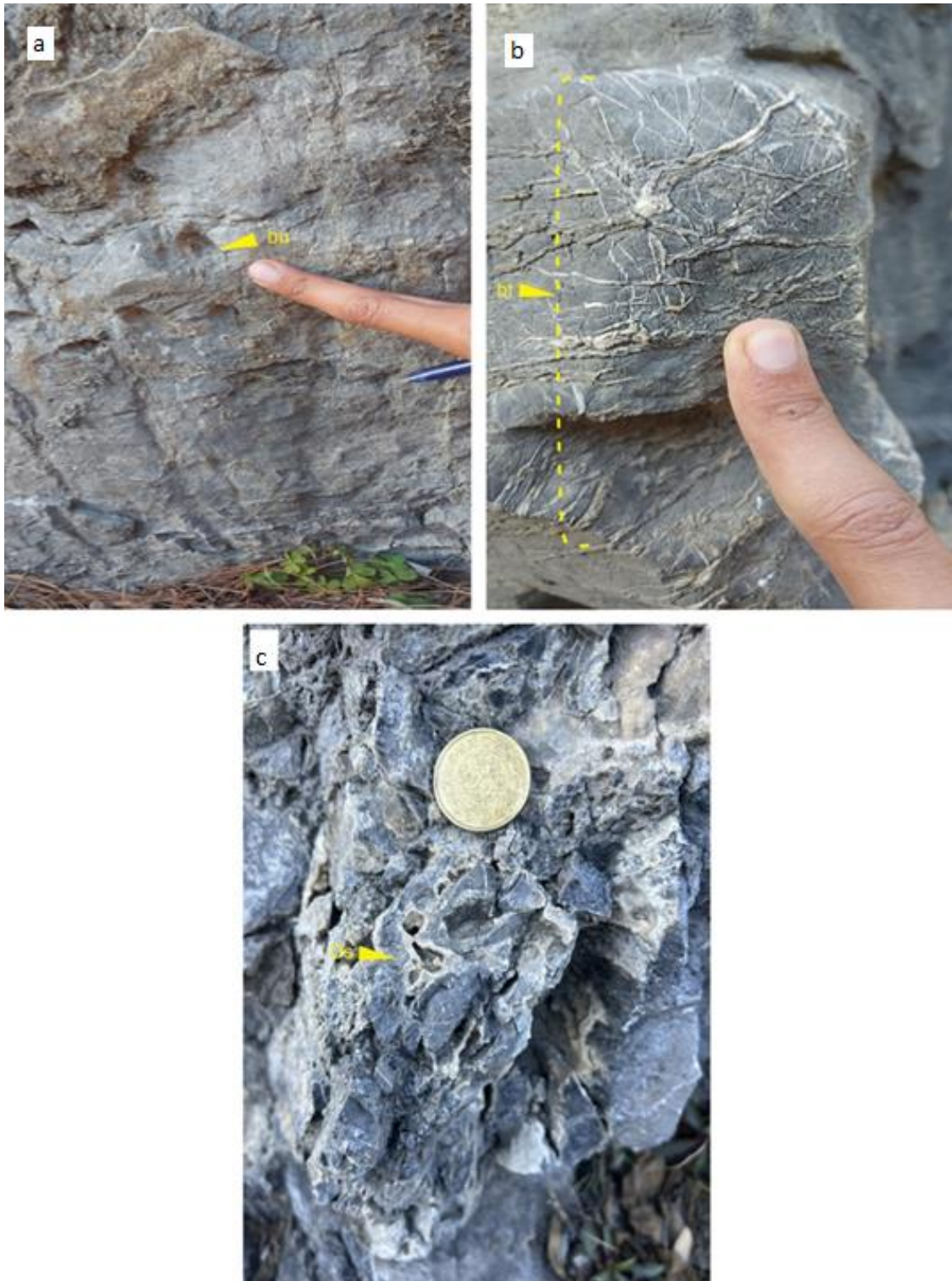


**Figure 6.1:** Field photographs (a) Burrowing (bu; burrows, bt; bioturbation and Ds; dissolution)



### 6.13 Paragenetic Sequence

A comprehensive paragenetic sequence (Figure 6.2) for the Eocene Margalla Hill Limestone has been developed based on the diagenetic investigations discussed above. Eogenetic processes such as micritization, bioturbation, burrowing, dissolution, and pyrite formation have extensively modified the primary depositional structures. Additionally, initial mechanical and chemical compaction and the cementation of sediments by blocky and botryoidal calcite cements represent early marine diagenetic activities. Mechanical compaction induced by tectonic forces and overburden pressure generated micro and macro fractures. Chemical compaction associated with this process led to the formation of stylolites in various strata of the formation.

Subsequent mesogenetic processes, both shallow and deep, further influenced mechanical and chemical compaction. The alteration of allochemical and bioclastic components within carbonate sediments under meteoric phreatic conditions has significant impact on reservoir quality. Carbonate grains underwent dissolution due to freshwater influx. Dolomitization, indicated by coarse-grained planar euhedral dolomite crystals in various facies, occurred during eogenetic conditions. Late-stage uplift events induced widespread fracturing, reflecting the region's tectonic activity (Chaudhry, 1990). Calcite-filled fractures, particularly near faulted contacts with underlying formations, provide evidence of telogenetic fracturing. The observed diagenetic characteristics of the facies also provide insights into the porosity of the formation strata: porosity increases with diagenetic events such as dissolution, dolomitization, and fracturing, while it decreases with chemical and mechanical compaction, bioturbation, burrowing, calcite veins, cementation, and micritization.

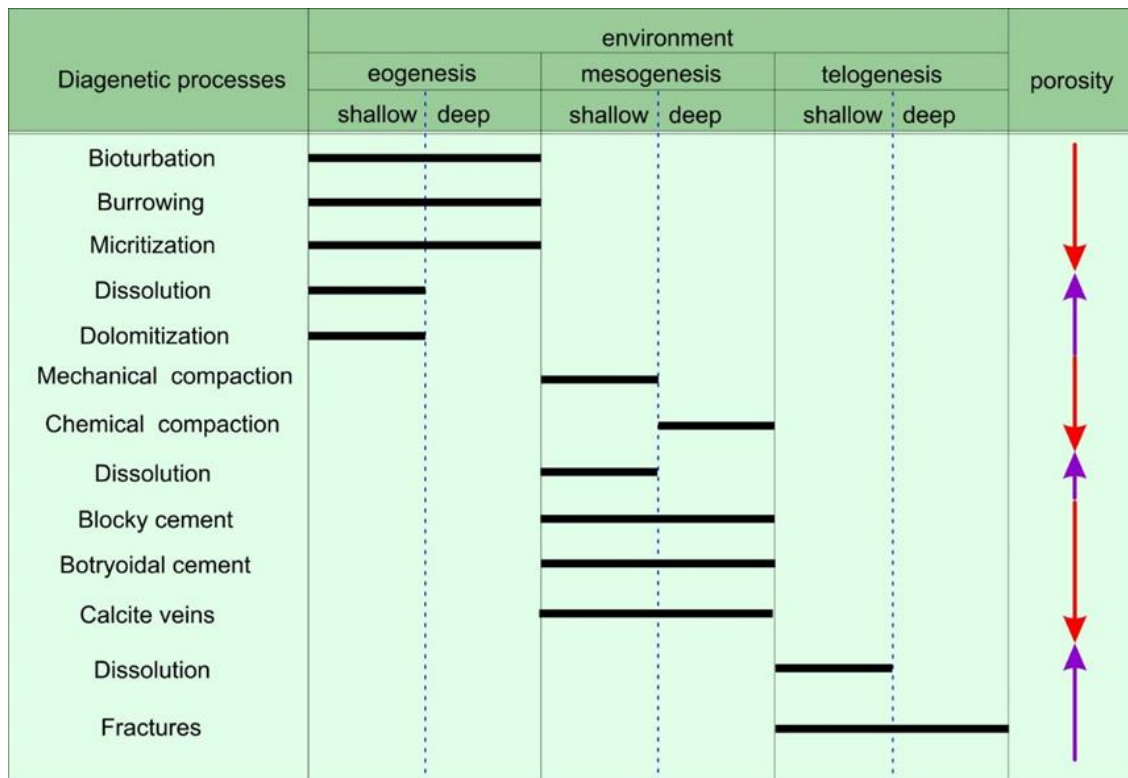


**Figure 6.2:** Representing paragenetic sequence of the study area

### 6.14 Effect of diagenesis on reservoir properties

The diagenesis of the Margalla Hill Limestone plays a crucial role in shaping the reservoir properties that are essential for hydrocarbon accumulation and storage. This formation has undergone multiple phases of deformation, resulting in extensive fracturing that significantly enhances its reservoir characteristics. Diagenetic processes, such as eogenetic micritization, bioturbation, dissolution, and dolomitization, modify the primary depositional structures, thereby improving porosity and permeability—key factors for reservoir quality. Although some alterations, including mechanical compaction and cementation, can reduce reservoir potential, the overall impact of diagenesis—particularly the dissolution of dolomitic and bioclastic components—tends to create favorable reservoir conditions. The presence of coarse-grained planar euhedral dolomite crystals highlights significant dolomitization, particularly in the dolomitic units, which

exhibit increased porosity and permeability due to the dissolution of dolomite and bioclasts (Moore, 2013).

Both dolomitic and limestone units within this formation are marked by substantial fracturing that enhances their reservoir characteristics, although early and late stages of cementation can diminish porosity and permeability. Initially, mechanical compaction reduces intergranular porosity, while subsequent blocky and botryoidal cements further modify these reservoir properties. Additionally, dolomite and calcite cements observed in the outcropped rock formations may hinder porosity and permeability (Moore, 2013). Chemical compaction processes, including the formation of stylolites and sutured contacts, typically reduce porosity, yet significant enhancements in reservoir properties arise from dolomite dissolution (Chatalov, 2014; Nabawy, 2020); Nabawy, Elgendy, & Gazia, 2019).

It is also noteworthy that the dolomitization process markedly improves intercrystalline porosity and permeability in the limestone. While dolomitization and dissolution generally enhance reservoir characteristics, compaction and cementation processes can negatively affect reservoir performance (Wadood, 2021).

### **6.15 Characterization of Margalla Hill Limestone as a Reservoir**

The The Margalla Hill Limestone, located within the tectonically complex Hazara sub-basin of the Lesser Himalayas, is characterized as a significant carbonate reservoir influenced by a combination of diagenetic processes, microfacies diversity, local geology, stratigraphy, and biostratigraphy. Its diagenetic history includes eogenetic processes like micritization, dissolution, and dolomitization, which enhance porosity and permeability, essential for hydrocarbon storage, despite some processes, such as compaction and cementation, potentially diminishing reservoir quality. Microfacies analysis reveals a range of depositional environments marked by bioclastic components and larger benthic

foraminifera, indicating favorable conditions for fluid migration. The stratigraphy, with the Margalla Hill Limestone conformably positioned between the Patala and Chorgali Formations, further enhances its reservoir capacity by reflecting distinct environmental transitions. Additionally, biostratigraphic analysis, identifying diverse fossil assemblages and key index fossils, aids in understanding the formation's geological history and hydrocarbon generation potential. Collectively, these factors underscore the Margalla Hill Limestone's significance as a reservoir with considerable potential for hydrocarbon accumulation.

## Chapter 7

# SEQUENCE STRATIGRAPHY

### 7.1 Introduction

Sequence stratigraphy is commonly defined as the "geological history of stratified rocks" (Emery, 1996). It integrates tectonics, sedimentation, and eustasy (Vail, 1987), ultimately resulting in the deposition of strata in distinct packets known as sequences. These sequences are typically further divided into system tracts based on the bounding sequence stratigraphic surfaces, distributions of parasequence sets, and their respective positions within the framework sequences (Van Wagoner, 1995). A "systems tract" serves as a link between modern depositional systems (Brown Jr, 1977). In clastic systems, these sequence stratigraphic components include;

- 1) transgressive systems tract (TST),
- 2) low-stand systems tract (LST), and
- 3) high-stand systems tract (HST) (Emery, 1996; Catuneanu, 2009)

For carbonate systems, regressive systems tract (RST) and transgressive systems tract (TST) are used, bounded on each side by sequence stratigraphic surfaces (Embry, 2017). Sequence stratigraphy is invaluable for understanding how facies tracts, stratigraphic units, and deposition components interact in basin interiors over time and space. Its applications range from delineating and exploring economic placer deposits, coal seams, and petroleum systems to gaining insights into the Earth's geological record from regional to global scales.

Carbonate deposits exhibit higher reactivity compared to clastic sediments, making them sensitive to even minor sea level changes that influence the chemistry of

pore waters trapped within them (Morad, S., Ketzer, J. M., & De Ros, L. F., 2013). Consequently, such sea level variations are closely associated with the distribution of diagenetic alterations in carbonate rocks, unlike clastic rocks (Tucker M. E., 1993; McCarthy, 1998; Morad, 2000).

Carbonate rocks formed in polar zones tend to be less reactive due to their low magnesium calcite content (Morad, S., Ketzer, J. M., & De Ros, L. F., 2013). Conversely, carbonates formed in tropical regions often contain aragonite and/or high-magnesium calcite, which are susceptible to transformation into other forms or minerals due to modest changes in sea level (Morad, S., Ketzer, J. M., & De Ros, L. F., 2013). Through microfacies analysis and outcrop data, this chapter aims to establish the general framework of sequence stratigraphy for the early Eocene Margalla Hill Limestone, highlighting its specific depositional history and diagenetic evolution.

## **7.2 Sequence Stratigraphy of Margalla Hill Limestone**

To develop a sequence stratigraphic framework for the early Eocene Margalla Hill Limestone within the sub-basin of the Hazara, NW Himalayan region, Pakistan, two stratigraphic sections, Ayubia and Nathiagali, have been selected for comprehensive analysis. The sea level curve for the Margalla Hill Limestone has been delineated through a detailed interpretation of microfacies and outcrop features. Based on the work of (Embry, 2017), the Margalla Hill Limestone is predominantly situated within a 3rd order cycle, which contains multiple 2nd order transgressive and regressive cycles. When correlating this 3rd order cycle with the curve proposed by (Haq, 1987), it shows a close alignment with the TA2 cycle. The system tracts for each section have been identified and are detailed as follows.

### **7.2.1 Ayubia section**

Within the Ayubia section, a total of ten systems tracts have been identified through microfacies analysis of depositional environments, comprising five Highstand Systems Tracts (HSTs) followed by an equal number of Transgressive Systems Tracts (TSTs) (Figure 7.1). The Highstand Systems Tracts (HSTs) are notably thicker than the TSTs, indicating that periods of stable and overall sea-level fall were more prolonged during highstand than transgressive phases where sea-level rise was rapid. The HSTs predominantly consist of Lagoonal Mudstone and Wackstone microfacies, whereas the TSTs are predominantly composed of open marine Wackstone microfacies. The sea-level curve derived from microfacies interpretation is correlated with the global sea-level curve proposed by (Haq, 1987).

### **7.2.2 Nathiagali Section**

The Margalla Hill Limestone in the study area exhibits second-order system tracts. In the Nathiagali section, petrographic and outcrop-based research has identified five Transgressive Systems Tracts (TSTs) and five Highstand Systems Tracts (HSTs), delineated by maximum flooding surfaces and transgressive surfaces (Figure 7.2). Individual TSTs are thicker than individual HSTs. Microfacies distribution shows similarities with other sections, where HSTs are predominantly composed of lagoonal Mudstone and Wackstone microfacies, while TSTs are characterized by open marine Wackstone and Packstone microfacies.

### **7.2.3 Correlation with Global Eustatic Curve**

The correlation eustatic curves in Figure 7.1 & 7.2 shows that the sequence stratigraphic model of the early eocene Margalla Hill Limestone does not share the same

architecture as the global sequence TA2 from (Haq, 1987). Local intensive tectonics in the region could explain the mismatch with the global curve.

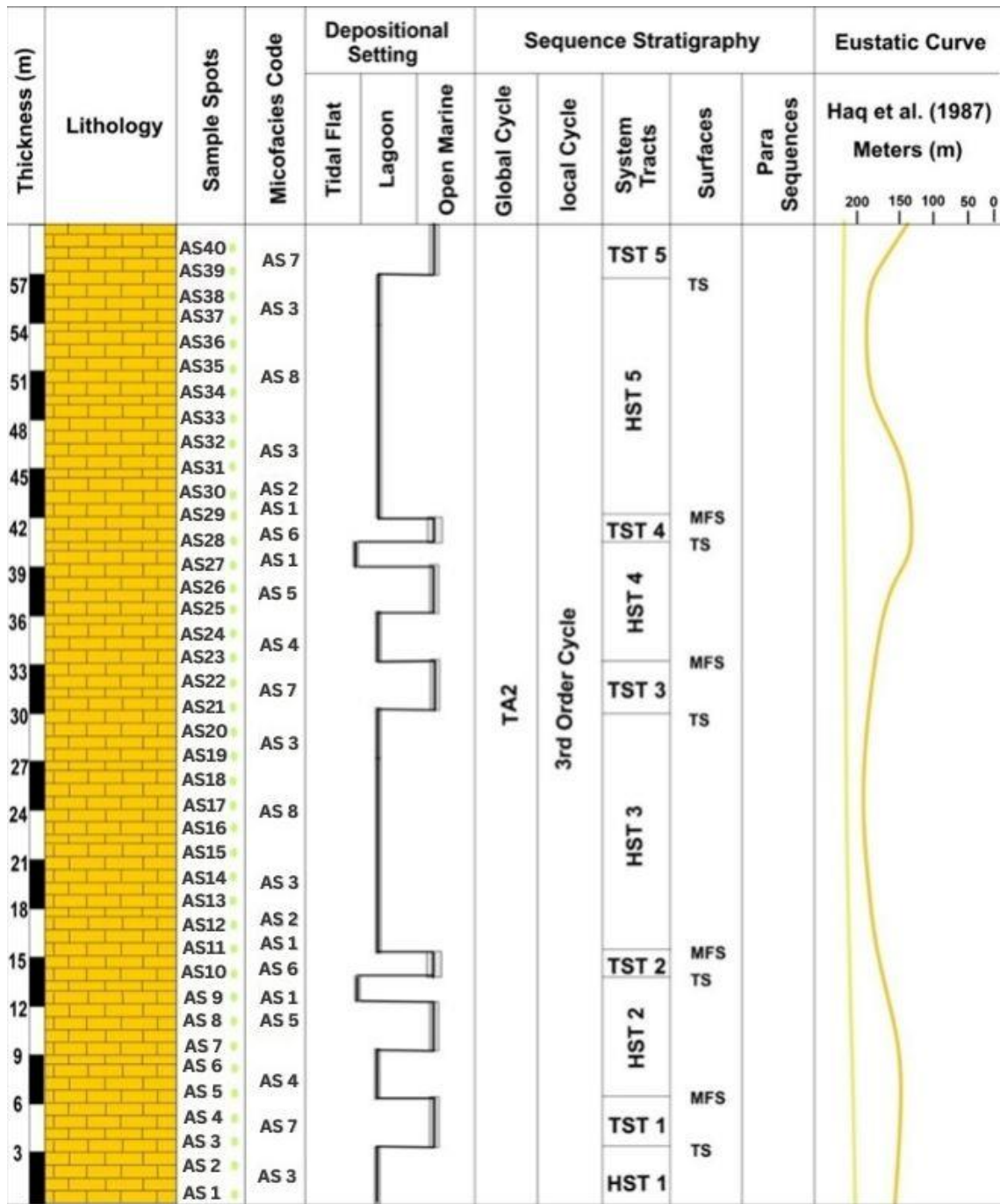


**Figure 7.1:** Stratigraphic log displaying variable lithology, microfacies distribution, depositional environments, sequence stratigraphy, and eustatic curve. light yellow colour line shows long term global eustatic changes and dark yellow colour line shows short term global eustatic changes. HST (Highstand system tract), TST (Transgressive system tract), MFS (Maximum Flooding surface) and TS (Transgressive surface).



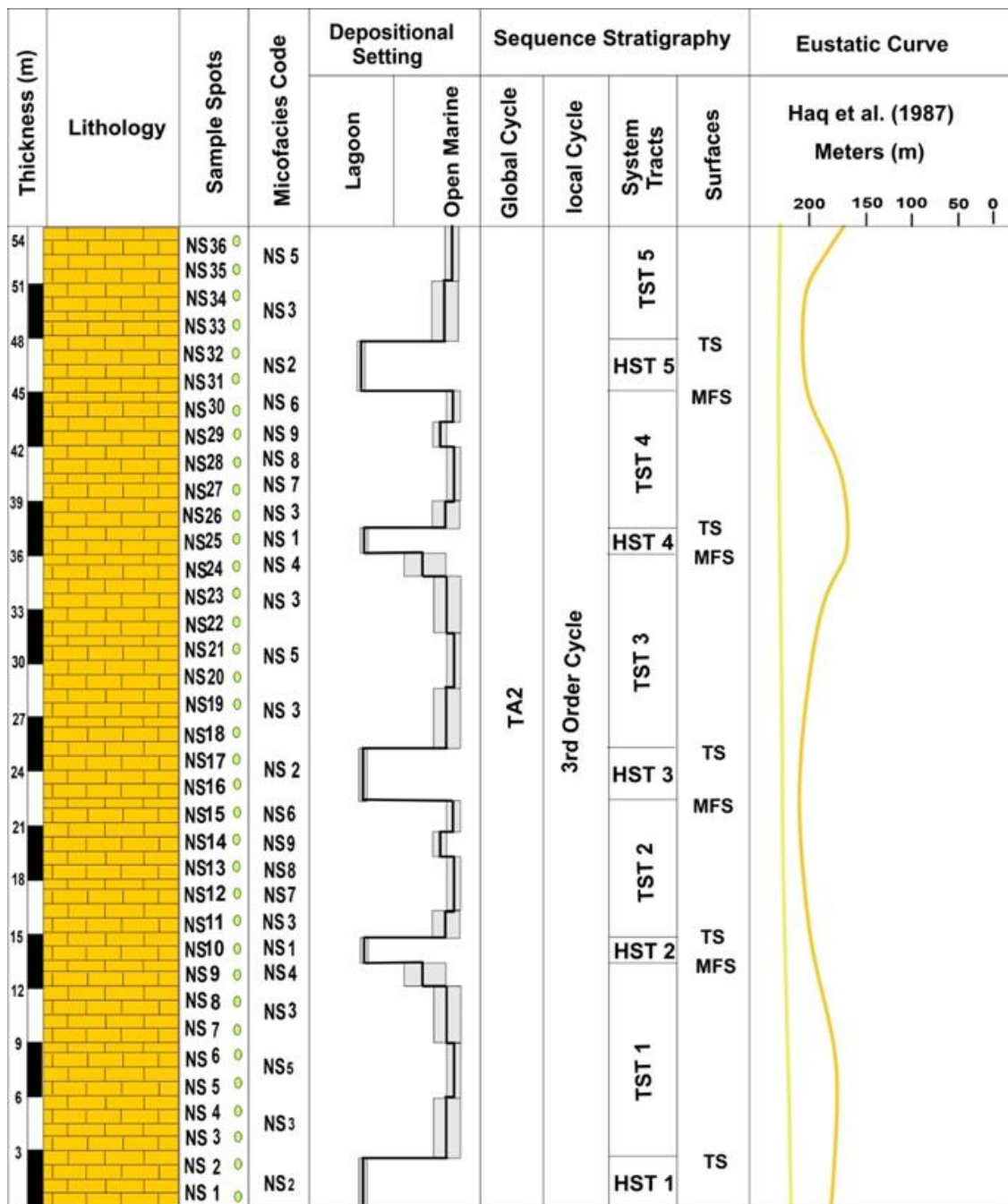


**Figure 7.2:** Stratigraphic log displaying variable lithology, microfacies distribution, depositional environments, sequence stratigraphy, and eustatic curve. light yellow colour line shows long term global eustatic changes and dark yellow colour line shows short term global eustatic changes. HST (High-stand system tract), TST (Transgressive system tract), MFS (Maximum Flooding surface) and TS (Transgressive surface).

#### **7.2.4 Correlation of Microfacies with Sequence stratigraphy of Ayubia section**

The microfacies analysis at Ayubia reveals eight distinctive facies across the Margalla Hill Limestone, representing low- to moderate-energy depositional environments ranging from tidal flats and lagoons to inner ramp settings. Sequence stratigraphic analysis integrates these microfacies with system tracts and surfaces, allowing us to interpret their roles within the transgressive-regressive (T-R) cycles. The mudstone and bioclastic mudstone microfacies, characterized by high micrite content and poor biogenic preservation, align with transgressive system tracts (TST), suggesting low-energy conditions within restricted tidal flat or lagoonal environments. The gradual increase in bioclast abundance and diverse foraminiferal assemblages in the bioclastic wackestone and algal wackestone microfacies likely reflects maximum flooding surfaces (MFS), representing a deeper, nutrient-rich setting at the peak of transgression.

Higher-energy facies, such as the Assilinid Nummulitic wackestone and Nummulitidae Alveolinal wackestone, indicate shallower, higher-energy conditions typical of highstand system tracts (HST) associated with the regressive phase. These wackestone facies, with well-preserved larger foraminifera (e.g., Assilina, Nummulites, Alveolina), indicate more open marine settings transitioning to proximal ramp environments as water depths decrease. The sequence stratigraphic analysis thus underscores a complete T-R cycle, where transgressive microfacies at the base transition upward into highstand microfacies, reflecting cyclical changes in sea level and sediment supply within the carbonate ramp system.

#### **7.2.5 Correlation of Microfacies with Sequence stratigraphy of Nathiagali section**

Microfacies analysis within the TSTs, such as Assilinid Wackstone, Nummulitidae-Lockhartian Wackstone, and Coralline-algal Wackstone, reflects

deposition in open marine settings, while HSTs show lagoonal facies like Mudstone and Bioclastic Wackstone, indicative of more restricted, lower-energy environments. Maximum Flooding Surfaces (MFS) demarcate transitions from transgressive to highstand conditions, showing repeated cycles of deepening and shallowing. The sequence stratigraphic analysis of the Nathiagali section in the Margalla Hill Limestone highlights that the Transgressive Systems Tracts (TSTs) are thicker than the Highstand Systems Tracts (HSTs), likely due to the pronounced influence of regional tectonics and rapid sea-level rise that prolonged transgressive phases.

The identified microfacies align with the stratigraphic markers in the sequence, where transgressive surfaces and MFSs show depositional shifts consistent with cycles of deepening and regression. The lagoonal mudstones and wackstones in HSTs suggest sedimentation during reduced accommodation space, while open marine packstones and wackstones in TSTs signal increased accommodation space during transgression. The sequence stratigraphic analysis reveals a complete T-R cycle in the Nathiagali section, where each Transgressive Systems Tract (TST) transitions upward into a Highstand Systems Tract (HST). This reflects periodic sea-level changes and sediment supply variations within the carbonate ramp system, with deeper marine transgressive microfacies at the base of each cycle progressively transitioning to shallower highstand microfacies at the top.

## Chapter 8

# DISCUSSION

The Margalla Hill Limestone contains fourteen significant species of larger benthic foraminifera, including *Nummulite mamillatus*, *Assilina spinosa*, and *Alveolina indicatrix*, which play an essential role in defining biostratigraphic zones. These age-diagnostic species allowed for accurate dating and zoning of Margalla Hill Limestone Biozone indicating that the formation occurred between the Late Ilerdian (SBZ9, 53 Ma) and the Lower Cuisian (SBZ10, 51.5 Ma) during the early Eocene, providing insights into the temporal and spatial distribution of these taxa. The identification of these key foraminifera species has helped establish a detailed framework for correlating biostratigraphy with physical stratigraphy, enhancing our understanding of the geological history of this region. The utility of larger benthic foraminifera acted as an effective tool for stratigraphic analysis in complex tectonic settings, advancing the knowledge of early Eocene depositional environments in the Hazara Basin and aiding in regional geological correlations.

The biostratigraphic and microfacies analysis suggests a depositional model consistent with a shallow marine environment, typical of a Tethyan carbonate platform. The presence of micrite and various microfacies types, including mudstones and wackestones, supports a carbonate ramp model with low-energy conditions conducive to mudstone deposition. This model reflects deposition across a proximal inner to middle ramp setting, where quiet water conditions, evidenced by the accumulation of micrite, allowed for the gradual deposition of carbonate materials, further affirming the open marine lagoon environment interpretation for the Margalla Hill Limestone.

The sequence stratigraphic analysis of the Margalla Hill Limestone identifies five Highstand Systems Tracts (HSTs) and five Transgressive Systems Tracts (TSTs) in both the Ayubia and Nathiagali sections. These tracts are separated by Maximum Flooding Surfaces (MFS) and Transgressive Surfaces (TS), marking fluctuations in sea levels

during deposition. The correlation of these tracts with local 3<sup>rd</sup> order cycle, specifically the global TA2 cycle (Haq et al. 1987), shows how local tectonic influences led to unique sea-level variations in the study area, impacting sedimentation patterns within the Hazara Basin.

The diagenesis of the Margalla Hill Limestone, including dissolution, dolomitization, and fracturing, plays a crucial role in enhancing reservoir properties by increasing porosity and permeability. While these processes promote reservoir quality, other diagenetic alterations, such as compaction and cementation, counteract these effects by reducing pore space. The study concludes that dissolution, dolomitization, and fracturing are vital to improving the reservoir characteristics, while compaction and cementation have a limiting effect.

## Chapter 9

# CONCLUSION

The identification of fourteen age-diagnostic species of larger benthic foraminifera, including notable taxa such as *Nummilite mamillatus* (Fichtel and Moll), *Nummilite ataticus* Leymerie, *Nummulite Globulus*, *Assilina spinosa* Davies and Pinfold, *Assilina subspinosa* Davies and Pinfold, *Assilina laminosa* Gill, *Assilina granulosa* (d'Archiac), *Lockartia tipper* Davies, *Lockhartia conditi*, *Alveolina Indicatrix*, *Alveolina* Sp, *Discocyclina Dispensa*, and *Discocyclina* Sp 1 has facilitated the establishment of biostratigraphic zones within the Margalla Hill Limestone. Zoning of Margalla Hill Limestone Biozone indicating that the formation occurred between the Late Ilerdian (SBZ9, 53 Ma) and the Lower Cuisian (SBZ10, 51.5 Ma) during the early Eocene. These zones have been effectively correlated with the physical stratigraphic data, thereby providing a clear framework for understanding the temporal and spatial distribution of these foraminifera species within the Margalla Hill Limestone.. This integration of correlating biostratigraphic analysis with physical stratigraphy underscores the effectiveness of using larger benthic foraminifera for detailed stratigraphic analysis and understanding the geological history of this region.

Detailed logging, microfacies analysis, and the presence of age-diagnostic larger benthic foraminifera indicate a shallow marine environment characteristic of a Tethyan carbonate platform. The sedimentological investigations revealed no evidence of a significant break in the slope or deep-water breccia, and mudstone deposition at this location suggests low-energy, quiet water conditions conducive to the deposition of mudstones. Therefore, the Carbonate Ramp model was effectively applied to explain the depositional setting. Many micrite crystals were observed, indicating that the currents were not strong enough to clear the mud. The Wackestone and Packstone indicate a moderate energy environment, with field observations and microfacies studies confirming that deposition occurred from the proximal inner ramp to the proximal middle ramp. These findings highlight the value of high-resolution biostratigraphic, sequence stratigraphic and logging analyses in reconstructing the depositional environment and refining our understanding of the early Eocene Margalla Hill Limestone.

The occurrence of a shallow water, low-energy, quiet water setting conducive to mudstone deposition, combined with presence of larger benthic foraminifera, points to an open marine lagoon environment for the early Eocene Margalla Hill Limestone. Various types of cements and compaction has reduced porosity and permeability by filling the available pore spaces, but the main diagenetic processes controlling reservoir quality are dissolution, dolomitization, and fracturing, which are believed to be important factors in improving reservoir quality. The Margalla Hill Limestone is composed of second-order sequences (TST and HST) that are generated from microfacies in the vertical section and are based on fluctuations in sea level. The study's sea-level curve, differing from the accepted worldwide model, highlights the significant influence of local tectonics on sedimentary processes.

## REFERENCES

- Adabi, M. H., & Rao, C. P. . (1991). Petrographic and geochemical evidence for original aragonite mineralogy of upper Jurassic carbonates (Mozduran formation), Sarakhs area, Iran. *Sedimentary Geology*, 72(3–4), 253–267. doi:[https://doi.org/10.1016/0037-0738\(91\)90014-5](https://doi.org/10.1016/0037-0738(91)90014-5)
- Adams, A. &. (1998). *Carbonate Sediments and Rocks Under the Microscope: A Colour Atlas*. CRC Press.
- Afzal, J. W. (2009). Revised stratigraphy of the lower Cenozoic succession of the Greater Indus Basin in Pakistan. *Journal of Micropalaeontology*, 28(1), 7–23.
- Afzal, J. W. (2011). Evolution of Paleocene to Early Eocene larger benthic foraminifer assemblages of the Indus Basin, Pakistan. *Lethaia*, 44(3), 299–320. doi:<https://doi.org/10.1111/J.1502-3931.2010.00247.X>
- Ahmad, S. (2011). Paleogene larger benthic foraminiferal stratigraphy and facies distribution: implications for tectonostratigraphic evolution of the Kohat Basin, Potwar Basin and the Trans Indus Ranges (TIR) northwest Pakistan.
- Ahmad, S., & Salad Hersi, O. (2021). Sedimentologic properties of mud-dominated deep-shelf carbonates of the Upper Indus Basin: The Paleocene-Eocene Patala Formation of the Hazara Sub-basin, Northern Pakistan.
- Antonellini, M., & Mollema, P. N. (2000). A Natural Analog for a Fractured and Faulted Reservoir in Dolomite: Triassic Sella Group, Northern Italy. *AAPG Bulletin*, 84(3), 314–344. doi:<https://doi.org/10.1306/C9EBCDDD-1735-11D7-8645000102C1865D>
- Radiozamani, K. (1973). The dorag dolomitization model, application to the middle Ordovician of Wisconsin. *Journal of Sedimentary Research*, 43(4), 965–984. doi:<https://doi.org/10.1306/74D728C9-2B21-11D7-8648000102C1865D>
- Baig, M. S. (2006). Active faulting and earthquake deformation in Hazara-Kashmir syntaxis, Azad Kashmir, northwest Himalaya, Pakistan. In *Extended Abstracts, International Conference on 8 October 2005 Earthquake in Pakistan: Its Implications and Hazard Mitigation* (pp. 27-28). Islamabad: Geological Survey of Pakistan.
- Baker, D. M. (1988). Development of the Himalayan frontal thrust zone: Salt Range, Pakistan. *Geology*, 16(1), 3-7.
- Barattolo, F. B. (2007). Upper Eocene larger foraminiferal - Coralline algal facies from the Klokova Mountain (southern continental Greece). *Facies*, 53(3), 361–375. doi:<https://doi.org/10.1007/S10347-007-0108-2/METRICS>
- Bathurst, R. G. (1976). Diagenesis of carbonate rocks. *132*(3), 342-343.



- Beck, R. A. (1995). Stratigraphic evidence for an early collision between northwest India and Asia. *Nature*, 373(6509), 55-58. doi:<https://doi.org/10.1038/373055a0>
- Benchilla, L. S. (2002). Sedimentology and diagenesis of the Chorgali Formation in the Potwar Plateau and Salt Range, Himalayan foothills (N-Pakistan). *American Association of Petroleum Geologists Search and Discovery article*, 90011.
- Bender, F. R. (1995). *Geology of Pakistan*. Berlin: Gebruder Borntraeger.
- Blendinger, W., & Meißner, E. (2006). Dolomite-limestone alternations—From outcrop to 3D model.
- Boggs Jr, S. (2009). Petrology of sedimentary rocks. *Cambridge university press*.
- Boschetti, T., Angulo, B., Cabrera, F., Vásquez, J., & Montero, R. L. (2016). Hydrogeochemical characterization of oilfield waters from southeast Maracaibo Basin (Venezuela): Diagenetic effects on chemical and isotopic composition. *Marine and Petroleum Geology*, 73, 228–248. doi:<https://doi.org/10.1016/J.MARPETGEO.2016.02.020>
- BouDagher-Fadel, M. K. (2008). Evolution and geological significance of larger benthic foraminifera. 540.
- Boudaughar-Fadel, M. K. (2018). *Evolution and geological significance of larger benthic foraminifera*. UCL Press. doi:<https://doi.org/10.2307/J.CTVQHSQ3>
- Brown Jr, L. F. (1977). Seismic-Stratigraphic Interpretation of Depositional Systems: Examples from Brazilian Rift and Pull-Apart Basins: Section 2. Application of Seismic Reflection Configuration to Stratigraphic Interpretation. 165, 213–248.
- Brown, J. S. (1943). Suggested use of the word microfacies. *Economic Geology*, 38(4), 325. doi:<https://doi.org/10.2113/GSECONGEO.38.4.325>
- Buxton, M. W. (1989). Short Paper: A standardized model for Tethyan Tertiary carbonate ramps. *Journal of the Geological Society*, 146(5), 746–748. doi:<https://doi.org/10.1144/GSJGS.146.5.0746>
- Calkins, J. A. (1975). *Geology of the southern Himalaya in Hazara, Pakistan, and adjacent areas (No. 716-C)*. US Govt. Print. Off.
- Catuneanu, O. A. (2009). Towards the standardization of sequence stratigraphy. *Earth-Science Reviews*, 92(1-2), 1–33. doi:<https://doi.org/10.1016/J.EARSCIREV.2008.10.003>
- Chatalov, A. &. (2014). Diagenesis of Palaeogene sandstones in the Padesh strike-slip basin. *Southwestern Bulgaria Geologica Balcanica*, 43(1-3), 3-26.
- Chatterjee, S. G. (2013). The longest voyage: Tectonic, magmatic, and paleoclimatic evolution of the Indian plate during its northward flight from Gondwana to Asia. *Gondwana Research*, 23(1), 238–267. doi:<https://doi.org/10.1016/J.GR.2012.07.001>
- Chaudhry, M. N. (1990). Position of the Main Central Thrust in the tectonic framework of Western Himalaya. *Tectonophysics*, 174(3-4), 321-329.

- Cheema, M. R. (1968). *Biostratigraphy of Changla Gali area. District Hazara, West Pakistan*. Punjab University, Pakistan.
- Choquette, P. W. (1987). Diagenesis# 12. Diagenesis in Limestones-3. The deep burial environment. *Geoscience Canada*, 14(1), 3-35.
- Choquette, P. W., James, N., McIlreath, I., & Morrow, D. (1990). Diagenesis. *Geoscience Canada*, 10(4).
- Ćosović, V. D. (2004). Paleoenvironmental model for Eocene foraminiferal limestones of the Adriatic carbonate platform (Istrian Peninsula). *Facies*, 50(1), 61–75. doi:<https://doi.org/10.1007/S10347-004-0006-9>/METRICS
- Coward, M. P. (1986). Collision tectonics in the NW Himalayas. *Geological Society, London, Special Publications*, 19(1), 203–219.
- Davies, L. a. (1937). The Eocene Beds of the Punjab Salt Range. *Memoirs of the Geological Survey of India, Palaeontologia Indica*, 24, 1–79.
- Dorgan, K. M. (2015). The biomechanics of burrowing and boring. *Journal of Experimental Biology*, 218(2), 176-183.
- Dunham, R. J. (1962). Classification of Carbonate Rocks According to Depositional Textures. 38, 108–121.
- Embry, A. F. (2017). Two approaches to sequence stratigraphy. In *Stratigraphy & Timescales* (Vol. 2, pp. 85–118). Academic Press.
- Emery, D. &. (1996). Sequence Stratigraphy. *Sequence Stratigraphy*, 45–88.
- Flügel, E. &. (2010). *Microfacies of Carbonate Rocks: Analysis, Interpretation and Application* (Vol. 976). Berlin: Springer.
- Flügel, E. (1982). Introduction to Facies Analysis. *Microfacies Analysis of Limestones*, 1–26. doi:[https://doi.org/10.1007/978-3-642-68423-4\\_1](https://doi.org/10.1007/978-3-642-68423-4_1)
- Flügel, E. (2004). *Microfacies of Carbonate Rocks: Analysis, Interpretation and Application*. Berlin: Springer.
- Gee, E. R. (1934). The Dhubri earthquake of the 3rd July, 1930. *Memoirs of the Geological Survey of India*, 65.
- Geel, T. (2000). Recognition of stratigraphic sequences in carbonate platform and slope deposits: Empirical models based on microfacies analysis of Palaeogene deposits in southeastern Spain. *Palaeogeography, Palaeoclimatology, Palaeoecology*, 155(3–4), 211–238. doi:[https://doi.org/10.1016/S0031-0182\(99\)00117-0](https://doi.org/10.1016/S0031-0182(99)00117-0)
- Ghazi, S. (2014). Microfacies and depositional setting of the Early Eocene Chor Gali Formation, Central Salt Range, Pakistan. *Pakistan Journal of Science*, 66(2).
- Gill, W. D. (1953). Facies and fauna in the Bhadrar beds of the Punjab Salt Range, Pakistan. *Journal of Paleontology*, 824–844.

- Gill, W. D. (1953). The genus *Assilina* in the Laki Series (Lower Eocene) of the Kohat-Potwar Basin, Northwest Pakistan. *Contributions from the Cushman Foundation for Foraminiferal Research*, 4, 76–84.
- Gingerich, P. D. (1977). A Small Collection of Fossil Vertebrates from the Middle Eocene Kuldana and Kohat Formations of Punjab (Pakistan). 24(18), 5.
- Gingerich, P. D. (1981). *Pakicetus inachus*, a new archaeocete (Mammalia, Cetacea) from the early-middle Eocene Kuldana Formation of Kohat (Pakistan).
- Gupta, B. C. (1934). The geology of central Mewar. *Office of the Geological Survey of India*.
- Halbouty, M. T. (1970). World's Giant Oil and Gas Fields, Geologic Factors Affecting Their Formation, and Basin Classification: Part II: Factors Affecting Formation of Giant Oil and Gas Fields, and Basin Classification. 9, 528–555.
- Haq, B. U. (1987). Chronology of fluctuating sea levels since the Triassic. *Science*, 235(4793), 1156–1167. doi:<https://doi.org/10.1126/SCIENCE.235.4793.1156>
- Heckel, P. H. (1972). Recognition of ancient shallow marine environments. In recognition of ancient sedimentary environments. *SEPM Society for Sedimentary Geology*. doi:<https://doi.org/10.2110/PEC.72.02.0226>
- Hottinger, L. (1960). Recherches sur les Alvéolines du Paléocène et de l'Eocène. Retrieved from <https://www.worldcat.org/title/recherches-sur-les-alveolines-du-paleocene-et-de-leocene-etc/oclc/859168830>
- Jacquemyn, C., El Desouky, H., Hunt, D., Casini, G., & Swennen, R. (2014). Dolomitization of the Latemar platform: Fluid flow and dolomite evolution. *Marine and Petroleum Geology*, 55, 43–67. doi:<https://doi.org/10.1016/J.MARPETGEO.2014.01.017>
- James, N. P., & Dalrymple, R. W. (2010). *Facies Models 4*. The Geological Association of Canada. Retrieved from <https://www.abebooks.com/9781897095508/>
- Johnson, B. D. (1976). Spreading history of the eastern Indian Ocean and Greater India's northward flight from Antarctica and Australia. *Geological Society of America Bulletin*, 87(11), 1560-1566.
- Jurgan, H., & Abbas, G. (1991). On the Chorgali Formation at the type locality. *Pakistan Journal of Hydrocarbon Research*, 3(1), 35–45.
- Kadri, I. B. (1995). *Petroleum Geology of Pakistan*.
- Kazmi, A. H. (2008). *Stratigraphy & Historical Geology of Pakistan*.
- Khan, A. H. (1970). Lithologic and biostratigraphic properties of the Paleocene Lockhart Formation, Hazara and Potwar basins, northeast Pakistan: Preliminary results.
- Khan, E. U. (2020). Microfacies analysis, diagenetic overprints, geochemistry, and reservoir quality of the Jurassic Samanasuk Formation at the Kahi Section, Nizampur Basin, NW Himalayas, Pakistan. *Carbonates and Evaporites*, 35, 1–17. doi:<https://doi.org/10.1007/S13146-020-00622-4>

- Kurganskaya, I. &. (2018). Carbonate dissolution mechanisms in the presence of electrolytes revealed by grand canonical and kinetic Monte Carlo modeling. *The Journal of Physical Chemistry C*, 122(51), 29285-29297.
- Latif, M. A. (1970). Explanatory notes on the geology of South Eastern Hazara, to accompany the revised geological map. *Wiener Jahrbuch für Geologie und Bergwesen (Wien Jb. Geol. BA)*, 15.
- Latif, M. A. (1970). Micropalaeontology of the Galis Group, Hazara, West Pakistan. *Wiener Jahrbuch für Geologie und Bergwesen (Wien Jb. Geol., B.-A.)*, 15, 63-66.
- Machel, H. G. (1999). Effects of groundwater flow on mineral diagenesis, with emphasis on carbonate aquifers. *Hydrogeology Journal*, 7(1), 94–107. doi:<https://doi.org/10.1007/S100400050182/METRICS>
- Machel, H. G., & Buschkuehle, B. E. (2008). Diagenesis of the Devonian Southesk-Cairn Carbonate Complex, Alberta, Canada: marine cementation, burial dolomitization, thermochemical sulfate reduction, anhydritization, and squeegee fluid flow. *Journal of Sedimentary Research*, 78(5), 366-389. doi:<https://doi.org/10.2110/JSR.2008.037>
- Margulis, L. (1990). Handbook of protoctista : the structure, cultivation, habitats, and life histories of the eukaryotic microorganisms and their descendants exclusive of animals, plants, and fungi : a guide to the algae, ciliates, foraminifera, sporozoa, water molds & slime. *The Jones and Bartlett series in life sciences (USA)*. Retrieved from <https://iucacat.iu.edu/iucacat/4154922>
- McCarthy, P. J. (1998). Recognition of interfluvial sequence boundaries: integrating paleopedology and sequence stratigraphy. *Geology*, 26(5), 387-390.
- Meigs, A. J. (1995). Middle-late Miocene (> 10 Ma) formation of the Main Boundary thrust in the western Himalaya. *Geology*, 23(5), 423-426. Retrieved from <https://pubs.geoscienceworld.org/gsa/geology/article-abstract/23/5/423/206310>
- Meysman, F. J. (2006). Bioturbation: a fresh look at Darwin's last idea. *Trends in Ecology & Evolution*, 21(12), 688-695.
- Middleton, G. V. (1973). Johannes Walther's law of the correlation of facies. *Geological Society of America Bulletin*, 84(3), 979–988.
- Mirza, K. A. (2022). Biostratigraphy, microfacies and sequence stratigraphic analysis of the Chorgali Formation, Central Salt Range, northern Pakistan. *Solid Earth Sciences*, 7(2), 104-125. doi:<https://doi.org/10.1016/J.SESCI.2021.11.003>
- Moore, C. H. (2013). Carbonate diagenesis: Introduction and tools. In *Developments in Sedimentology* (Vol. 67, pp. 67-89). Elsevier.
- Morad, S. K. (2000). Spatial and temporal distribution of diagenetic alterations in siliciclastic rocks: Implications for mass transfer in sedimentary basins. *Sedimentology*, 47(SUPPL. 1), 95–120. doi:<https://doi.org/10.1046/J.1365-3091.2000.00007.X>

- Morad, S. K. (2013). Linking Diagenesis to Sequence Stratigraphy: An Integrated Tool for Understanding and Predicting Reservoir Quality Distribution. *Linking Diagenesis to Sequence Stratigraphy*, 1–36. doi:<https://doi.org/10.1002/9781118485347.CH1>
- Muhammad, T. K., & Osman, S. H. (2022). Shallowing-upward nature of the Chorgali Formation, Potwar and Hazara sub-basins, N. Pakistan: a clue during the closing stage of the eastern Neo-Tethys Ocean. Retrieved from <https://geoconvention.com/>
- Muslim, M. (2019). Diagenetic studies of the Cretaceous turbidities, Sulaiman Range, Pakistan: Implications for reservoir quality. *Journal of Himalayan Earth Sciences*, 52(1), 106-119.
- Nabawy, B. S. (2020). Mineralogic and diagenetic controls on reservoir quality of paleozoic sandstones, Gebel El-Zeit, North Eastern Desert, Egypt. *Natural Resources Research*, 29(2), 1215-1238.
- Nelson, C. R. (2000). Effects of geologic variables on cleat porosity trends in coalbed gas reservoirs. *SPE Unconventional Resources Conference/Gas Technology Symposium*, 59787, 651–655. doi:<https://doi.org/10.2118/59787-MS>
- Nichols, G. J. (2007). Processes, facies and architecture of fluvial distributary system deposits. *Sedimentary Geology*, 195(1–2), 75–90. doi:<https://doi.org/10.1016/J.SEDGEO.2006.07.004>
- Norman, K. (2015). Stylolitization of Limestone: A Study about the Morphology of Stylolites and Its Impacts of Porosity and Permeability in Limestone.
- Pascoe, E. H. (1920). Petroleum in the Punjab and North-West Frontier Province. *Geological Survey of India*.
- Patriat, P. &. (1984). India–Eurasia collision chronology has implications for crustal shortening and driving mechanism of plates. *Nature*, 311(5987), 615-621.
- Pinfold, E. S. (1918). Notes on structure and stratigraphy in the north-west Punjab. *Rec. Geol. Surv. India*, 49(Pt 3), 137-160.
- Powell, C. M. (1979). A speculative tectonic history of Pakistan and its surrounding: Some constraints from the Indian Ocean. In K. &. In Dejong (Ed.), *Geodynamics of Pakistan* (pp. 5-24). Quetta: Geological Survey of Pakistan.
- Racey, A. (1994). Biostratigraphy and palaeobiogeographic significance of Tertiary Nummulitids (Foraminifera) from Northern Oman. In I. M. (Ed.) (Ed.), *Micropalaeontology and Hydrocarbon Exploration in the Middle East* (pp. 343–370). Chapman & Hall.
- Racey, A. (1995). Lithostratigraphy and larger foraminiferal (nummulitid) biostratigraphy of the Tertiary of northern Oman. *Micropaleontology*, 41, 1-123. doi:<https://doi.org/10.2307/1485849>

- Rahman, M. U. (2021). Alveolinids from the Lower Indus Basin, Pakistan (Eastern Neo-Tethys): Systematic and biostratigraphic implications. *Geological Journal*, 56(7), 3644-3671. doi:<https://doi.org/10.1002/GJ.4119>
- Raiswell, R. (1997). A geochemical framework for the application of stable sulphur isotopes to fossil pyritization. *Journal of the Geological Society*, 154(2), 343-356.
- Read, J. F. (1985). Carbonate platform facies models. *AAPG bulletin*, 69(1), 1-21.
- Reid, R. P. (2000). Microboring versus recrystallization: further insight into the micritization process. *Journal of Sedimentary Research*, 70(1), 24-28. doi:<https://doi.org/10.1306/2DC408FA-0E47-11D7-8643000102C1865D>
- Rosales, I. P.-A. (2018). Microfacies, diagenesis and oil emplacement of the Upper Jurassic Arab-D carbonate reservoir in an oil field in central Saudi Arabia (Khurais Complex). *Marine and Petroleum Geology*, 96, 551-576.
- Sam boggs, J. (2006). *Principles of sedimentology and stratigraphy*. Upper Saddle River, NJ: Pearson Prentice Hall.
- Sameeni, S. J. (2013). Biostratigraphy of Chorgali formation, Jhalar area, Kala Chitta range, Northern Pakistan. *Science International (Lahore)*, 25(3), 567-577.
- Schaub, H. (1981). Nummulites et Assilines de la Tethys paleogene, taxinomie, phylogenie et biostratigraphie avec deux volumes d'atlas.
- Scotese, C. R. (1988). Plate tectonic reconstructions of the Cretaceous and Cenozoic ocean basins. *Tectonophysics*, 155(1-4), 27-48. doi:[https://doi.org/10.1016/0040-1951\(88\)90259-4](https://doi.org/10.1016/0040-1951(88)90259-4)
- Searle, M. (1991). Geology and Tectonics of Karakoram Mountains. *Geological Magazine*, 129(358).
- Serra-Kiel, J. H. (1998). Larger foraminiferal biostratigraphy of the Tethyan Paleocene and Eocene. *Bulletin de la Société géologique de France*, 169(2), 281-299.
- Shah, S. M. (1977). Stratigraphy of Pakistan. *Mem. Geol. Surv. Pakistan*, 12, 1-138.
- Shah, S. M. I., Ahmed, R., Cheema, M. R., Fatmi, A. N., Iqbal, M. W. A., Raza, H. A., & Raza, S. M. (1977). *Stratigraphy of Pakistan*. Quetta: Geological Survey of Pakistan (Memoir, 12).
- Siddiqui, S. U. (1998). Ratana Field: A Case History. In *Proceedings of the Pakistan Petroleum Convention, Islamabad*, 22-51.
- Surdam, R. C. (1985). Organic-inorganic reactions during progressive burial: key to porosity and permeability enhancement and preservation. *Philosophical Transactions of the Royal Society of London. Series A, Mathematical and Physical Sciences*, 315(1531), 135-156. doi:<https://doi.org/10.1098/RSTA.1985.0034>
- Swati, M. A. (2013). Biostratigraphy and depositional environments of the Early Eocene Margalla Hill Limestone, Kohala-Bala area, Haripur, Hazara Fold-Thrust Belt, Pakistan. *Journal of Himalayan Earth Sciences*, 46(2), 65.

- Taha Jamal, R. A., Haneef, M., Saboor, A., Ali, N., & Uddin, M. A. F. S. Z. (2015). Microfacies and diagenetic fabric of the Chorgali Formation in Bhuchal Kalan, Kallar Kahar, Salt Range, Pakistan. *Journal of Himalayan Earth Sciences*, 48(1), 14–25.
- Tahirkheli, R. A. (1982). Geology of Hindu Kush, Himalayas and Karakoram in Pakistan. *Geological Bulletin, University of Peshawar*, 15, 51.
- TahirKheli, R. K. (1979). Geology of kohistan and adjoining eurasian and indo-Pakistan continents, Pakistan. *Geological Bulletin of University of Peshawar*, 11(1), 1-30.
- Teillet, T. F. (2019). Diagenetic history and porosity evolution of an Early Miocene carbonate buildup (Upper Burman Limestone), Yadana gas field, offshore Myanmar. *Marine and Petroleum Geology*, 589-606, 589-606. doi:<https://doi.org/10.1016/J.MARPETGEO.2019.06.044>
- Treloar, P. J. (1992). Thrust geometries, interferences and rotations in the Northwest Himalaya. *Thrust tectonics*, 325-342. doi:[https://doi.org/10.1007/978-94-011-3066-0\\_30](https://doi.org/10.1007/978-94-011-3066-0_30)
- Tucker, D. H. (2007). Geology and complex collapse mechanisms of the 3.72 Ma Hannegan caldera, North Cascades, Washington, USA. *Geological Society of America Bulletin*, 119(3-4), 329-342. doi:<https://doi.org/10.1130/B25904.1>
- Tucker, M. E. (1990). Carbonate Sedimentology. *Blackwell, Oxford*, 482.
- Tucker, M. E. (1993). Carbonate diagenesis and sequence stratigraphy. *Sedimentology Review/1*, 51-72.
- Umar, M. S. (2015). Stratigraphic and sedimentological attributes in Hazara Basin Lesser Himalaya, North Pakistan: their role in deciphering minerals potential. *Arabian Journal of Geosciences*, 8, 1653-1667.
- Vail, P. R. (1987). Seismic Stratigraphy Interpretation Procedures. In A. W. Bally (Ed.), *Atlas of Seismic Stratigraphy* (Vol. 1, pp. 1–10). AAPG (American Association of Petroleum Geologists) Studies in Geology.
- Van Wagoner, J. C. (1995). Sequence stratigraphy and marine to nonmarine facies architecture of foreland basin strata, Book Cliffs, Utah, USA. 137–223.
- Wadood, B. K. (2021). Investigating the impact of diagenesis on reservoir quality of the Jurassic shallow shelfal carbonate deposits: Kala Chitta Range, North Pakistan. *Geological Journal*, 56(2), 1167-1186.
- Worden, R. H. (2003). Sandstone diagenesis: the evolution of sand to stone. *Sandstone diagenesis: Recent and ancient*, 1-44.
- Yoshida, M. &. (2018). Voyage of the Indian subcontinent since Pangea breakup and driving force of supercontinent cycles: Insights on dynamics from numerical modeling. *Geoscience Frontiers*, 9(5), 1279-1292. doi:<https://doi.org/10.1016/J.GSF.2017.09.001>

- Zhang, H. D. (2006 ). Carbonate diagenesis controlled by glacioeustatic sea-level changes: a case study from the Carboniferous-Permian boundary section at Xikou, China. *Journal of China University of Geosciences*, 17(2), 103-114. doi:[https://doi.org/10.1016/S1002-0705\(06\)60014-9](https://doi.org/10.1016/S1002-0705(06)60014-9)
- Zhang, Q. W. (2013). Evolution of the Paleocene-Early Eocene larger benthic foraminifera in the Tethyan Himalaya of Tibet, China. *International Journal of Earth Sciences*, 102, 1427-1445. doi:<https://doi.org/10.1007/S00531-012-0856-2/METRICS>



# MS Thesis M Ismail Geology

---

## ORIGINALITY REPORT

---

12%

SIMILARITY INDEX

6%

INTERNET SOURCES

11%

PUBLICATIONS

3%

STUDENT PAPERS

---

## PRIMARY SOURCES

---

- |   |   |    |
|---|---|----|
| 1 | <a href="https://ourspace.uregina.ca">ourspace.uregina.ca</a><br>Internet Source  | 3% |
| 2 | Ullah, Aman. "Lithofacies Properties, Biostratigraphy, Cyclicity and Depositional Environment of the Margala Hill Limestone, Hazara Basin, Northern Pakistan.", The University of Regina (Canada), 2020<br>Publication                            | 2% |
| 3 | Submitted to Higher Education Commission Pakistan<br>Student Paper  | 1% |
| 4 | Kamran Mirza, Nosheen Akhter, Ayesha Ejaz, Syeda Fakiha Ali Zaidi. "Biostratigraphy, microfacies and sequence stratigraphic analysis of the Chorgali Formation, Central Salt Range, northern Pakistan", Solid Earth Sciences, 2021<br>Publication | 1% |
| 5 | Khan, Muhammad Tufail. "Sedimentology and Biostratigraphy of the Chorgali Formation, Potwar and Hazara Sub-Basins, Upper Indus  | 1% |

# Basin of Pakistan: Implications for the Closing Stage of the Eastern Neo-Tethys Ocean", The University of Regina (Canada), 2023

Publication

---

6

Basit Ali, Mumtaz Ali Khan, Muhammad Hanif, Masood Anwar, Beenish Ali, Mustafa Yar, Ijaz Ahmed. "Physico-mechanical and petrographic analysis of the Margalla Hill Limestone, Islamabad, Lesser Himalaya, Pakistan", Carbonates and Evaporites, 2023

Publication

---

1 %

7

Shuja Ullah, Muhammad Hanif, Ahmed E. Radwan, Chuanxiu Luo et al. "Depositional and diagenetic modeling of the Margala Hill Limestone, Hazara area (Pakistan): Implications for reservoir characterization using outcrop analogues", Geoenergy Science and Engineering, 2023

Publication

---

<1 %

8

[www.researchgate.net](http://www.researchgate.net)

Internet Source

---

<1 %

9

Asghar Ali, Shah Faisal, Khaista Rehman, Suleman Khan, Nijat Ullah. "Tectonic imprints of the Hazara Kashmir Syntaxis on the Northwest Himalayan fold and thrust belt, North Pakistan", Arabian Journal of Geosciences, 2015

Publication

---

<1 %

10

Irshad Hussain, Zuo-Chen Li, Misbah Fida, Jabir Hussain et al. "Sub-Himalayan Mesozoic-Cenozoic tectonic-stratigraphic properties and deformation features in the western limb of Hazara Kashmir syntaxis, Pakistan", *Arabian Journal of Geosciences*, 2023

Publication

<1 %

11

Rafiq Ali Khan, Sajjad Ahmad, Shehla Gul. "Fracture and Fracture Pressure Analysis of the Carbonate Reservoir: Implications for Hydrocarbon Exploration and Drilling in Pakistan", *Research Square Platform LLC*, 2023

Publication

<1 %

12

Darngawn, Jehova Lalmalsawm. "Sedimentology, Ichnology and Sequence Stratigraphy of Jurassic Sediments of Khadir, Bela and Chorar Islands, Island Belt Zone, Kachchh, Western India", *Maharaja Sayajirao University of Baroda (India)*, 2023

Publication

<1 %

13

Submitted to University of Portsmouth

Student Paper

<1 %

14

[www.currentscience.ac.in](http://www.currentscience.ac.in)

Internet Source

<1 %

15

Sajjad Ahmad. "Tectonostratigraphic evolution of the Paleogene basins in North Pakistan:

<1 %

# Implications for the timing of closure of Eastern Tethys and India-Asia Collision", Research Square Platform LLC, 2023

Publication

16

[ouci.dntb.gov.ua](http://ouci.dntb.gov.ua)

Internet Source

<1 %

17

[core.ac.uk](http://core.ac.uk)

Internet Source

<1 %

18

Submitted to University of Durham

Student Paper

<1 %

19

Ahmad, Shakeel. "Late Paleocene-Early Eocene Outer Shelf Depositional System of the Upper Indus Basin: the Patala Formation of the Hazara and Potwar Sub-Basins, Northern Pakistan", The University of Regina (Canada), 2023

Publication

<1 %

20

[docslib.org](http://docslib.org)

Internet Source

<1 %

21

[pdffox.com](http://pdffox.com)

Internet Source

<1 %

22

[www.britannica.com](http://www.britannica.com)

Internet Source

<1 %

23

[c.coek.info](http://c.coek.info)

Internet Source

<1 %

[www.scielo.org.mx](http://www.scielo.org.mx)

24

Internet Source

&lt;1 %

25

"The lowermost Silurian of Jämtland, central Sweden: conodont biostratigraphy, correlation and biofacies", Transactions of the Royal Society of Edinburgh Earth Sciences, 03/2005

Publication

&lt;1 %

26

Ahmer Bilal, Renchao Yang, Muhammad Saleem Mughal, Hammad Tariq Janjuhah, Muhammad Zaheer, George Kontakiotis. "Sedimentology and Diagenesis of the Early-Middle Eocene Carbonate Deposits of the Ceno-Tethys Ocean", Journal of Marine Science and Engineering, 2022

Publication

&lt;1 %

27

[era.library.ualberta.ca](http://era.library.ualberta.ca)

Internet Source

&lt;1 %

28

[nceg.uop.edu.pk](http://nceg.uop.edu.pk)

Internet Source

&lt;1 %

29

Ercan Özcan, Johannes Pignatti, Christer Pereira, Ali Osman Yücel, Katica Drobne, Filippo Barattolo, Pratul Kumar Saraswati. "Paleocene orthophragminids from the Lakadong Limestone, Mawmluh Quarry section, Meghalaya (Shillong, NE India): implications for the regional geology and

&lt;1 %

paleobiogeography", Journal of  
Micropalaeontology, 2018

Publication

30

Khaista Rehman, Asghar Ali, Sajjad Ahmed,  
Wajid Ali, Aamir Ali, Muhammad Younis Khan.  
"Spatio-temporal variations of b-value in and  
around north Pakistan", Journal of Earth  
System Science, 2015

Publication

<1 %

31

Wei Wei, Xiaomin Zhu, Mingxuan Tan,  
Chenbingjie Wu, Dianbin Guo, Hui Su.  
"Distribution of diagenetic alterations within  
depositional facies and sequence  
stratigraphic framework of fan delta and  
subaqueous fan sandstones: evidence from  
the Lower Cretaceous Bayingebi Formation,  
Chagan sag, China–Mongolia frontier area",  
Geosciences Journal, 2015

Publication

<1 %

32

[es.scribd.com](http://es.scribd.com)

Internet Source

<1 %

33

[fdocuments.us](http://fdocuments.us)

Internet Source

<1 %

34

[idoc.tips](http://idoc.tips)

Internet Source

<1 %

35

[pu.edu.pk](http://pu.edu.pk)

Internet Source

<1 %

36 Applied Stratigraphy, 2005.

Publication

<1 %

---

37 Morad, S., J.M. Ketzer, and L.F. De Ros.  
"Linking Diagenesis to Sequence Stratigraphy:  
An Integrated Tool for Understanding and  
Predicting Reservoir Quality Distribution",  
Linking Diagenesis to Sequence Stratigraphy  
Morad/Linking Diagenesis to Sequence  
Stratigraphy, 2013.

Publication

<1 %

---

38 Niraj Kumar, George van Driem, Phunchok  
Stobdan. "Himalayan Bridge", Routledge,  
2020

Publication

<1 %

---

Exclude quotes Off

Exclude matches Off

Exclude bibliography Off